Characterization of radio wave propagation into buildings at 1800 MHz

Martijn, E.F.T.

Award date:
2000

Eindhoven University of Technology
Faculty of Electrical Engineering
Division of Telecommunication Technology and Electromagnetics
Radiocommunications Group

Characterization of radio wave propagation into buildings at 1800 MHz

by E.F.T. Martijn

Master of Science Thesis
carried out from November 1999 till August 2000

Supervisors:
dr.ir. A. Mawira (KPN Research)
dr.ir. M.H.A.J. Herben (EUT)

Graduation professor:
prof.dr.ir. G. Brussaard (EUT)

Abstract

This report treats the characterization of radio wave propagation into buildings. Measurements of the signal strength have been carried out in four KPN buildings in The Hague at 1800 MHz, these have been compared with outdoor measurements at street level in the vicinity of the buildings. Additionally, one wideband measurement has been carried out in two office rooms of a KPN building in Leidschendam.

The first experiment was carried out in a small cell. The results indicated an average penetration loss of approximately 12-13 dB with a standard deviation of 5-6 dB. In general, an increase has been found in the average signal strength when the receiver is moved upward in a building (up to floor seven), the worst case situation being at ground floor. This is in accordance with several other studies done on this subject. The observed increase has been found to be dependent on factors such as the antenna radiation pattern in buildings close to the transmitter with line of sight, and the local urban clutter. The relationship between the floor height and extra gain with respect to the ground floor level is not linear, however the floor height gain is often represented as a linear relationship governed by a single factor. In this experiment, this factor has been found to be approximately 2dB/floor.

Statistically, the small-scale variations noticed in the received signal strength can be modeled as having a Rayleigh distributed probability function. This has been demonstrated in several other studies and has been confirmed here. In other studies, the large-scale fluctuations have been often modeled as having a lognormal distribution, in this project this has been shown to be the case when considering the lower floors. Significant differences have been observed at higher floors between areas directly facing the transmitter and areas not facing the transmitter.

The larger variability in the indoor average received signal strength compared to the outdoor average signal strength causes larger errors when predicting the path losses. For cells with radii of 1km or more a simple and a coarser type of modeling is enough to predict the coverage. In general, a model containing a distance-power law, lognormal large-scale fluctuations and superimposed Rayleigh distributed small-scale fluctuations is used for urban areas. This approach can also be used in the case of into building propagation. We used the model of Hata as a starting point and showed that it is possible to calculate path losses with RMS errors of 5 dB for the ground or first floor and up to approximately 8 dB for higher floors. The model presented by COST included extra information on the losses due to indoor radio wave propagation such as transmission through internal walls, to calculate the signal strength. This was not possible with the Hata model, consequently it was possible to further decrease the error; in our analysis the COST model calculated the path loss in line of sight rooms with a root mean square error of 5.7 dB.

In the second experiment, an existing uniform circular array antenna for outdoor measurements was adapted in order to measure the impulse response of the channel and angles of arrival of the radio wave components in a microcell type of scenario. The choice of an array with smaller radius resulted in still a reasonable indication of the true angles of arrival despite a decrease in resolution. We have seen that propagation through building walls can be the main propagation mechanism, even through multiple building walls. Furthermore, the adaptation provided the information for comparison with the unmodified antenna array in an indoor situation. The ray tracing model uFipre was used for simulations; it showed capable of correctly calculating received signal strengths and the time dispersion of the channel.

With the further increase in mobile communication, the need for more capacity will have to be satisfied with implementation of smaller cell configurations. When moving from small cells to microcells, the modeling of radio wave propagation moves from calculations with simple, empirical-statistical models to more complex deterministic models. In any case the main problem in the prediction of into building coverage in small cells will be the acquisition of enough measurement data for empirical-statistical modeling. In microcells on the other hand both indoor measurements and further improvement of deterministic models and advanced tools like angle of arrival measurement systems will be of great importance.

Acknowledgements

I would like to express my sincere gratitude to prof.dr.ir. G. Brussaard, dr.ir. A. Mawira and dr.ir. M. Herben. Thank you for the good coaching and reviewing of my report.

I would also like to thank ir. Y. de Jong, ir. J. Schmidt, ir. N. Scully, ir. M. Koelen and mr. L. Wijdemans, for their useful advises and contributions in the taking of measurements and analyses.

Ewart

Contents

List of Figures

Chapter 1 Introduction

In personal wireless communication systems a great deal of the radio coverage inside buildings is still being provided with the use of Base Stations (BS) located outside the buildings. The Mobile Station (MS) of a user inside a building will receive radio waves affected by both the outdoor as well as the indoor environment. In addition to the properties of the outdoor radio channel, the MS will experience extra attenuation and the effects of indoor multipath propagation. This will deteriorate the signal to noise ratio (SNR) even more and may limit the maximum achievable data rate due to delayed radio arrivals.

This project deals with the propagation of radio waves into buildings in an urban area for frequencies around 1800 MHz. The first objective of our research is to get a good understanding of the fundamental propagation mechanisms involved in radio wave propagation from outside into buildings and vice versa. The second objective of this project is to produce a simplified empirical-statistical model for the prediction of signal strengths involving the penetration of radio waves into buildings.

In order to achieve these objectives two experiments were carried out to obtain sufficient data to characterize radio wave propagation into buildings. The first experiment was carried out in a DCS 1800 system cell and the main purpose was to determine the characteristics concerning cell coverage. Signal strength measurements were carried out around and inside buildings in The Hague to study the building penetration loss and at different floor levels to measure the height dependence. The second experiment consisted of a wideband measurement to determine the time delay characteristics and to visualize the arrival of radio waves into a room (the angles of arrival). The data were collected on the downlink with the BS as the transmitter and the MS as the receiver.

First the basic theory concerning radio wave propagation and penetration into buildings will be explained, and then a description of the first experiment will follow. In chapter four the results of this experiment will be presented and discussed. In chapter five the propagation model will be treated. The second experiment and its results will be presented in chapter six. Finally, chapter seven contains the conclusions of this study.

This project was carried out at KPN Research within the framework of projects for planning of the cellular DCS 1800 and UMTS systems.

Chapter 2 The multipath radio channel

2.1 Propagation mechanisms

In personal wireless communications, the radio channel can be described as a multipath propagation channel where the system user can be standing still or moving. At both the BS and the MS, the received signal will be a combination of multiple radio waves arriving from different directions and with different magnitudes and phases. The propagation of radio waves is generally described with three basic mechanisms; these are reflection, diffraction and scattering [1].

Electromagnetic waves arriving from a certain direction at a surface with large dimensions compared to the wavelength are (partially) reflected by this surface. The intensity of the reflected wave depends on the radio wave frequency, the type of material, the polarization of the wave and the angle of incidence. Diffraction can be explained as an apparent *bending of radio waves* around obstacles. Reflection and diffraction can be modeled using the Geometrical Optics (GO) and Uniform Theory of Diffraction (UTD) [2]. Scattering is the dispersion of radio waves due to contact with objects with irregular structures or surfaces (vegetation, furniture); the size of these irregularities is in the order of the wavelength of the propagating waves.

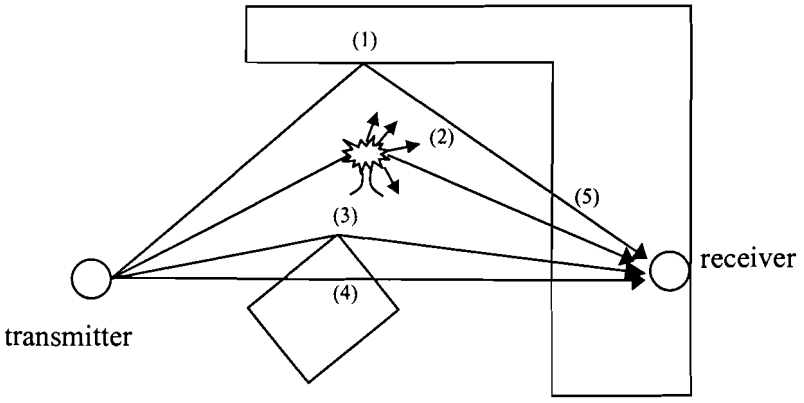

Figure 2.1 Representation of the propagation mechanisms (1)reflection,(2)scattering, (3)diffraction, (4)transmission and (5)penetration into a building

Besides reflection, diffraction and scattering there are other important mechanisms involved in radio wave propagation. Transmission through buildings can play an important role in built-up areas. Transmission occurs in combination with reflection and absorption of the radio waves by the obstructing material. Since in our case the receiver is located inside a building we look at this mechanism as a transmission through the outer walls, thus as a penetration into the building rather than a transmission through the building.

Where necessary the propagation mechanisms will be clarified and applied to explain certain measurement results. In section 2.4, the building penetration will be discussed.

2.2 Propagation characterization

A radio wave travelling through a certain environment will deteriorate in strength due to the above-mentioned mechanisms and free space loss. These effects can be characterized as large-

scale path losses and small scale fading. The concepts large- and small-scale refer to the dimensions of the area studied. Large-scale effects are noticed over longer distances while small-scale effects are noticed over smaller distances.

In the characterization of the mobile radio channel (vehicular communication) the radio wave propagation is modeled by describing the received signal power with the product A(d)B(x,y)C(x,y). The factors A and B describe the large-scale fluctuations, these are the variations in received signal strength when travelling over large distances ($d>>\lambda$). The factor C represents the fast fluctuations called small-scale or fast fading caused by multipath propagation. Figure 2.2 shows the positioning of the receiver relative to the transmitter.

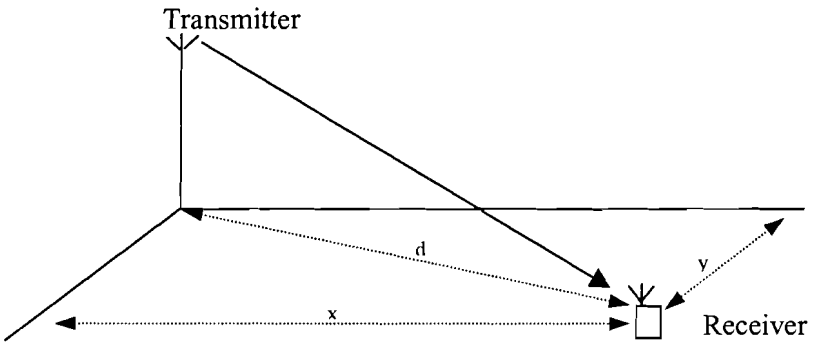

Figure 2.2 Positioning of the receiver in the field

2.2.1 Propagation factor A(d)

The factor A(d) consists of two parts, the free space propagation and a two-ray model. It describes the received signal in a line of sight (LOS) situation with the receiver situated on plane earth at a large distance d compared to the transmitter and receiver heights (h_t and h_r).

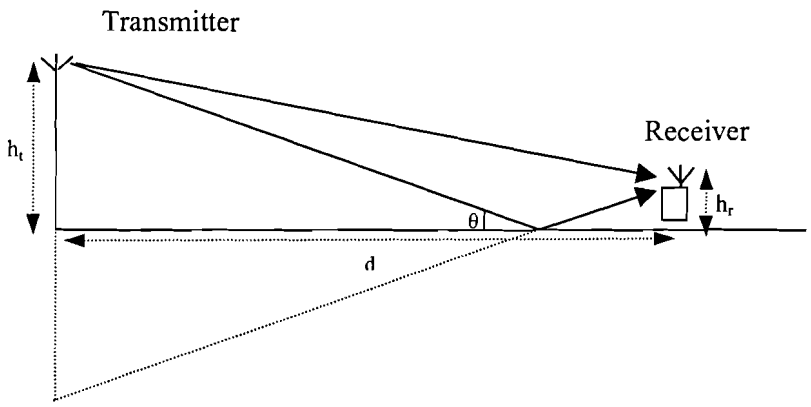

Figure 2.3 Two ray model, combined reception of a direct radio wave and a component reflected by the earth

Given a known transmitted power P_t, the antenna gains relative to an isotropic radiator G_t and G_r, and the distance d between the transmitter and receiver positions, the free space propagation model returns the received signal strength in a LOS case.

$$P_r(d) = P_t G_t G_r \left(\frac{\lambda}{4\pi d}\right)^2 \qquad \textit{Equation 2.1}$$

The two-ray model adds to the free space model the effect of nearby (earth) reflection (figure 2.3). If we assume that only a direct and a reflected radio wave arrive at the receiver and a distance between transmitter and receiver that is (very) large compared to the transmit and receive antenna heights, then the radio equation becomes [3]:

$$P_r(d) = P_t G_t G_r \left(\frac{h_t h_r}{d^2} \right)^2 \qquad d >> h_t \text{ and } d >> h_r \qquad \textit{Equation 2.2}$$

where h_t is the height of the transmit antenna and h_r is the height of the receive antenna.

In formula 2.2, we see a d^{-4} dependence of the received signal power. This means that each doubling of the distance d leads to a decrease of the received signal power of 12 dB. The formula also shows a 6 dB increase in received signal power with each doubling of the transmitter or receiver antenna height.

The above-mentioned dependencies may differ significantly in practice, even in LOS situations the position of the receiver is often close to multiple reflectors and scatterers causing multipath propagation and thus changing the dependencies. In practice, the received signal power is modeled for large areas with the use of empirical models (§2.3).

2.2.2 Propagation factor B(x,y)

The factor B(x,y) is a stochastic variable representing the effect of the buildings and other large objects on the received signal. The surrounding environmental clutter is different for different locations. This factor is typically a lognormally distributed variable [3].

2.2.3 Propagation factor C(x,y)

The factor C(x,y) is also a stochastic variable, it represents the fast fading that occurs due to multiple radio waves arriving simultaneously at the receiver from different angles and with different properties. In our case the effects are:

1. Rapid changes (fades and enhancements) in signal strength over small distances (in the order of wavelengths) or time intervals.
2. Time dispersion (echoes) caused by multipath propagation delays.

The behavior of the factor C can be described statistically by the probability density function of the received signal envelope and its variance. Typically, in the absence of a dominant (strong) component the signal envelope is comprised of a number of waves with similar strength and follows a Rayleigh distribution [4]. The probability density function for the Rayleigh process is

$$p(r) = \frac{r}{\sigma^2} * e^{\left(\frac{-r^2}{2\sigma^2}\right)} \qquad \textit{Equation 2.3}$$

where r is the signal amplitude and σ is related to the mean amplitude r_{mean}.

$$\sigma = \sqrt{\frac{\pi}{2} r_{mean}} \qquad \textit{Equation 2.4}$$

The signal phase is assumed to be uniformly distributed over $[0,2\pi]$. In cases where there is a line of sight (i.e. a dominant stationary signal component) between transmitter and receiver the small scale signal envelope distribution is Ricean [5].

2.3 Empirical path loss models

The accurate modeling of the reception of radio waves penetrating into buildings can be a difficult task. The radio channel is a multipath channel in which multiple radio waves arrive from different angles and with different amplitudes, phases and polarization. The complexity of the urban and indoor environment creates an undeterministic situation. In the outdoor environment neighboring buildings, vegetation and moving objects such as cars will have an effect on the radio waves. In the indoor environment, the radio waves will be affected by a large number of close range obstructing, reflecting and scattering objects from different sizes, shapes and materials. Also the problem becomes a 3-D one, the receiver could not only be at a certain distance (x,y position) from the transmitter, but also the height z becomes an important variable (receiver could be at higher floor levels in a building). Fortunately, the Doppler effects noticed in vehicular communications can be neglected in the case of indoor reception by assuming that the user communicates is in a (quasi) static position and surrounded by quasi static scatterers.

For the planning of radio cells with a radius of approximately 1 km with relatively high base stations (small cells) the received signal power is predicted with the use of empirical-statistical models. Empirical-statistical models are chosen above their deterministic counterparts because of their simplicity and adequacy to accurately calculate the average received signal power for grid areas as small as 50x50m. The effects of fast fading (factor C presented in §2.2.3) are normally excluded from these models and if necessary have to be taken into account separately.

The models calculate the so called *basic transmission loss* L_b, which is commonly used to characterize the large-scale propagation [6]. Here L_b is defined as:

$$L_b = P_t - P_r - L_t - L_r + G_t + G_r \qquad \text{[dB]} \qquad \textit{Equation 2.5}$$

where L_t and L_r are losses in the transmitting and receiving antennas circuits respectively. In this definition the effects of the antenna gains have been factored out, therefore it represents the path loss between isotropic antennas.

In general, most empirical path loss models have the following form.

$$L_b = u + v\log(d) + \sum_i w_i \qquad \text{[dB]} \qquad \textit{Equation 2.6}$$

Where u and v are only dependent on general configuration parameters such as the transmitter height, the receiver height and the frequency. The factors w_i represent various effects connected to the environment and other small effects. One of the simplest models of this form can be deduced from equation 2.2, here it is rewritten as a path loss equation when transmitting with isotropic antennas.

$$L_{b\_tworay} = 40\log(d) - 20\log(h_t) - 20\log(h_r) \qquad \text{[dB]} \qquad \textit{Equation 2.7}$$

This theoretical model is only valid for line of sight cases with a large d compared to the transmitter and receiver heights. These conditions are normally not met in urban areas, therefore this model is simply not applicable.

Rappaport also presents a simple model of this form [1]. Here the outdoor large-scale fluctuations are modeled with the log-distance path loss model:

$$L_{b\_Rappaport} = L_0(d_0) + 10n\log(\frac{d}{d_0}) + \chi_\sigma \qquad \text{[dB]} \qquad \textit{Equation 2.8}$$

The average path loss at a distance d from the transmitter is calculated. The factor $L_0(d_0)$ is the path loss at a reference distance d_0 (e.g. 10m or 1 km). The exponent n (also called the *rate of decay*) can take different values in different environments. In a free space environment n=2, for the two-ray model n=4 and in an urban environment n could be from 2.5 up to 5. Finally the factor X_σ represents the factor B in section 2.2.2, it is the Gaussian distributed random variable in dB with μ=0 and a certain standard deviation σ.

When modeling the path loss through areas with different building densities or through media with different electromagnetic properties (e.g. from freespace into a building), the propagation path is often divided in parts (see figure 2.4). The path loss model is then comprised of components with different exponents to account for each part [7]. Here it is given in exponential form,

$$L_{b\_areas} = (\frac{4\pi d_1}{\lambda})^{n_1}(\frac{d_2}{d_1})^{n_2}(\frac{d_3}{d_2})^{n_3}\cdots(\frac{d_i}{d_{i-1}})^{n_i} \qquad \textit{Equation 2.9}$$

with $d_{i-1} \le d \le d_i$

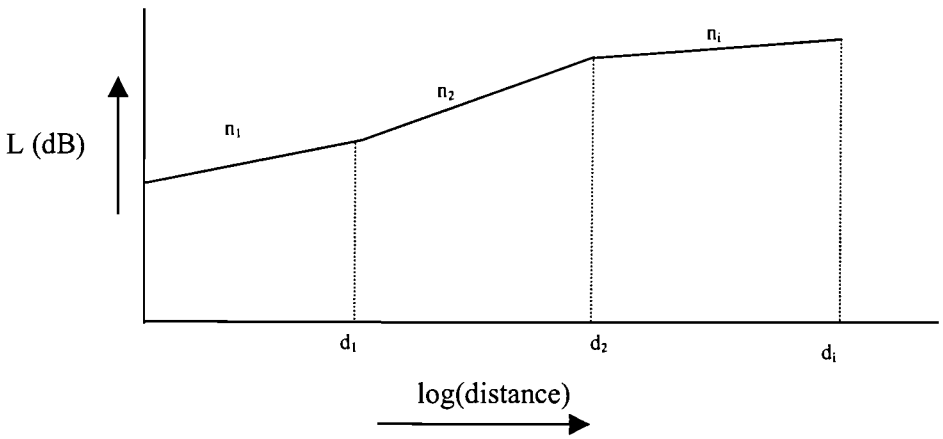

Figure 2.4 Propagation over i different areas

The problem with this model is that it is not reciprocal.
Different models were proposed for the estimation of the building penetration loss, these models include building properties such as floor area, number of walls, number of rooms and also local transmission conditions such as the angle of illumination. The case of transmission through a building is a similar to the above-mentioned situation. An alternative for the model in equation 2.9 for the case of building transmission in microcells was proposed by Koelen [8]. It replaces the exponents with a constant decay rate (-2) and uses a specific building loss instead. The loss relative to free-space loss for a single radio wave component travelling through a building is given by

$$L_{b\_Koelen} = \alpha d_{in} - 40\log|T_s(\theta)| \quad [\text{dB}] \qquad \textit{Equation 2.10}$$

where α indicates a specific building loss in dB per meter, d_{in} is the distance propagated in the building and T_s is the soft transmission coefficient which is a function of the angle of illumination θ.

The European organization COST also recently presented a model including a specific building loss and transmission losses in the COST 231 project [9]. This model is applicable for path loss calculations in the case of outdoor-indoor transmission. The model has two variants, one for line of sight (LOS) and one for non line of sight (NLOS)

$$L_{b\_COST\_LOS} = 32.4 + 20\log(f) + 20\log(S+d) + W_e + WG_e \cdot (1-\frac{D}{S})^2 + \max(\Gamma_1, \Gamma_2) \quad [\text{dB}]$$

Equation 2.11

$$L_{b\_COST\_NLOS} = L_{outside} + W_e + W_{ge} + \max(\Gamma_1, \Gamma_3) - G_{FH} \quad [\text{dB}] \qquad \textit{Equation 2.12}$$

where

$$\Gamma_1 = W_i \cdot p$$

$$\Gamma_2 = \alpha \cdot (d-2) \cdot (1-\frac{D}{S})^2$$

$$\Gamma_3 = \alpha \cdot d$$

and

$$G_{FH} = \begin{cases} n \cdot G_n \\ h \cdot G_h \end{cases}$$

The variables in these equations are illustrated in figure 2.5

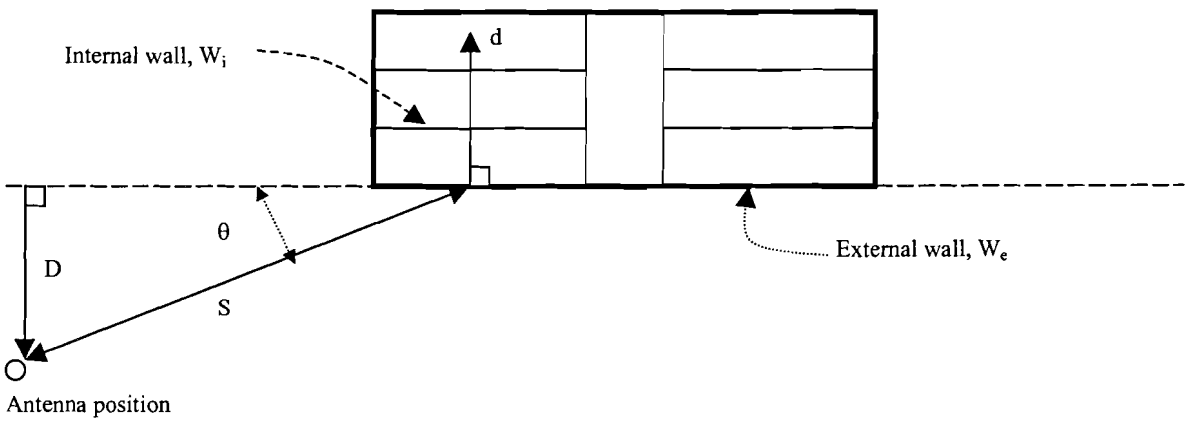

Figure 2.5 Topview of the illumination of a building with the definition of the incident angle θ and distances D, S and d. The distance d is a path through internal walls.

The frequency is given in GHz, W_e is the loss in the externally illuminated wall at an angle $\theta=90^0$, WG_e is the additional loss in the external wall when $\theta=0^0$, W_{ge} is an additional variable loss. W_i is the loss in the internal walls and p is the number of penetrated walls. The factor α is the transmission loss inside the building given in dB/m, G_n is a floor height gain in dB/floor (n is the number of floors) and G_h is the height gain in dB/m (h is the height in meters).

In the LOS model the entire path loss from outdoor transmitter to indoor receiver is calculated using information about the condition of illumination (θ), external building properties and also internal building properties. In the NLOS model the total path loss is calculated as a summation of the already known outdoor path loss and the additional building penetration loss (including both external and internal properties). Here the case of outdoor transmission with indoor reception is approached by combining a good outdoor model with factors that account for the building loss.

A well known empirical model used for the outdoor prediction of path loss is the model of Hata [10].The Hata model was derived from the graphical path loss data provided by Okumura [11]. It gives the median path loss as a function of the transmit frequency, the receiver and transmitter heights and the distance between transmitter and receiver.

$$L_{b\_Hata} = 69.55 + 26.16\log(f) - 13.82\log(h_t) - a(h_r) + (44.9 - 6.55\log(h_t))\log(d) \text{ [dB]}$$

Equation 2.13

Where

$150 \le f \le 1500$ [MHz]
$30 \le h_t \le 200$ [m]
$1 \le d \le 20$ [km]

$a(h_r)$ is a correction factor for mobile antenna height and is for a small or medium sized city:

$$a(h_r) = (1.1\log(f) - 0.7)h_r - (1.56\log(f) - 0.8) \quad \text{[dB]}$$

Equation 2.14

where $1 \le h_r \le 10\text{m}$.

Despite of the restrictions given for this model, it has been extensively used with success. However, the model has been developed with data gathered in Japanese cities. Therefore often some modifications are done prior to the application of the model, an example is the extension to 2 GHz developed by COST for European cities

$$L_{b\_COST} = 46.3 + 33.9\log(f) - 13.82\log(h_t) - a(h_r) + (44.9 - 6.55\log(h_t))\log(d) + C_m$$

Equation 2.15

Where $a(h_r)$ is defined in equation 2.14 and Cm is 0 dB for medium sized cities and 3 dB for metropolitan centers. The ranges of parameters are:

$1500 \le f \le 2000$ [MHz]
$30 \le h_t \le 200$ [m]
$1 \le h_r \le 10$ [m]
$1 \le d \le 20$ [km]

2.4 Building penetration loss

The definition of building (penetration) loss originally formulated by Rice [12] is the difference between the median field intensity in the *streets* and the field intensity at a location on the main floor of a building. This is the building loss at a location on the 1st floor of a building for a given distance from the transmitter. The 1st floor was chosen because it has been found the most difficult portion of a building to cover. Note that the 1st floor in the Rice paper is equivalent to the ground floor in Europe. The median field intensity in the streets was determined at a receiver height of 1.8 m.

The *local* building loss of a building is defined by Rice as the difference between the median field intensity in the *streets adjacent* to the individual building and the field intensity at a location on the 1st floor of the building. The building loss is a concept concerning the overall coverage in a certain cell while the local building loss is a concept concerning the coverage of an individual building. The local building losses of a series of buildings can be combined to calculate the *over-all* building loss.

It is also possible to categorize penetration loss; the four categories would be wall loss, room loss, floor loss and building loss [9].
The *wall (penetration) loss* is the specific loss when a radio wave is transmitted through a wall. It is basically a local concept that applies specifically to a single wall (or portion of it) with certain material properties and a certain mode of illumination (LOS or NLOS). The loss caused by the wall of a building is difficult to measure due to the almost inevitable reflections inside a room.

The *room loss* is the median loss in a single room, it is comprised of the wall penetration loss(es) and other losses due to the interior environment. The room loss is determined by taking the median of all measured values within the room. The *floor loss* is calculated by taking the median of all room losses on the same floor. Between the different floors, a difference in loss can be noticed which can be denoted as a *floor height* factor. The *building loss* is the median floor loss taken over all the floors of a building.

We can see that here the characterization of penetration losses is done by first separately determining the median loss in the rooms of a building and then combining these values to provide a floor loss and subsequently a building loss.

In the above-mentioned definitions the median is used as statistical parameter, this is done because the median (which is the 50% marking value) is independent of the type of statistical distribution of the measured values. In this project we will simply use the mean value (the average), in practice the median and the mean lie closely together.

2.4.1 The definition

In this project the *building penetration loss* is defined as *the difference between the average signal strength in the local area around the building situated at a certain distance from the transmitter and the average signal strength on the ground floor of that building*. For convenience, it is also simply called the *building loss*. The *ground* floor is equivalent to the American *first* floor used by Rice in his definition.

The *room loss* is defined as the difference between the average signal strength in the outdoor area adjacent to a room located on the ground floor of a building and the average signal strength in that room. The building loss is calculated by averaging over all the room losses on the ground floor. The produced loss factor can be used as an addition to the predicted signal loss for the surrounding local area. The loss for the higher floors is related to the calculated building penetration loss through a certain floor height factor.

The above-mentioned building penetration loss is useful when predicting the coverage over a relatively large area, e.g. 100x100m. However, in reality there is a difference in propagation modes for different parts of a building, for instance one or two sides could be in the Line Of Sight (LOS) of a transmitter while the other sides are not (NLOS). There could even be a difference when all the sides of a building are in a NLOS situation but with one (or two) sides having an orientation towards the transmitter (OTT) while the other sides do not have this orientation (NOTT), see figure 2.6.

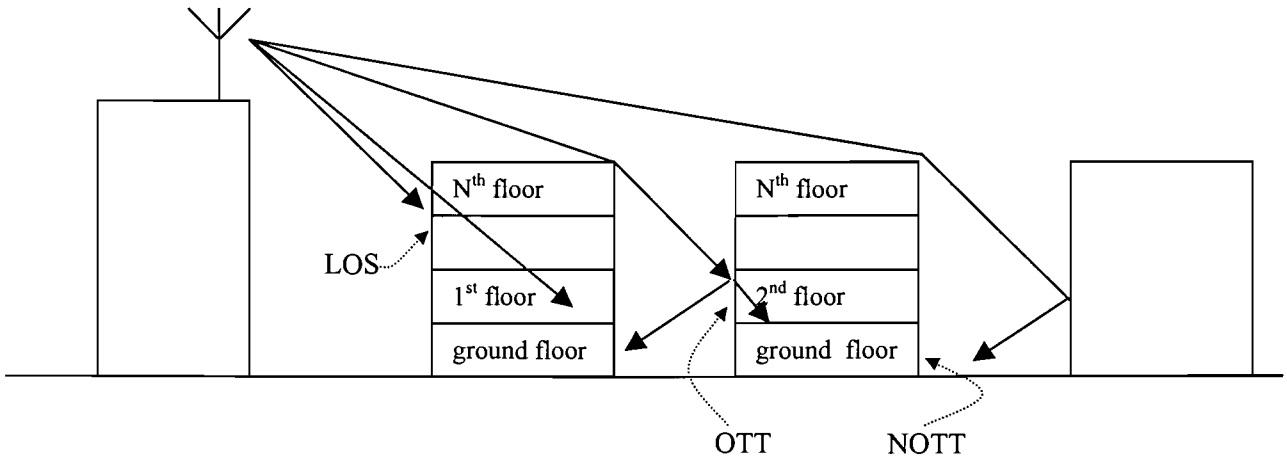

Figure 2.6 Propagation modes LOS and NLOS classified in situations where a building part or room is oriented towards the transmitter (OTT) or not (NOTT).

For this reason a *local area loss* is defined, this figure represents the difference between the average signal strength in the outdoor area adjacent to a building and the average signal strength on the ground floor at the particular side of that building. In figure 2.7 the local and room areas in a building are illustrated.

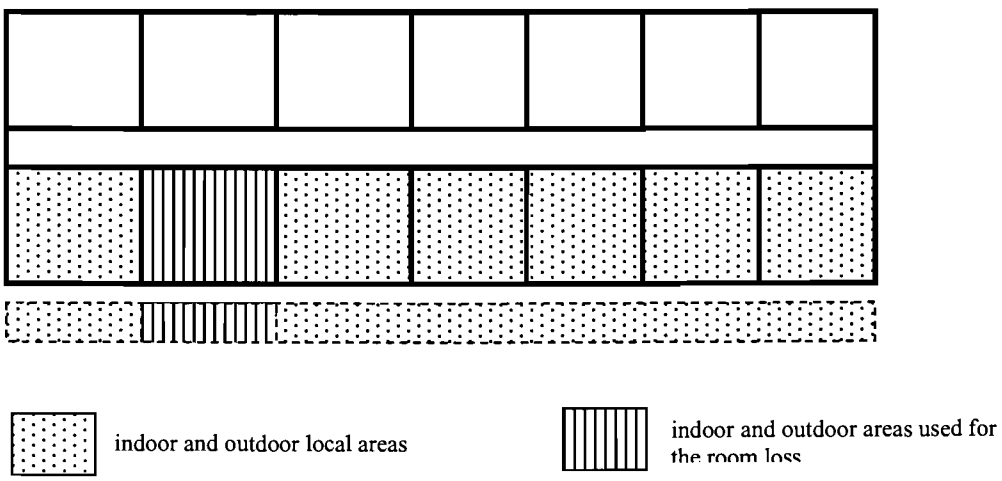

Figure 2.7 Topview of indoor and outdoor local and room areas

In this project the terms LOS and NLOS are used as follows. A floor of a building with a direct path between one of its sides and the transmitter is called a *LOS floor*, if there is no direct path between one of its sides and the transmitter it is a *NLOS floor*. When there is a direct path

between the transmitter and the external wall of a certain part of a floor (i.e. a local area) or a room on a floor, this is called a *LOS area* or *LOS room*. On the other hand when there is no direct path between the transmitter and external wall of an area or room, the area or room is called a *NLOS area* or *NLOS room*. Notice that in this definition it is possible to have a NLOS area or room on a LOS floor! Finally, if the floor is a NLOS floor (i.e. no side is directly illuminated), then all areas and rooms on that floor are in NLOS and can optionally be distinguished with the OTT and NOTT terms. This is illustrated in figure 2.8.

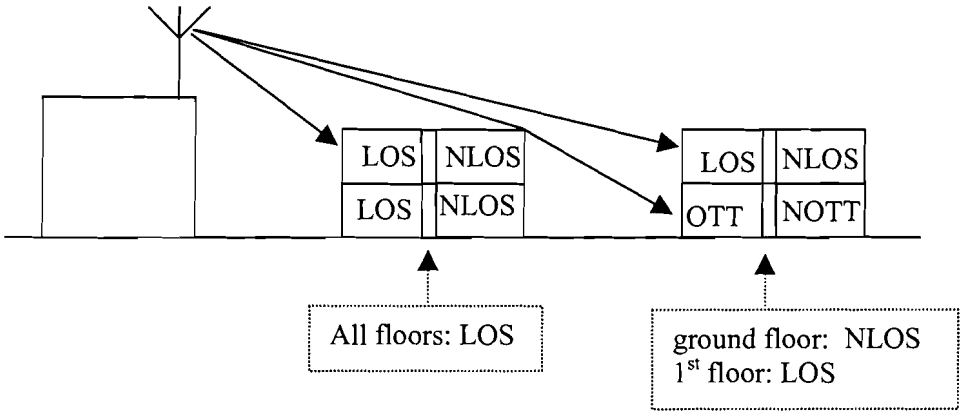

Figure 2.8 LOS and NLOS floors and areas/rooms

Chapter 3 The TEMS experiment

3.1 Intro

In this experiment, measurements were taken in four office buildings in an urban area covered by a DCS 1800 cell. The cell can be considered a small cell with the transmitter located above rooftop and a cell radius of approximately 1 km. The main objective of this experiment was to obtain statistical data of the signal strength outside and inside the buildings in order to be able to draw conclusions about the building penetration loss. The measurements were carried out with the Ericsson TEMS measurement system.

To be able to model the path loss the dependence of the signal strength on a number of parameters was also analyzed. These parameters are the distance between transmitter and receiver, the receiver height (i.e. the floor height) and the angle of penetration of the buildings in line of sight situations. The data consists of the parameter RxLev which represents the received signal strength level and the above-mentioned parameters gathered from maps and databases. The RxLev was measured only on the downlink.

3.2 Relevant properties of the DCS 1800 system

DCS 1800 system is the counterpart of GSM900 operating around 1800 MHz. In this section, only the properties of DCS1800 that are relevant to this experiment will be treated. The specifications are taken from the 05 series of the GSM Technical Specification phase 2+ .

3.2.1 Transmission and reception

The DCS system operates in the following band:
Lower band (mobile transmit, base receive): 1710 – 1785 MHz.
Upper band (base transmit, mobile receive): 1805-1880 MHz.

The channel spacing is 200 kHz and there is a total number of 374 duplex channels.
The maximum sensitivity is approximately –100 dBm for DCS 1800 handhelds.

3.2.2 Radio link measurements

In the GSM system radio link measurements are used in the handover and RF power control processes. These measurements are reported as the RxLev, this parameter is the average of the received signal level measurement samples in dBm*. These samples are taken within one SACCH (Slow Associated Control Channel) multiframe of approximately 480 milliseconds. All other measurements taken during previous periods are discarded. Each SACCH consists of 104 TDMA frames, for every TDMA frame one measurement is made with the option of omitting up to 4 frames. Thus in total approximately 100 samples are taken within one SACCH multiframe. From these samples the RxLev is determined by averaging and reported every 480 milliseconds. This means that the signal strength is not measured in the same way as in a continuous wave (CW) measurement.

* The reference level is one milliwatt, the abbreviation dBm stands for dB with respect to 1 mW. The power dissipated by a signal of 1 μV in a 50 Ω resistor is $2*10^{-11}$mW which corresponds with –107 dBm.

3.3 Measurement equipment TEMS Light

TEMS Light is a GSM measurement system developed by Ericsson. It consists of a MS and a portable computer. The system can measure and record all important parameters transmitted by all BS located in the vicinity of the MS.

TEMS has two measurement modes for the type of measurements that were performed, the idle mode and the dedicated mode. In the idle mode no call is established and the measurements are taken at a rate of 0.5 samples per second. In the dedicated mode a call is established and the measurement rate is 2 samples per second. The dedicated mode was chosen because this is the fastest mode. The measurement speed had to be at maximum to be able to cover the large areas within the permitted measurement time and available battery time.

The measurement range of the received signal strength is from 0 dBm down to –110 dBm, which is taken as the noise floor. The accuracy of the measured RxLev is ± 1 dB.
The RxLev is given in this report as the measured signal strength level in dBm added with a constant.

$$\text{RxLev} = \text{Measured signal strength (dBm)} + 110$$

With TEMS the number and position of the samples are determined in time and not in traveled distance as would be the case with the well known method of a measurement-cart with special wheel. Therefore it is the job of the person taking the measurements to locate the sample positions correctly on the map on the portable computer and to take enough samples.

3.4 Measurement method

The measurements were done by a single person walking in the office rooms and carrying the MS and a portable computer for data acquisition. The TEMS equipment was carried across the body with the MS positioned just above the shoulder (see figure 3.1). The approximate height is 1.5 m and this method roughly resembles the use of mobile phones when the person is standing in a room.

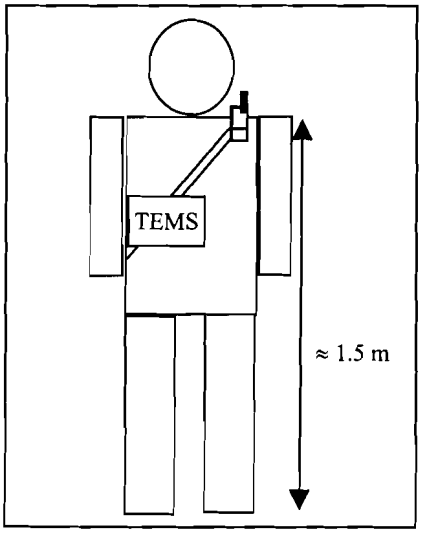

Figure 3.1 Positioning of the measurement equipment on the person taking the measurements

3.4.1 Sampling

Measurements with TEMS are time based, approximately every half a second an RxLev value averaged over one hundred samples is reported. This means that the sampling of a room will depend on the walking speed and route traveled in that room during the measurement. Concerning the traveled route in a room it must be said that the entire area of the room could not be covered because of the furniture. Furthermore the walking speed is not constant, therefore the measurements taken in one room are not a symmetrical representation of the received signal.

The walking speed depends on the total time available to cover all the areas within a building, this is limited by the available battery time and access time to the building. The speed was approximately 15cm/second, this would give about two samples every 15 cm (two samples per wavelength). In every room the total measurement time was about one minute, giving approximately 120 RxLev samples per room.

The number of samples taken outdoor is listed in figure 3.2.

Building	No. of samples	Samples/m
SK	952	7.8
PB	620	8.4
AB	2210	11
WA	1422	12.2

Figure 3.2 Number of samples taken in the outdoor measurements

As mentioned earlier TEMS reports the RxLev with a maximum error of 1 dB, this can be calculated as follows. The standard deviation σ of a Rayleigh process is 5.57 dB [4] and the number of independent samples n taken for every reported RxLev is 100. If we take the confidence level at 95%, then the confidence interval k is calculated with [13],

$$k = \frac{c\sigma}{\sqrt{n}} \qquad \text{Equation 3.1}$$

and is equal to 1 dB (k=1). Here the parameter c=1.960 for 95% confidence.
This means that the true RxLev μ for the measured portion of an area lies within 1 dB of the measured RxLev $\overline{x}$ $\left(\mu = \overline{x} \pm 1dB\right)$.

When taking 120 samples per room, i.e. 120 RxLev reports of which each one is already averaged over 100 samples, we obtain an accurate estimation of the average signal strength for the area covered in a room. It should be noted however, that the reported RxLev also depends on the calibration accuracy of the receiver. For this experiment we assumed that the TEMS receiver is accurately calibrated, however the true calibration accuracy is not known.

3.5 The transmitter

The transmitter is that of a KPN DCS 1800 BS located on top of the MBP building in The Hague. A total of 3 antennas radiate into three different directions (3 sectors). One antenna radiated the area in which the buildings SK, PB and AB are located while another antenna radiated the area were the WA building is located (see figure 3.4). The transmitter and antennas of the base station had the following specifications:
Transmit power: $P_t = 41$ dBm
Antenna gain: $G_t = 18$ dBi
Cable Losses: $L_c = 8$ dB
Effective Radiated Isotropic Power: EIRP = 51 dBm
Antenna height: $H_t = 40$ m
Polarization: either +45° or –45°, one channel is transmitted in one polarization direction.
Antenna radiation patterns:

Horizontal 3dB beamwidth = 65°
Vertical 3dB beamwidth = 7°
Electrical downtilt: 6°
No physical downtilt

Frequencies:

For the buildings SK, PB and AB: ARFCN = 832; f = 1869 MHz (upper band)
For the building WA: ARFCN = 562; f = 1815 MHz (upper band)

3.5.1 Site descriptions

The measurements were carried out in 4 KPN buildings illuminated by the transmitter from the top of a fifth KPN building in The Hague (see figure 3.4).

KPN buildings and their locations:
MBP→ the transmitter location, W. Van Pruisenweg 52
SK→ Schenkkade 100
PB→ Prinses Beatrixlaan 10
AB→ Prinses Beatrixlaan 9
WA→ Binckhorstlaan 36

In the Appendix a layout for every measured floor of the buildings is plotted, in figure 3.3 the building information is given.

Building	Height (m)	Number of floors	Floor area (m^2)	Position	Internal description
SK	14 & 27	7	1600	LOS with some vegetation in front of the rooms oriented towards the transmitter.	On floors 1& 3 mainly open offices with partitions. On floors 5 & 7 mainly normal closed offices rooms
PB	41	12	3000 (measured area:300)	NLOS at street level with direct path to Tx being obstructed by SK. LOS at higher floor levels	The measured room is a large room on the entire front side, at some floors (7&8) divided by partitions
AB	27	7	1300	NLOS at street level. Two obstructing buildings with heights around 26 and 16m. LOS on floors 4 &7	Mainly normal office rooms
WA	-	2	3100	LOS with vegetation in front of the rooms at the front area (see appendix). NLOS for the rest of the building. There is a tall building obstructing to the right of the direct path (see figure 3.4)	Mainly normal office rooms and some rooms containing equipment.

Figure 3.3 Building information

The exact types of building material are not known, but the office buildings SK, PB and AB are believed to be made of reinforced concrete and normal (not coated) glass, while building WA is made of brick and normal glass.

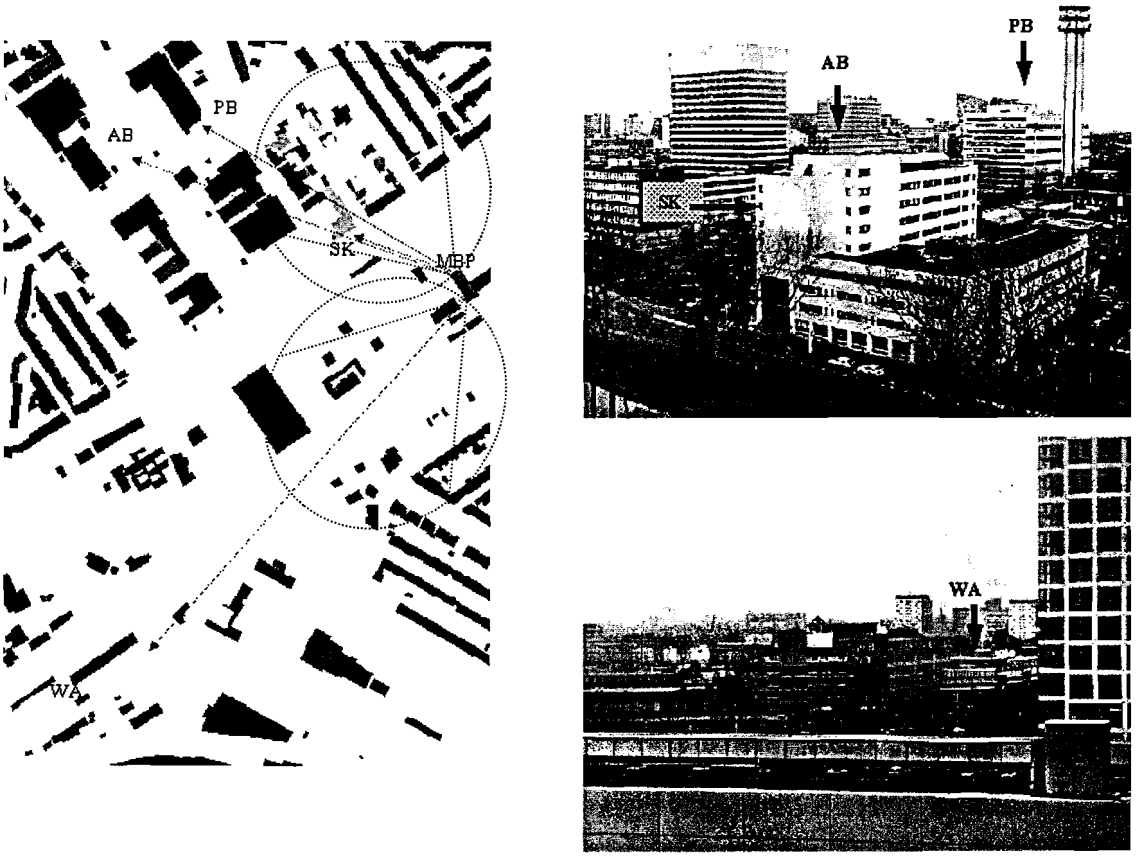

Figure 3.4 Left a map of the site in The Hague, to the right panoramic views of the measured buildings seen from the MBP building where the BS is located

Chapter 4 Experimental Results

4.1 Intro

In all the measured buildings with the exception of building WA it was not possible to get substantial data at ground level. The reason is that the ground floor is often used for other purposes such as the reception desk and storage places, even in cases when there were office rooms at ground level it was often impossible to access them because of security measures. Therefore the measurements began at the first floor in the three other buildings. This will be taken into account when drawing conclusions for the penetration loss.

First the results will be discussed per building, in the buildings SK, AB and WA the floors were divided into areas with different conditions of illumination and orientation towards the transmitter (LOS, OTT, NOTT), see figure 2.6. The idea is to illustrate the differences and explain the observations. Important are the statistical properties of the received RxLev in the different sections of the buildings. In the area plots (see figure 4.2) and appendix the areas are indicated per building with the names *left*, *right* and *front*. The indoor areas (e.g. *left in*) cover the rooms with an outer wall adjacent to the corresponding outdoor area (e.g. *left out*). To generate the cumulative distribution functions all the samples taken in an area are used and not the averages per room. Then in section 4.5 the overall results will be treated, the results of building PB will be treated in this section.

4.2 Results of building SK

The cumulative probability distribution of all measured RxLev around the building SK and indoor for all the measured floors, is plotted in figure 4.1.

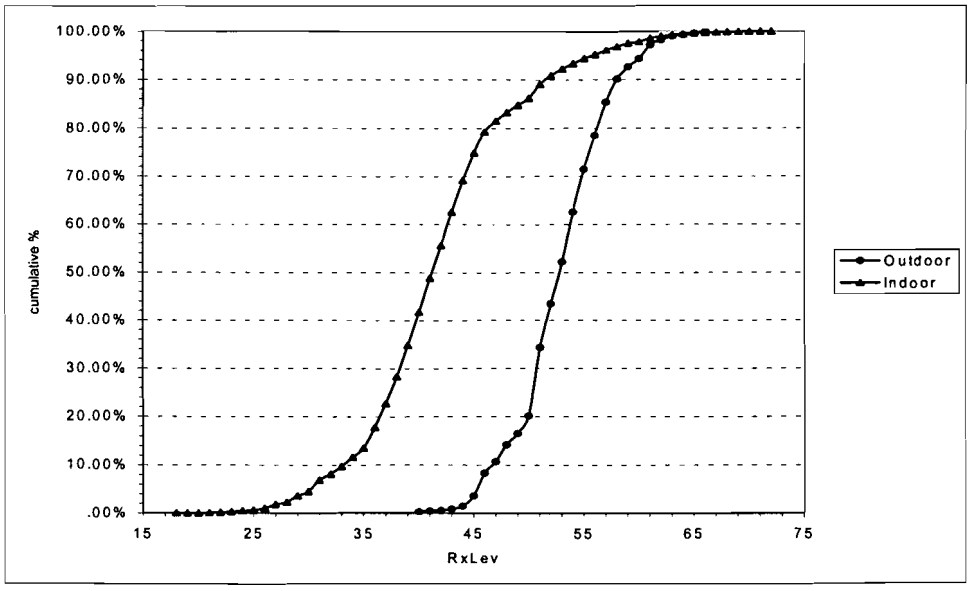

Figure 4.1 Cumulative distribution function (CDF) of Total building SK

The first aspect noticed when comparing the received signal strength level in a building with the level outdoor in the vicinity of the building is the extra attenuation and spreading introduced by the building structure and interior. The mean RxLev outdoor and indoor are 53.2 dB and 42.2 dB respectively, this gives a loss of 11 dB. The standard deviation outdoor is 4.3 dB and indoor it is 7.3 dB.

4.2.1 The first floor

In figure 4.2 a sketch of the building SK is plotted with the average RxLev around and in the building at the first floor. The arrow indicates the direction of the transmitter. The question marks indicate the area where it was impossible to measure the outdoor signal strength.
Notice that, 1. there is not much fluctuation in the difference between indoor and outdoor values along the outer walls and 2. the indoor values corresponding to the outdoor 'question mark' area are the lowest for this floor. This suggest that these values are related to the unknown outdoor values (could be verified with angle of arrival measurements). These outdoor values are probably also lower because of the particular building structure and direction of illumination. Consequently, the data gathered in the rooms adjacent to the 'question mark' area were omitted in the calculations.

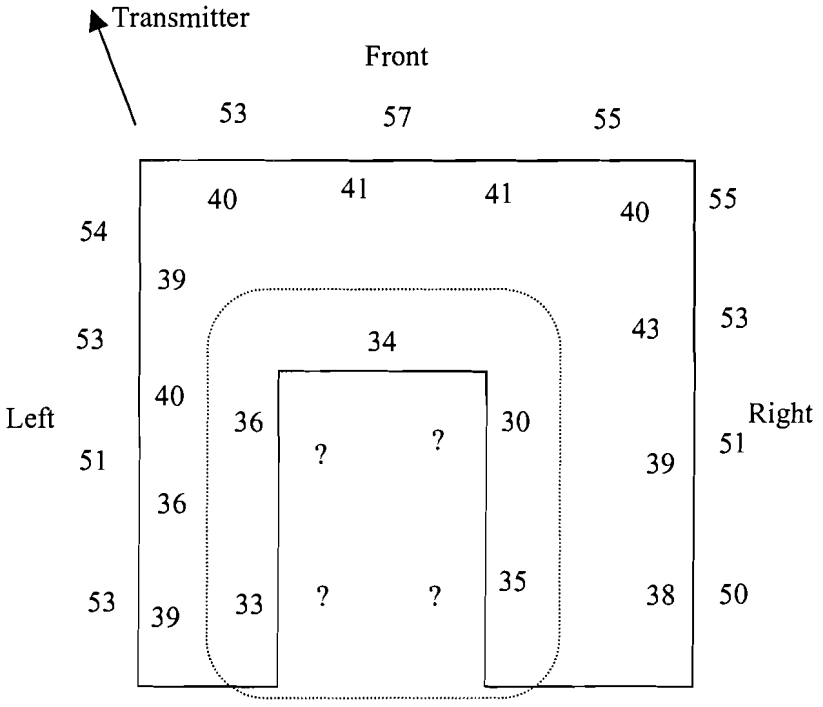

Figure 4.2 Average values for areas on the first floor of building SK

The cumulative distribution for the first floor of building SK is plotted in figure 4.4, the mean values and standard deviations are given in figure 4.3.

Area	Mean RxLev	σ
Left out	52.6	4.7
Front out	54.0	3.6
Right out	51.7	4.5
Left in	38.5	3.9
Front in	40.7	4.0
Right in	40.4	5.4

Area	mean: out – in
Left	14.1
Front	13.3
Right	11.3

Figure 4.3 Mean and standard deviation for areas at SK floor 1

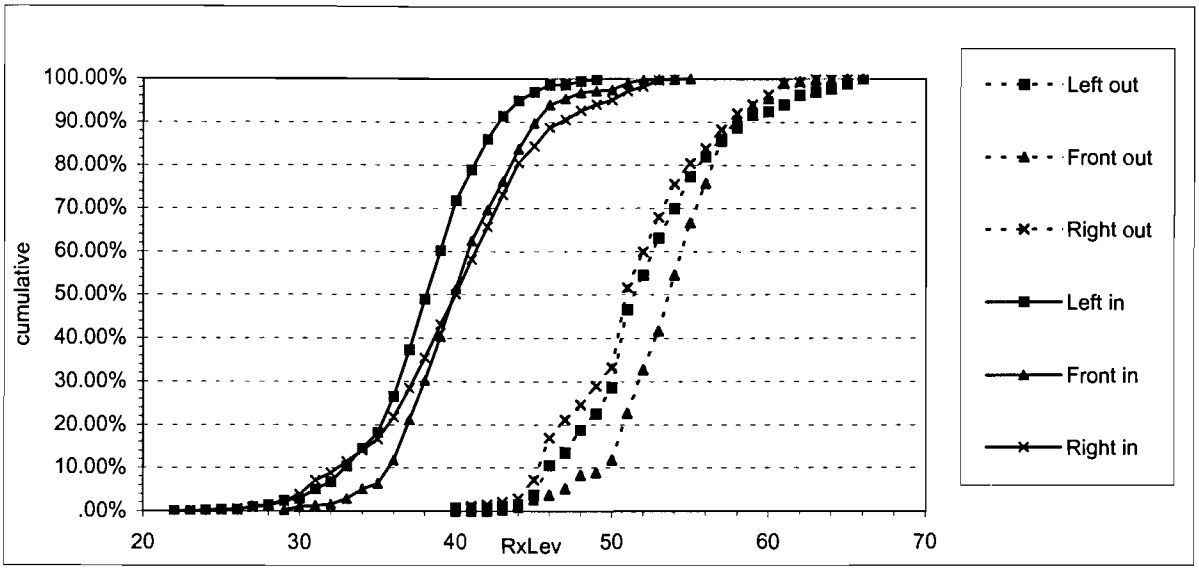

Figure 4.4 CDF for building SK outdoor and floor 1

In figure 4.3 we can see a difference of 11 to 14 dB between the mean RxLev outdoor and indoor. The building SK lies at close range from the transmitter, therefore the difference could partly be caused by the antenna radiation pattern, which has a small vertical beamwidth. Other possibilities are reflection and transmission loss through the wall.

Antenna radiation pattern:
The antenna pattern is given in figure 4.5 for the measured floor levels, here the gain in the main direction is taken at 0 dB.

Floor	Antenna pattern [dB] (main direction = 0 dB)
ground	-12.7
first	-12.4
third	-13.1
fifth	-6.8
seventh	-1

Figure 4.5 Antenna radiation pattern per floor

The difference between the ground floor and the first floor because of the radiation pattern is only 0.3 dB. This means that the difference between indoor and outdoor average signal must be explained with transmission loss through the wall. The transmission loss can be calculated with the electrical properties of the building material and the angle of illumination of the wall.

The electromagnetic transmission through an infinitely long wall is illustrated in figure 4.6, [14].

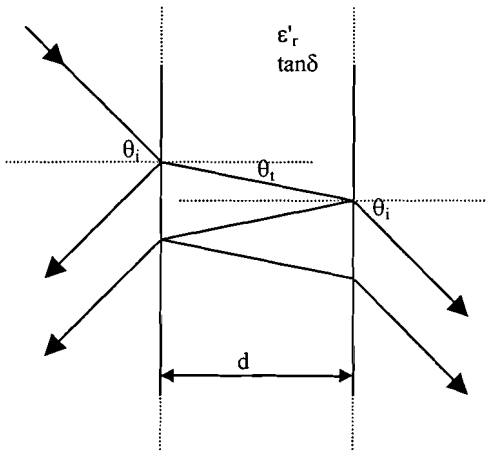

Figure 4.6 Transmission through a building wall

The angle θ_i is given by

$$\theta_i = \arccos\{\cos\varphi\cos\phi\} \qquad \textit{Equation 4.1}$$

where is φ and ϕ are the angles indicating the direction of wave propagation in vertical and horizontal plane (see figure 4.7).

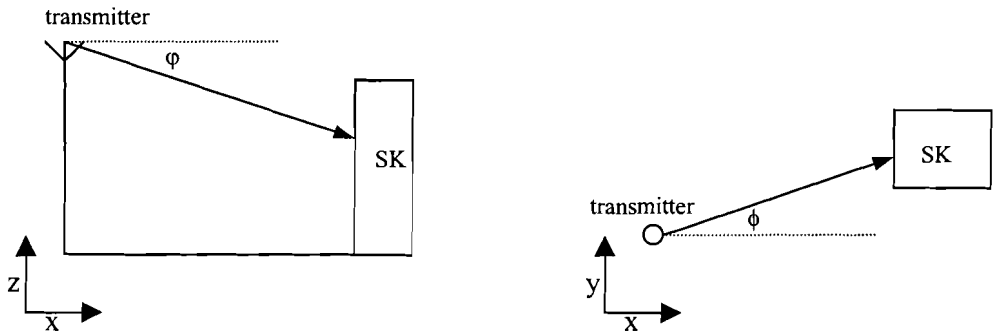

Figure 4.7 Direction of propagation in horizontal and vertical plane

The angle θ_t is given by

$$\theta_t = \arctan\left\{\frac{\sin\theta_i}{\mathrm{Re}[\sqrt{\varepsilon_r - \sin^2\theta_i}\,]}\right\} \qquad \textit{Equation 4.2}$$

If we assume reception of only the vertical component of the radio wave both indoor and outdoor then the reflection coefficient R for an air/material boundary is given by

$$R = \frac{\cos\theta_i - \sqrt{\varepsilon_r - \sin^2\theta_i}}{\cos\theta_i + \sqrt{\varepsilon_r - \sin^2\theta_i}} \qquad \textit{Equation 4.3}$$

with

$$\varepsilon_r = \varepsilon'_r (1 - j\tan\delta) \qquad \textit{Equation 4.4}$$

The transmission coefficient T is given by

$$T = R + 1 \qquad \textit{Equation 4.5}$$

For the transmission material/air the factor ε'_r becomes $1/\varepsilon'_r$, this will lead to R_2=-R_1 and T_1T_2=1-R^2_1, where the indexes 1 and 2 indicate the air/material and material/air boundaries. Due to the complex nature of the permittivity of the material, a wave propagating through the material will be attenuated and phase shifted. For the calculation of the transmission coefficient of the entire wall, assumed to be infinitely long, multiple reflections and transmissions have to be taken into account. The propagation factor for the wave in the material will be

$$G = e^{\left(-j\frac{2\pi}{\lambda}d\left(\sin\theta_i \tan\theta_t + \sqrt{\varepsilon_r - \sin^2\theta_i}\right)\right)} \qquad \textit{Equation 4.6}$$

Radio waves leaving the wall at different points will have mutual phase. This is expressed in the phase factor,

$$F = e^{j\frac{2\pi}{\lambda}2d\sin\theta_t \tan\theta_t} \qquad \textit{Equation 4.7}$$

The transmission coefficient for the entire wall becomes

$$T_w = T_1T_2G + T_1T_2G^3R_2{}^2F + T_1T_2G^5R_2{}^4F^2 + \cdots = T_1T_2G\sum_{n=0}^{\infty}(G^2R_2{}^2F)^n$$

$$= \frac{T_1T_2G}{1 - G^2R_2{}^2F} \qquad \textit{Equation 4.8}$$

The contribution of internal reflections is very small compared to transmission at the material-air boundaries. Therefore the higher order terms are neglected and equation 4.8 becomes

$$T_w = T_1T_2G \qquad \textit{Equation 4.9}$$

The loss due to reflection/transmission at the wall is

$$L_t = 20\log(T_w) \qquad \textit{Equation 4.10}$$

L_t is plotted in figure 4.8 as a function of θ_i, here we have chosen for the external wall ε'_r=5.3, tanδ=1.8*10^{-4} which are typical values used in simulations [8] and d=0.1m.

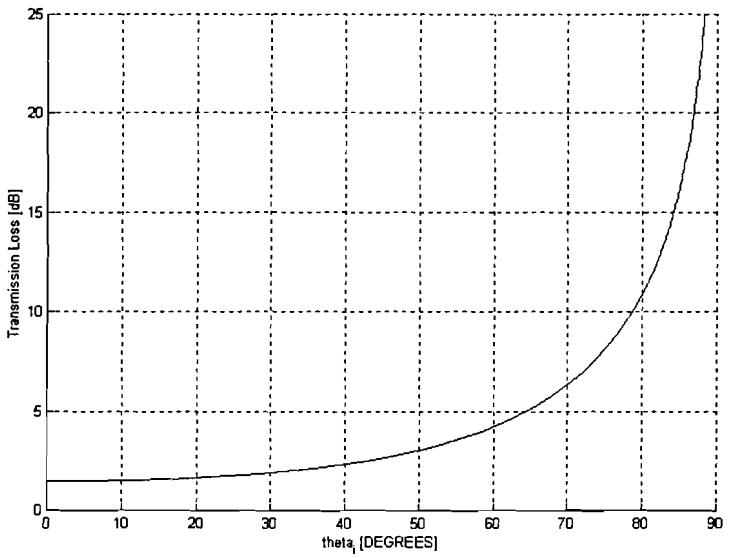

Figure 4.8 Wall transmission loss

For the *left* and *front* areas of building SK the angle θ_i varies from 35 to 65 degrees, this gives a calculated wall transmission loss of 2 to 5 dB. According to this analysis the difference between the measured average signal strength can only in part be attributed to losses due to external wall. However it should be noted that this is a simplified analysis in which the used electrical parameters may not be the true parameters of the wall. Furthermore aspects as insulation and humidity were not considered.

Also a difference of 1.4 dB is noticed between the mean RxLev for *left out* and *front out*, this is also the case for *left in* and *front in*. The difference is probably caused due to scattering from the vegetation on the propagation path from transmitter to the left area, the path to the front area has less vegetation (see figure 3.4).

For the first floor of SK it can be said that there is not much fluctuation in the difference between the measured outdoor and indoor mean RxLevs. In the right area (NLOS) the differences are the smallest and the spread is the largest.

4.2.2 A comparison of all floors

For all four floors and outdoor the cumulative distribution function is plotted in figure 4.9.
The first observation is that the measured RxLev values increase with increasing floor level. At floors five and seven there were measured RxLev values that are higher than the outdoor values at street level.

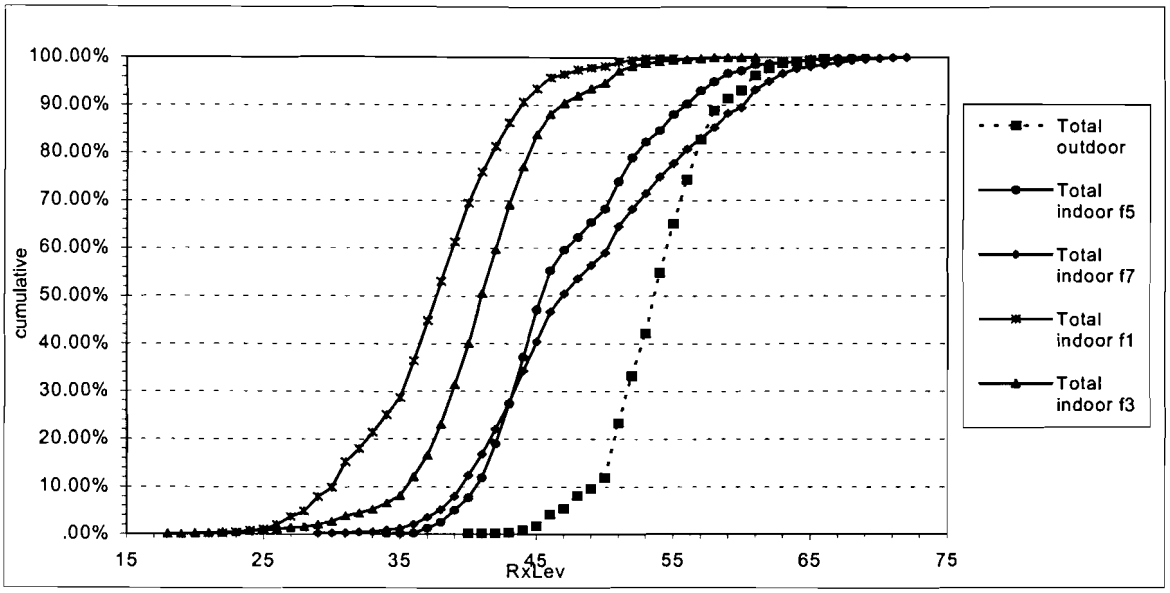

Figure 4.9 Mean RxLev taken over all floors and total outdoor

The approximate increase in signal strength between floors caused by the antenna radiation pattern are:

ground floor to first floor: 0.3 dB
first floor to third floor: -0.7 dB
third floor to fifth floor: 6.3 dB
fifth floor to seventh floor: 5.8dB

The differences on the lower floors are not caused by the radiation pattern, however on the higher floors the effect is larger. The distributions at the floors 5 and 7 also show a departure from the typical distribution indicating a combination of two distributions in one. This is because both the floors five and seven consist of a part that has LOS and a part that has NLOS. In figure 4.10 the distributions of the floors five and seven are plotted for the LOS and NLOS areas.

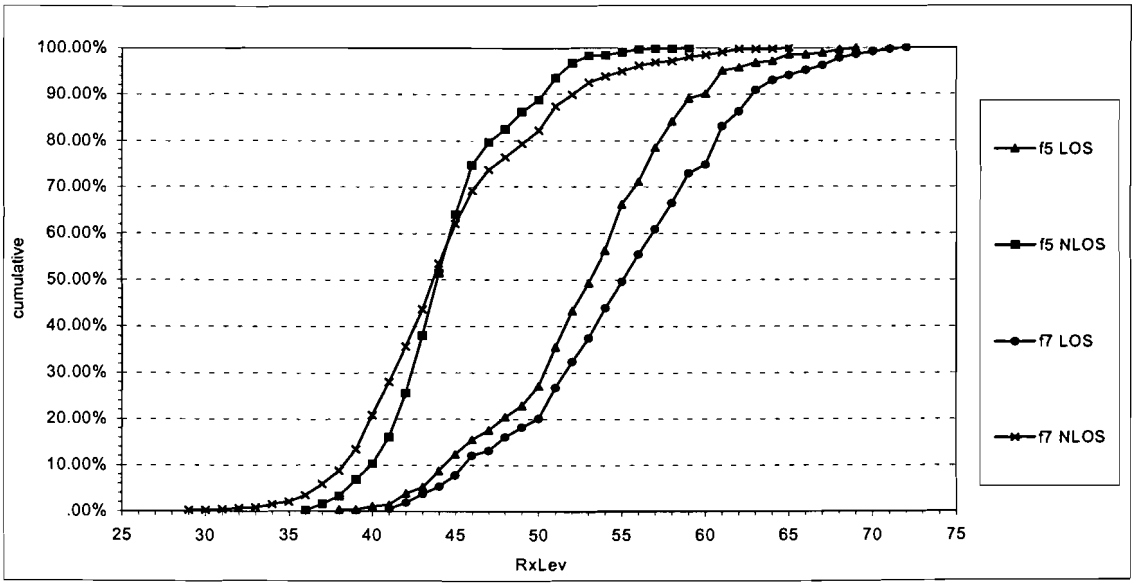

Figure 4.10 CDF for the LOS and NLOS areas of SK floors5 and 7

The mean values and standard deviations are given in figure 4.11.

Area	Mean RxLev	σ
f5 LOS	53.2	5.7
f5 NLOS	44.9	3.8
f7 LOS	55.5	6.5
f7 NLOS	44.9	5.6

Figure 4.11 Mean and standard deviation for LOS and NLOS areas at SK floor 5 and 7

The observations here are: 1. There is a difference of 2.3 dB between the LOS of both floors, while the NLOS averages are the same, but with an increase in spread for the highest floor. This indicates more effect of the radiation pattern for the LOS area.. This effect disappears for the NLOS area. 2. The difference between LOS and NLOS mean RxLev on the same floor is 8.3 dB and 10.6 dB for the fifth and seventh floor respectively. The difference between LOS and NLOS areas on one floor is also noticed for lower floors, but this difference is larger at higher floor levels. 3.The spread for the LOS areas is larger than the spread for the NLOS areas.

4.3 Results of building AB

4.3.1 The first floor

In figure 4.12 a sketch is given of the distinctive areas in building AB.

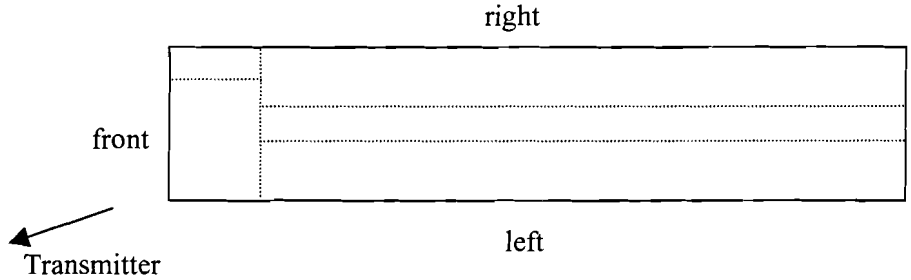

Figure 4.12 Area representation for building AB

Figure 4.13 shows that the difference between the distributions of the outdoor and indoor *front* areas is very small. This is also the case for part of the left *area* .

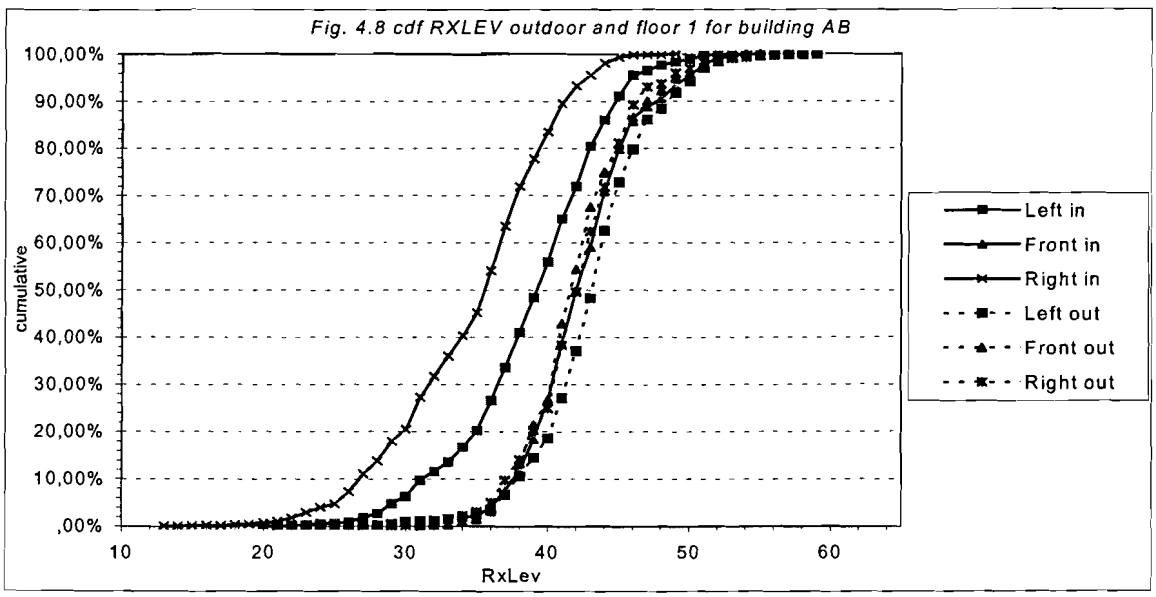

Figure 4.13 CDF for areas at AB floor 1

The mean values and standard deviations are:

Area	Mean RxLev	σ
Left out	43.5	4.2
Front out	42.5	3.7
Right out	42.5	3.8
Left in	39.2	5.1
Front in	42.8	3.9
Right in	35.1	5.5

Area	mean: out – in
Left	4.3
Front	-0.3
Right	7.4

Figure 4.14 Mean and standard deviation for areas at AB floor 1

One possible explanation for this observation is the occurrence of diffraction. The radio waves arriving at street level in the *front* area are diffracted at the edges of the building SK and obstructing building OBS at 325m from the transmitter (see figures 3.4 and 4.15). We will consider double diffraction at sharp edges of these two buildings. The diffraction losses will be calculated with the model of Picquenard [15] for a receiver at ground level and a receiver at the first floor. We take the first floor height at 3.25m based on the number of floors and total length of the building.

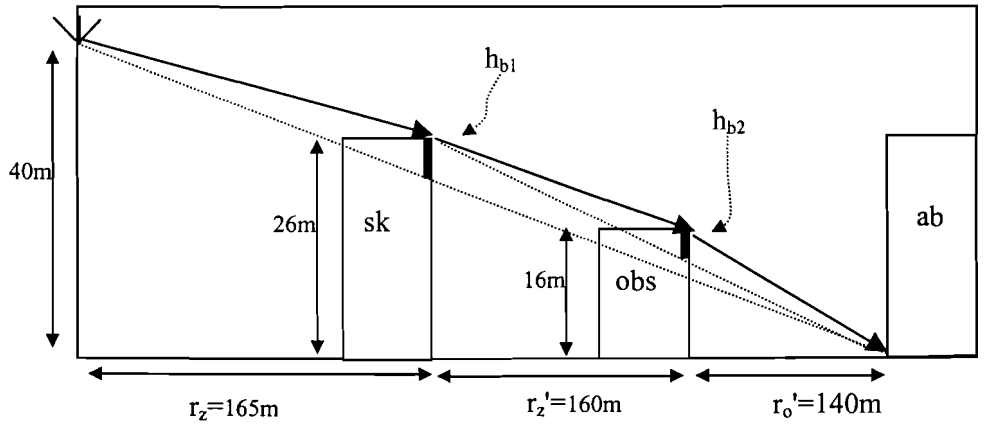

Figure 4.15 Model of Picquenard for diffraction at two obstacles

First we calculate the parameter v:

Obstacle SK:

$$v_{sk} = -h_{b1}\sqrt{\frac{2}{\lambda}\left(\frac{1}{r_z}+\frac{1}{r_0}\right)} \qquad \textit{Equation 4.11}$$

where $r_0 = r_z' + r_o'$

Obstacle OBS:

$$v_{obs} = -h_{b1}\sqrt{\frac{2}{\lambda}\left(\frac{1}{r'_z}+\frac{1}{r'_0}\right)} \qquad \textit{Equation 4.12}$$

Then the diffraction loss is calculated with one of the following equations [7],

$$L_d = 0 \quad \text{[dB] with } v \geq 1$$

$$L_d = -20\log(0.5 + 0.62v) \quad \text{[dB] with } 0 \leq v \leq 1$$

$$L_d = -20\log(0.5\exp(0.95v)) \quad \text{[dB] with } -1 \leq v \leq 0 \qquad \textit{Equation 4.13}$$

$$L_d = -20\log(0.4 - \sqrt{0.1184 - (0.1v + 0.38)^2}) \quad \text{[dB] with } -2.4 \leq v \leq -1$$

$$L_d = -20\log(-0.225/v) \quad \text{[dB] with } v < -2.4$$

In the first case with receiver at ground level, the calculated diffraction losses are L_{diff_sk}=6.5 dB, L_{diff_obs}=17.1dB, for a total loss of 23.6 dB. This value corresponds with the measured signal strength at ground level.

$RxLev_{calculated}$=EIRP+110-$L_{free\text{-}space(d=465m)}$-$L_{diffraction}$=51+110-91-23.6=46.5

In the second case with receiver at first floor level, the calculated diffraction losses are L_{diff_sk}=3.1 dB, L_{diff_obs}=8.0dB, for a total of 11.1 dB. The difference in diffraction loss for the two cases is 12.5 dB. This explains why the indoor and outdoor values in the front area lie closely together.

In figure 4.13 we can also see that the outdoor levels lie closely together. Indoor there is a 2 dB difference between *left in* which is an NLOS case with outer wall oriented towards the transmitter (OTT) and *right in* which is a NLOS case with the outer wall not oriented towards the transmitter. Obviously the areas around the building are on average affected in the same way by diffraction at neighboring buildings and other mechanisms such as reflection and scattering. However indoor we see a decrease in received RxLev when moving from OTT to NOTT and thus moving 'deeper' into to the building seen from the transmitter perspective.

4.3.2 A comparison of all floors

In figure 4.16 we can notice the same observation as in section 4.2.2.for building SK, the measured values increase with increasing floor height. The difference is that here the explanation cannot be given by means of the radiation pattern of the antenna. When moving from the fourth to the seventh floor (both in LOS) the effect of the antenna pattern would be a decrease in signal strength of approximately -2 dB. On the contrary we notice a slight increase when moving upwards. This indicates that there must be another effect taking place. This effect is often referred to as a *clutter* effect and will be treated in section 4.5.5. It should also be noted that again the values at higher floors are higher than at street level .

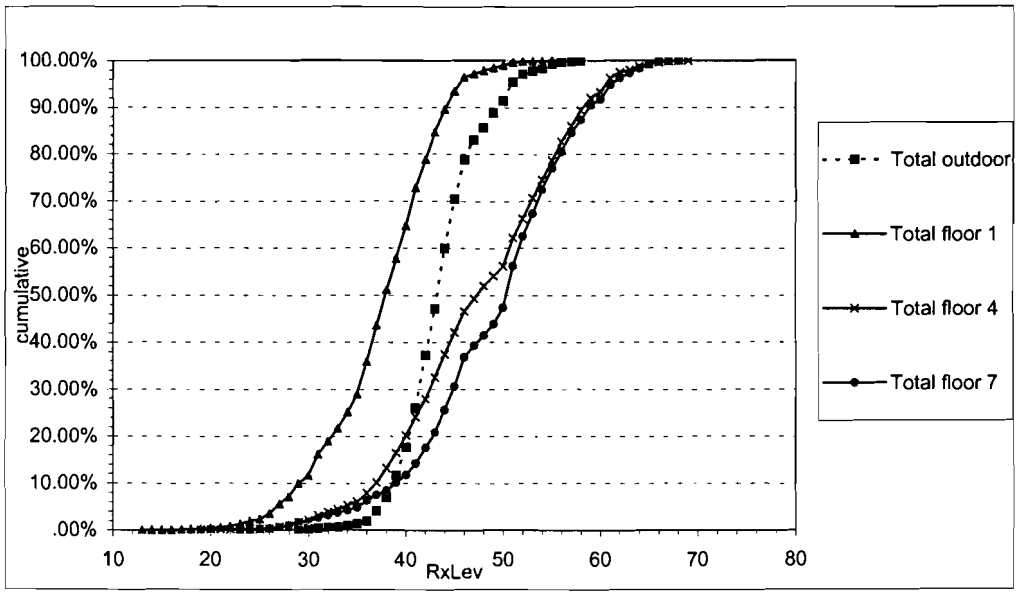

Figure 4.16 CDF for AB outdoor and floors 1,4 and 7

The distributions of floors 4 and 7 also consist of two sections, when dividing these floors in LOS and NLOS areas we get the plot in figure 4.17.

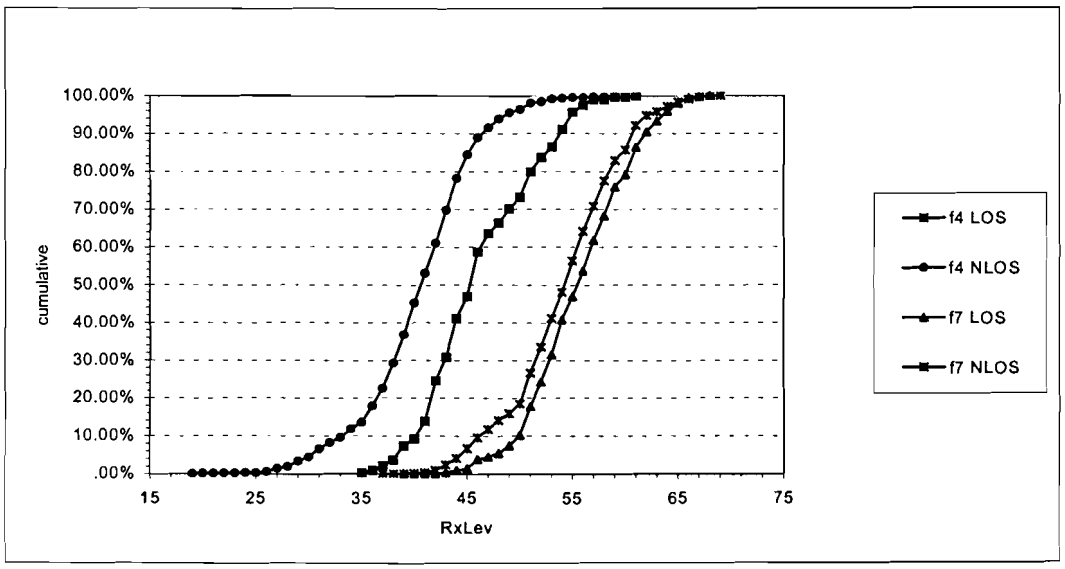

Figure 4.17 CDF for LOS and NLOS areas on AB floor 4 and 7

The mean values and standard deviations are given in figure 4.18.

Area	Mean RxLev	σ
f4 LOS	54.5	5.3
f4 NLOS	40.8	5.4
f7 LOS	56.0	4.8
f7 NLOS	46.6	5.2

Figure 4.18 Mean and standard deviation for LOS and NLOS areas on AB floors 4 and 7

In the appendix we can also see a difference between the average signal strength in the LOS and NLOS regions on floors 4 and 7. The difference is 14 dB for floor 4 and 10 dB for floor 7.

4.4 Results of building WA

In figure 4.19 a sketch is given of the distinctive areas in building WA together with a neighboring building.

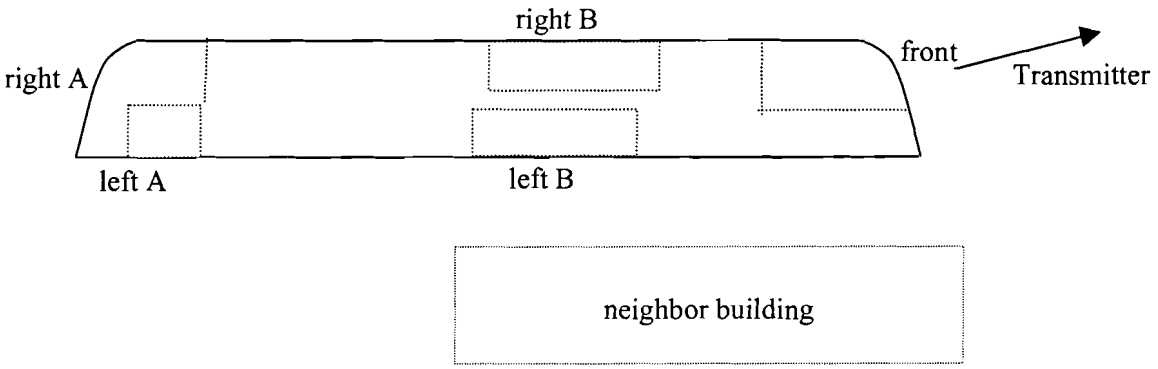

Figure 4.19 Area representation for building WA

For building WA the areas *front* and all areas *B* are plotted in figure 4.20. The area *left B* has a higher outdoor level than *right B*. The explanation given here is that of a 'tunneling' effect being caused by the neighboring building on the left side (see figures 3.4 and 4.19). This can be noticed indoor also, there is a difference of more than 5 dB between *left B* and *right B*. This indicates that the indoor level here is determined directly by the outdoor level adjacent to the area in question.

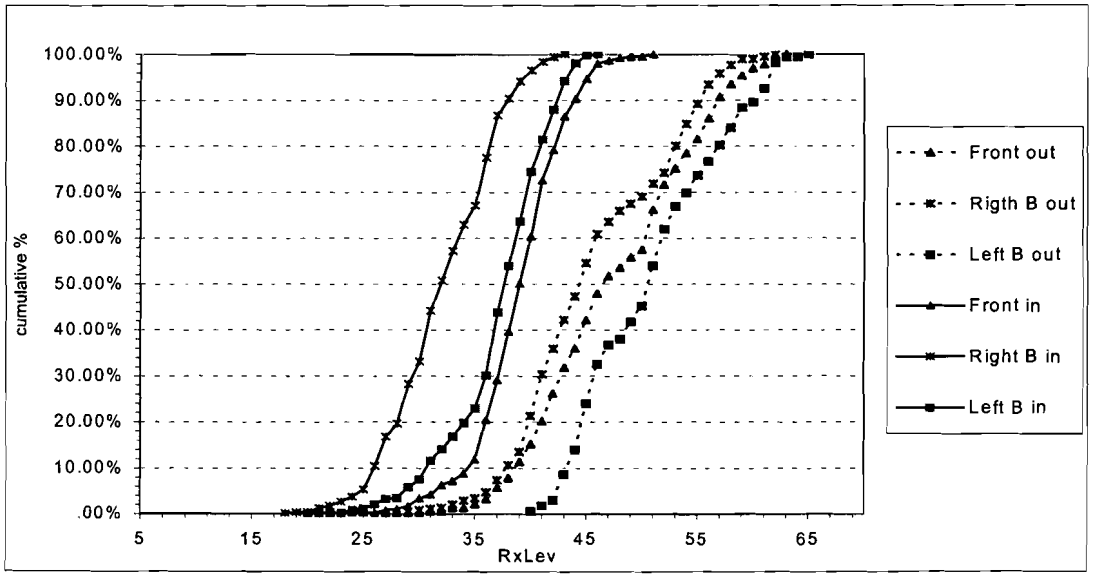

Figure 4.20 CDF for Front and B areas in building WA

In figure 4.21 again the area *front* is plotted together with all the areas *A* . Here we can see that area *left A* has the largest loss, one possible explanation is that at *left A* the previous tunneling still has an effect causing a high outdoor level, however the neighboring building is not long enough to act as a reflector for this area.

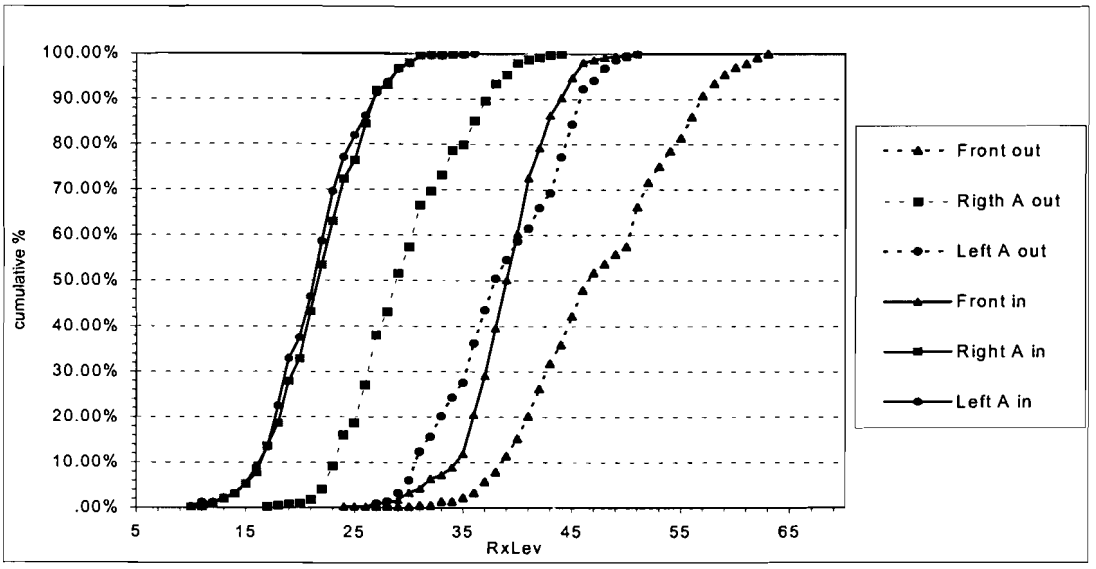

Figure 4.21 CDF for Front and A areas in building WA

4.5 Overall experimental results

In figure 4.22 an overview of the four buildings is given per measured floor. The mean RxLev measured both inside and outside and the standard deviation calculated over the entire floor are given. From the mean RxLevs per room both inside and outside the room loss is calculated. The building loss and its standard deviation are calculated over the mean values of all the room losses on the first floor of the buildings. The floor-height factor (or floor height gain) is defined as the difference between the average RxLevs of two consecutive floors. For example the calculated difference between the averages on floors 4 and 7 is divided by 3 to give an increase (positive factor) or decrease (negative factor) per floor. The factor can be given in dB per meter. However, since all the buildings have approximately the same floor height the value is given in dB per floor, which is an easier factor to work with. For more detailed figures see the appendix.

Buil-ding	Floor	Mean RxLev outs	SD RxLev outs	Mean RxLev ins	SD RxLev ins	Building loss (dB)	SD Building loss (dB)	Floor-height factor (dB/floor)	Approx. Distance Tx-Rx (m)	Building height (m)
SK	1	52.9	1.9	37.7	2.1	13.2	2.5		130	
	3			41.5	2.6			1.9		14
	5			47.6	4.5			3.0		
	7			48.8	5.5			0.6		26
AB	1	42.6	1.1	37.7	4.2	4.8	4.0		465	
	4			48.3	7.5			3.5		
	7			51.3	5.6			1.0		27
WA	G	41.7	8.7	29.6	7.2	12.2	3.8		745	-
PB	1	56.6	5.1	53.0	6.8	3.6	6.8		365	
	2			53.7	4.7			0.7		
	5			57.9	9.0			1.4		
	6			59.6	5.0			1.7		
	7			59.0	4.9			-0.6		
	8			58.2	5.7			-0.8		
	9			58.1	9.0			-0.1		
	10			57.5	4.3			-0.6		
	12			52.9	5.5			-2.3		41

Figure 4.22 Overall results per floor of the measured buildings

4.5.1 Building penetration loss

The buildings AB and PB have building penetration losses around 4-5 dB and the buildings SK and WA have building losses around 12-13 dB. From the analysis in the previous sections we explained that the low losses for building AB is a result of a difference in outdoor path loss between the first floor and street level. A measurement at the ground floor would have given a more accurate building loss. For building PB we have a similar situation, the building is situated at approximately the same distance as AB and is also obstructed by building SK at ground level. The first floor however lies at approximately 3.5m height and therefore encounters less outdoor path loss.

For building SK there is not much difference in the antenna radiation pattern for the street level and first floor, therefore we can conclude that the building loss measured here is close to the loss that would have been measured on the ground floor. In building WA the measurements were carried out at ground floor and are therefore valid for building loss calculations.

From the above we can conclude that the average building loss factor is approximately 12.5 dB with a standard deviation of 5.3 dB. These results are in accordance with the results of some other studies done at 1800 MHz. After extensive measurements in an urban area with transmitter above rooftop, Turkmani and de Toledo found for 1800 MHz an average penetration loss of 13.4 dB with a standard deviation of 7.6 dB [16]. COST proposed as parameters for the path loss model for NLOS (equation 2.11) an attenuation of 12 to 14 dB for external concrete walls.

4.5.2 Correlation

To measure the dependence between the mean RxLev measured outside in the streets adjacent to each rooms and the mean RxLev measured in the room, the correlation coefficient was calculated. The measured values are given in the appendix, see figure 4.23 for a scatter plot of these values. The overall computed correlation coefficient was 0.7. This means that we can assume a certain relation between the RxLev measured in a room and the RxLev measured just outside the room.

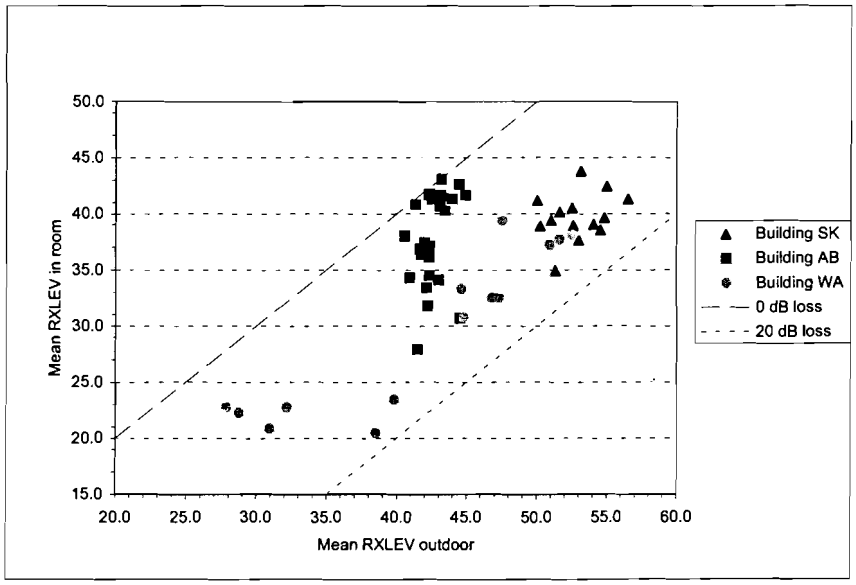

Figure 4.23 Scatter plot of the mean RxLev values measured in rooms on the first floor (ground floor for WA) and values measured outdoor in the street adjacent to the rooms

4.5.3 Effect of transmission condition on signal strength

In four cases the difference between LOS and NLOS on a single floor was analyzed, namely on the fifth and seventh floors in building SK and on the fourth and seventh floor in building AB. In all four cases a significant difference was measured between the average signal strength in LOS and NLOS (see figure 4.24).

floor	LOS-NLOS [dB]
SK f5	8.3
SK f7	10.6
AB f4	13.7
AB f7	9.4

Figure 4.24 Mean difference between LOS and NLOS areas

4.5.4 The signal strength/distance factor

In figure 4.25 the mean RxLev measured both indoor and outdoor for all rooms on the first floor (WA on the ground floor) is given as a function of the distance.

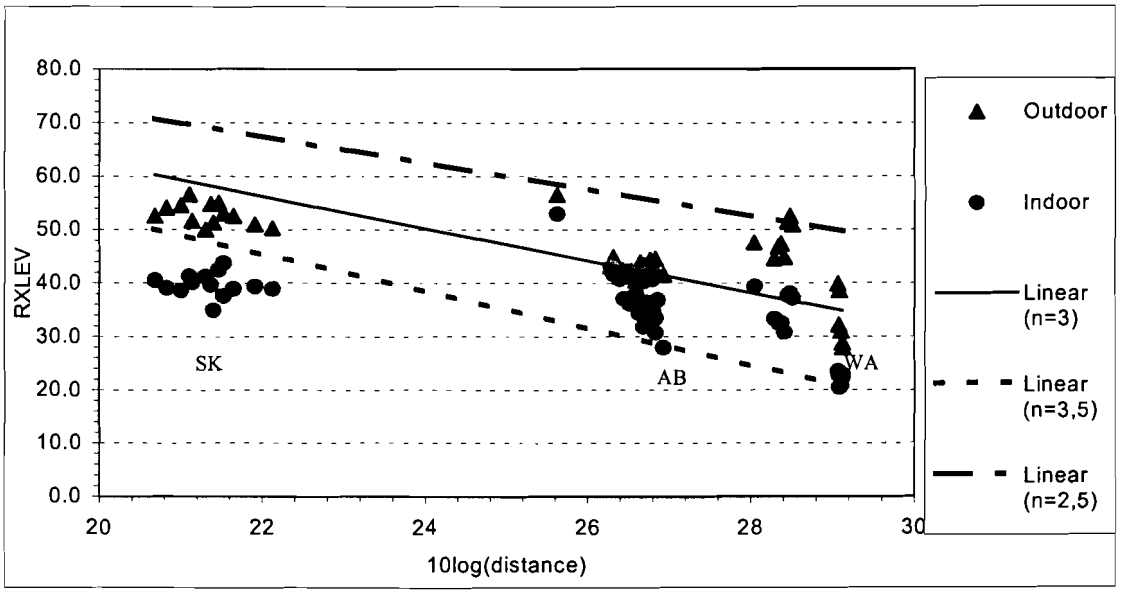

Figure 4.25 Outdoor and indoor RxLev as a function of the Tx-Rx distance

Also three n*log(distance) functions are drawn with n= 2.5; 3 and 3.5. The outdoor values for building AB correspond best with n=3. The outdoor values of building SK are below the n=3 line, this can be explained with the radiation pattern of the antenna. The rooms at the first floor are radiated with 12.4 dB less power. If we compensate this difference then the values of SK would also correspond with the n=3 line. The values of WA closer to the transmitter also depart from the n=3 line towards n=2.5. This can be explained with figure 3.4 (site description), the area between the transmitter and the front part of WA has a lower building density than for AB. Therefore the radio waves travelling to WA are less deteriorated by the environment compared to the waves travelling to AB. The path to AB is obstructed by SK and another building causing extra diffraction losses.

4.5.5 Floor-height factor

It is normally not possible to calculate or predict a penetration loss using an outdoor reference at higher floor levels. The floor-height factor can be used to give an estimate of the received signal level at higher floors.

If we calculate a floor-height factor from the data 'as is', then we get the following results. In figure 4.26 the difference between the mean RxLev measured outdoor at ground level and the mean RxLev measured indoor at different floors is plotted. For the buildings SK, AB and PB we see a negative trend for increasing floor level, for building PB the trend becomes negative above the 7th floor.

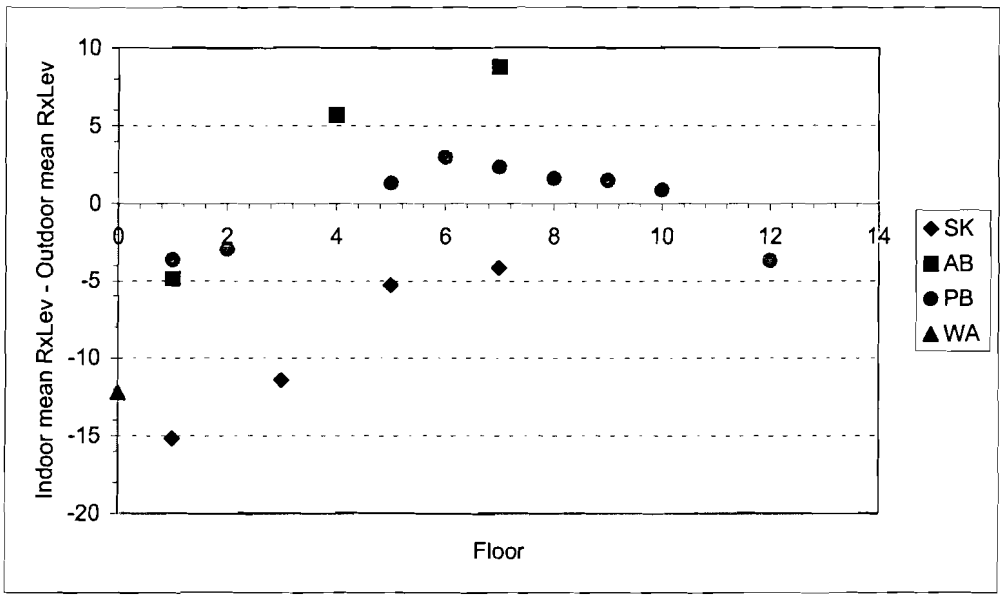

Figure 4.26 Difference [Indoor Mean RxLev - Outdoor Mean RxLev] for all floors of the four buildings

Calculated trendlines for the difference (y) are:

SK: y = 2.0*floor - 16.8 $R^2 = 0.94$
AB: y = 2.3*floor - 5.9 $R^2 = 0.91$
PB<7: y = 1.3*floor - 5.3 $R^2 = 0.95$
PB>6: y = -1.0*floor + 9.7 $R^2 = 0.84$

The given linear trendlines are calculated using the least square method. The R-squared value indicates the goodness of fit, in this case the calculated dependencies lie close to the best fit (R^2=1). From these calculations we get the following floor-height factors,
SK and AB → 2.0 to 2.3 dB/floor
PB till floor 6→ 1.3 dB/floor
PB above floor 6 → -1.0 dB/floor

These figures are in accordance with results found in other studies. In [17] this factor was found to be 1.4 dB/floor up to the sixth floor and –0.4 dB/floor for higher floors. Tanis [18] found values of 1.2 dB/floor and 2.4 dB/floor up to the fifth floor. Also in COST 231 [9] floor height gains from 1.5 to 2 dB/floor were given.

However in the preceding analyses we could see that there are several aspects to be considered.

First the difference in mean RxLev between floors 3, 5 and 7 in SK can be explained as an effect caused by the radiation pattern of the transmitting antenna.

Second, the antenna radiation pattern shows a decrease in signal strength when moving upwards in the buildings AB and PB. The radiation pattern has an electrical downtilt of 6 degrees which means that the ground reflection point of the strongest wave component from the transmitter is around 375m. The buildings AB and PB are just beyond this point and should experience a decrease for higher floors instead of an increase, however this is not the case.
The noticed difference between the floors of these two buildings can be best regarded as an effect of the surrounding environment, the urban clutter. In an urban area, the lower floors are affected by the 'depth' of their position in the area. The waves arriving at lower floors encounter more diffraction, reflection and scattering than waves arriving at the higher levels. After the seventh floor, we notice a negative dB/floor value. This is probably the point where the negative coefficient caused by the antenna radiation pattern takes over from the positive coefficient caused by departure from the clutter.

Third, in the case of building AB it was shown that increases around 10 dB are also possible when considering the first few meters (the difference between ground floor and first floor). Notice that Hata's path loss model given in equation 2.13 also suggests a large height gain at lower heights. For the first 10 meters the Hata model gives a height gain of 2.9 dB per meter at 1800 MHz, this would give a gain of about 10 dB when moving from the ground floor to the first floor.
And fourth, as shown in section 4.5.3. there are substantial differences in the average received signal strength when comparing rooms at LOS and NLOS on higher floors.

Summarizing we can say that in general there is an increase in the average signal strength when the receiver is moved upwards in a building (up to floor seven). In this experiment the observed increase has been found to be dependent on factors such as the antenna radiation pattern in buildings close to the transmitter (with (partial) LOS), and the local urban clutter. The relationship between the floor height and extra gain with respect to the ground floor level is not linear, even on the same floor significant differences can be noticed between rooms with LOS and NLOS. However the floor height gain is often represented as a linear relationship governed by a single factor.

4.5.6 Effects of horizontal sun shields

The effect of aluminum sun shields was measured in two rooms in the buildings PB and AB. First The signal strength was measured with all the sun shields removed from the windows and then with all the sunshields closed. Figure 4.27 gives the results of these measurements.

Building & Floor	Condition	Mean RxLev without shields	Mean RxLev with shields	Extra loss (dB)
PB f10	LOS	57.5	53.8	3.7
AB f7	LOS	55.4	53.3	2.1

Figure 4.27 Results of measurements with and without sun shields

From this figure we can conclude that these sun shields can cause an additional attenuation of about 3 dB. In [19] additional losses of 7 dB for windows with aluminum shields were reported.

4.6 Small scale statistics

In many experiments, it was shown that in cases where there are many radio wave components with similar amplitudes arriving at the receiver, the signal envelope follows a Rayleigh distribution [5]. In LOS situations where there clearly is one component stronger than the others,

the distribution may become Rician. This section treats the testing of the data to determine the statistical nature of the measured groups of samples per room. The test was performed with the chi-square goodness of fit test [13]. The considered distributions were the Rayleigh, Rice and lognormal distributions.

The data were first divided per room, the samples were then adjusted in order to get amplitude values r instead of power values. Next the samples were divided in intervals containing at least 5 samples each. This is a requirement resulting from the fact that for a finite number of samples the random variable only approximates the chi-square distribution used in the test.

Next, the theoretical number of samples per interval was calculated for the three considered distributions. The deviation χ_o^2 between measured and theoretical values is computed with,

$$\chi_0^2 = \sum_{j=1}^{K} \frac{(b_j - e_j)^2}{e_j} \qquad \textit{Equation 4.14}$$

Where K is the number of intervals, b_j is number of measured samples per interval and e_j is the theoretically expected number of samples per interval.

Given a certain significance level the test will accept or reject the hypothesis that the distribution of the samples corresponds with a certain theoretical distribution. In this test, the significance level was 1%, meaning that only 1% of the correct hypotheses would be rejected anyway. In the event that more than one distribution was accepted by the test, the distribution with the smallest deviation was chosen.

4.6.1 Results

The results indicate a *lognormal* distribution for 60 of the measured rooms, for 16 rooms a *Rayleigh* distribution was accepted and for 2 rooms a *Rician* distribution was accepted. The explanation for these results lies in the internal averaging procedure of the TEMS. Normally the true statistical nature is verified with either continuous wave or wideband measurements. However, the measurements in this experiment were taken with a system that applies internal averaging of samples, and changes the statistical nature of the true samples. Additionally the averaging does not occur over fixed distances since it is time-based and the walking speed is not constant. We can conclude that the TEMS measurement system is best suited for the measurement of large-scale characteristics rather than for accurate measurements of small-scale characteristics. We will return to the small-scale statistics in chapter 6, next the large-scale statistics will be treated.

4.7 Large scale statistics

In sections two, three and four of the chapter several cumulative distributions of measured samples were presented. Normally these samples would contain both small scale effects as well as large scale effects, however as shown earlier the small scale characteristics are averaged out for a great deal. Therefore, it can be expected that the large scale fluctuations will dominate the statistical nature of these distributions measured with TEMS.

In this section, the statistics of the local mean will be treated. It has been well established in literature that the local mean is lognormally distributed in outdoor, indoor and outdoor to indoor propagation as well, [11,12,17]. In this project, a graphical method was chosen to test the data, this is because the groups of data were too small for a chi-square analysis. In order to graphically test whether the data is lognormally distributed or not a statistical procedure described by A. Mawira [23] was used. This procedure uses the so-called *Rank-ordered statistics* to assign the

probabilities [24]. First the data is selected for a particular area, e.g. an entire floor or building. Then its points are sorted in ascending order from position 1 to i, and assigned a cumulative probability given by

$$P_i = \frac{i}{(N+1)} \qquad \textit{Equation 4.15}$$

where N is the total number of samples considered. With P_i as input, the probability Q_i is computed from a normal distribution with mean equal to zero and standard deviation equal to one. Finally, the inverse of Q_i is plotted as a function of the measured RxLev. In this procedure a normal distribution would give a straight line:

$$Q_i = \frac{\text{RxLev} - \mu}{\sigma} \qquad \textit{Equation 4.16}$$

where μ is the median and σ is the standard deviation.

In figure 4.28, the room averages measured in building SK are plotted. The measured distribution approximately follows the straight line in the middle, but departs at the tails. In the lower right corner a sub-group of high RxLevs is noticed, these values were measured in the rooms having LOS at the higher floors.

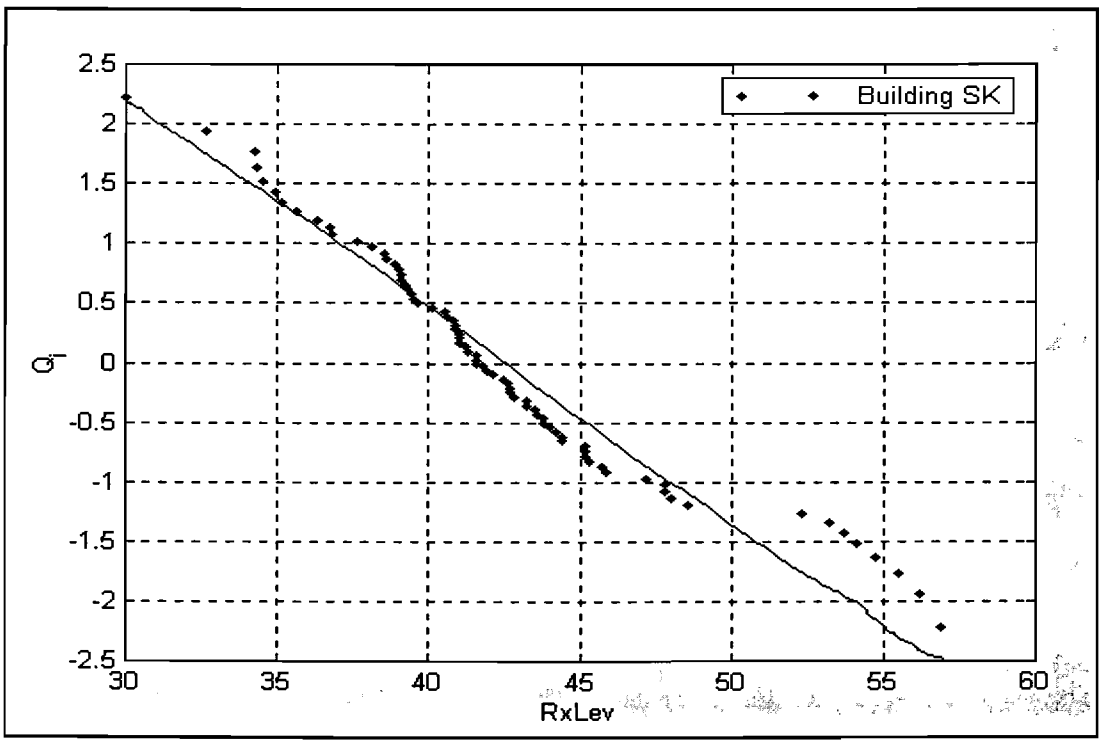

Figure 4.28 Cumulative probability distribution of mean RxLev per room in Building SK

For the buildings AB and WA, the distributions are plotted in figure 4.29. The data points of Building AB in the upper left part of the plot coincide with the straight line, while the middle and lower right part significantly depart from it.

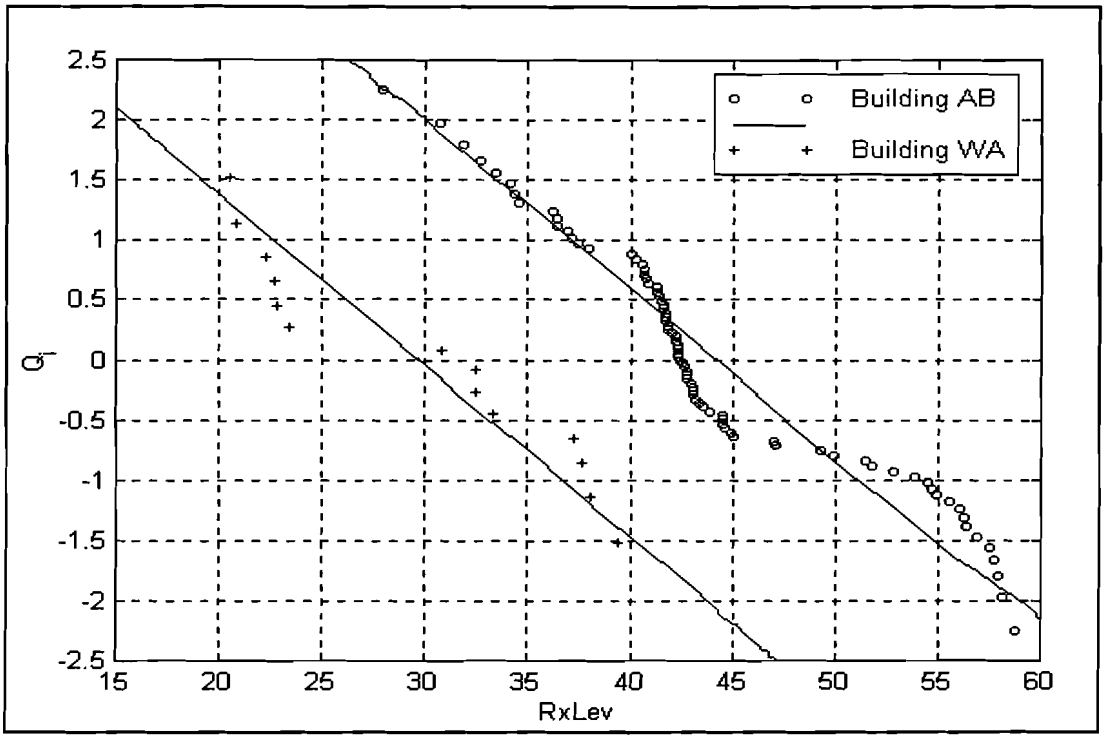

Figure 4.29 Cumulative probability distribution of mean RxLev per room in Buildings AB and WA

In figure 4.30, the distribution per floor is given for building SK. Here we can see a relatively good fit for the first and third floor of the building SK, however for floors 5 and 7 the measured samples lie scattered around the straight lines.

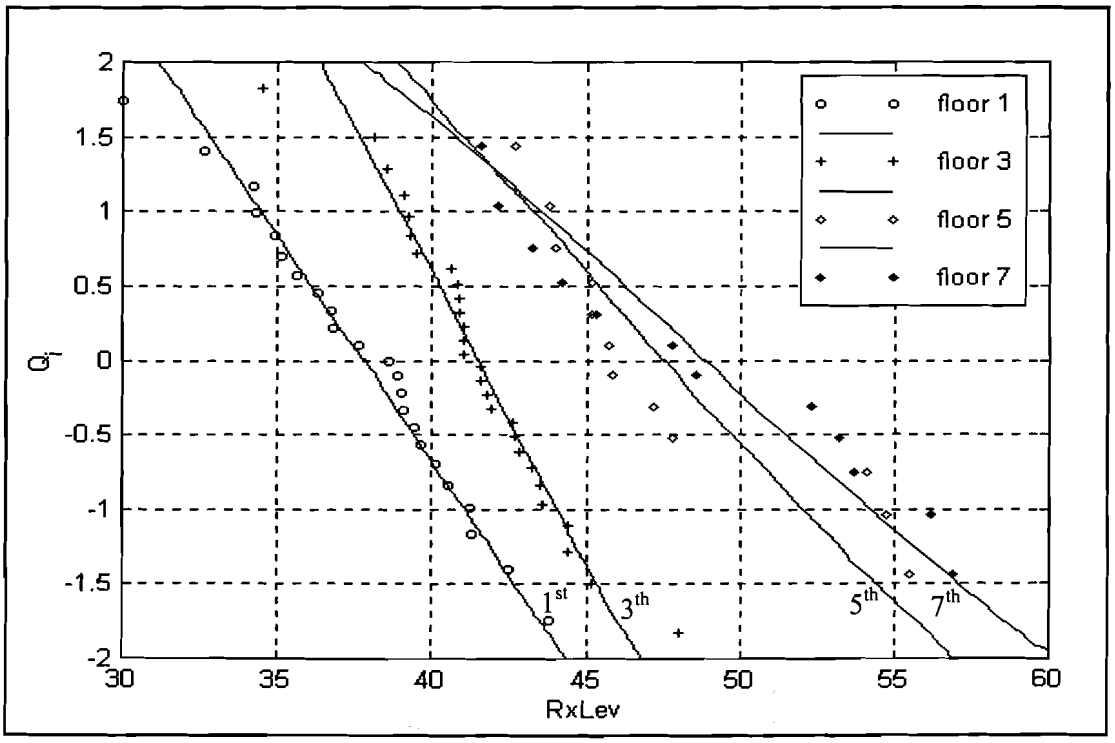

Figure 4.30 Cumulative probability distribution of mean RxLev per room for 4 floors in SK

In the results per floor from building AB (figure 4.31), there is no close fit to the normal distribution. It seems that the data points are divided in two sub-groups for each of the three floors.

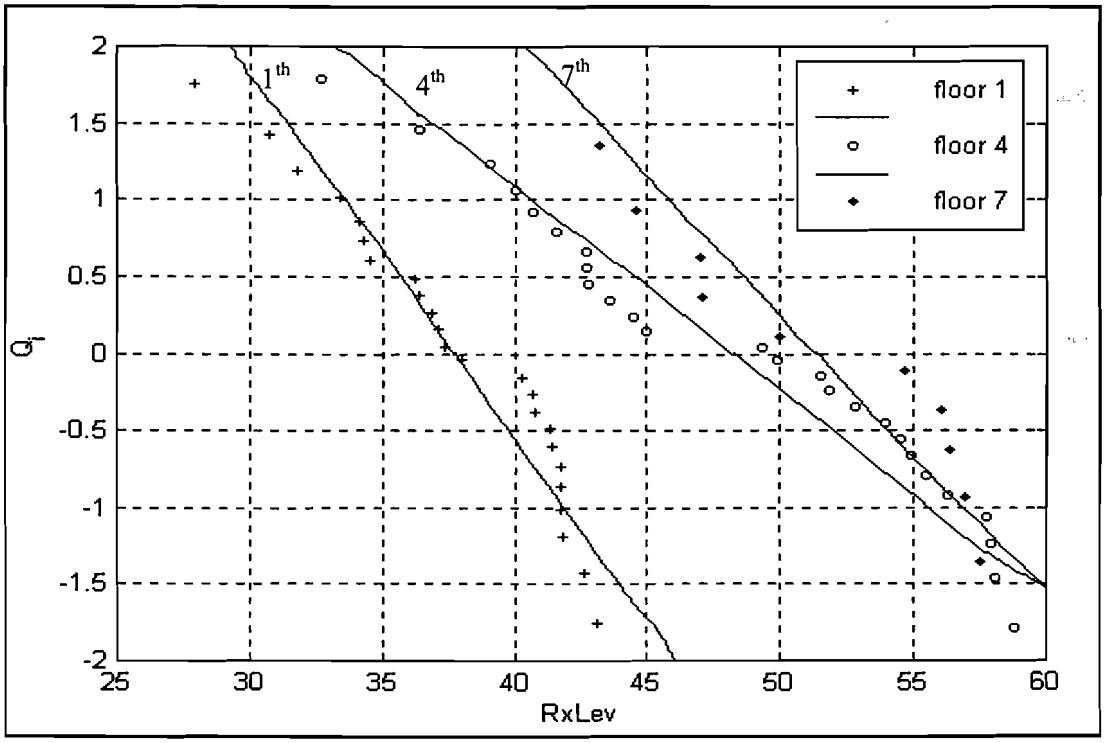

Figure 4.31 Cumulative probability distribution of mean RxLev for 3 floors in AB

The division of higher floors into LOS and NLOS sub-groups was already noticed in the previous sections. On the other hand, the differences in RxLev were less at lower floors; this is confirmed in this analysis.

In the mobile radio channel, a receiver moving in a large circle around the transmitter will experience a lognormal distribution around an average signal level that strongly depends on the log of distance to the transmitter. However, in the treated four cases the average signal strength per room does not naturally show a normal distribution. At the same distance from the transmitter the receiver may encounter different distributions of the signal strength for different floors, or even on the same floor.

Chapter 5 Modeling

5.1 Introduction

Most of the models developed for the prediction of path loss in the case of into building propagation have used the technique proposed by Rice. First the median signal level in the neighboring streets is predicted and then the building penetration loss is added as a factor. Other researchers [9,16,20] included in their models the angle of illumination and building properties that may influence the loss, properties such as the floor area, number of rooms and number of penetrated internal walls. However, our objective is to give a simple empirical-statistical model of the form given in equation 2.6. The data used for this model are the average signal strengths received per room. Therefore, it will estimate a total path loss at ground floor including the room loss.

As a basis, we use the model developed by Hata presented in section 2.3. First, the outdoor path loss in the vicinity of the measured buildings is calculated with the model. Then the path loss in the case of indoor reception is calculated by compensating the receiver height (1st floor) in SK, AB and PB with a constant factor. The idea is to first add a penetration loss to the calculated outdoor path loss at ground level and then add a constant factor as correction for the receiver height. Next, the path loss for indoor reception is calculated by including the receiver height differences in the factor $a(h_r)$ of the model. This will be done for the first floor of the buildings SK, AB and PB, and the ground floor of building WA. The idea is to calculate the outdoor path loss at a certain height and then add a factor to account for the penetration loss.

After the Hata model for ground level, the case of higher floor levels will be treated. Finally the models developed by COST will be treated, these models calculate the path loss with use of additional information such as the angle of illumination and internal building properties.

The path loss calculated is defined as,

$$\begin{aligned} L_b &= P_t + G_t - L_t - P_r \\ &= P_t + G_t - L_t - RxLev + 110 \end{aligned} \qquad \text{[dB]} \qquad \textit{Equation 5.1}$$

Here the receiver antenna gain G_r and receiver cable losses L_r are set to 0 dB. To indicate the accuracy of the model the *prediction error* is calculated. The prediction error is the difference between the calculated path loss and the measured path loss. The root mean square of this error is:

$$RMSE = \sqrt{\frac{1}{n}\sum_{j=1}^{n}(\hat{L}_{predicted} - L_{measured})^2} \qquad \text{[dB]} \qquad \textit{Equation 5.2}$$

where n is the total number of rooms considered.

The data consisted the average RxLev calculated outside and inside a total of 53 rooms at the first floor level (ground floor for building WA) and the average RxLev calculated inside 90 rooms for the higher floor levels. The main parameters used for the modeling are the distance between transmitter and receiver, the receiver height and the angle of penetration in the COST LOS case. Where necessary the receiver heights were converted from floors to meters. The corrections made to the data are to account for the antenna pattern for the building SK at close range and

corrections for the first floor in the buildings SK, AB, and PB. The corrections for building SK are: street level: +12.7 dB; floor 1: +12.4 dB; floor 3: +13 dB; floor 5: +7 dB; floor 7: +1 dB.

5.2 The Hata model extension

In this section, the well-known Hata model (equation 2.13) is used for outdoor prediction. For our case the model can be modified in two ways, 1. the constant factor can be modified (addition of a w_i to u in equation 2.6), and 2. the exponent or rate of decay can be modified (v in equation 2.6).

The Hata model is here rewritten for 1800 MHz, a transmitter height of 40m, a receiver height of 1.5m for all cases, and the distance d between transmitter and receiver in meters.

$$L_{hata} = 69.55 + 85.16 - 22.14 - (4.32 - 4.28) + (44.9 - 10.49)\log(d/1000) + w_1$$

$$= 29.39 + 34.4\log(d) + w_1 \qquad \text{[dB]} \qquad \textit{Equation 5.3}$$

In the analysis, we calculated the RMSE for the model in seven cases.

Case1: The outdoor path loss was calculated with the Hata model unmodified (n=v/10=3.44 and w_1=0). The calculated RMSE was 7.5 dB.

Case 2: The outdoor path loss was calculated with n=3.44 and variation of w_1 to get the minimum RMSE (i.e. best fit of the model to the data). The minimum RMSE was in this case 5.0 dB and the best w_1= -6 dB.

In figure 5.1 the results of cases one and two are plotted.

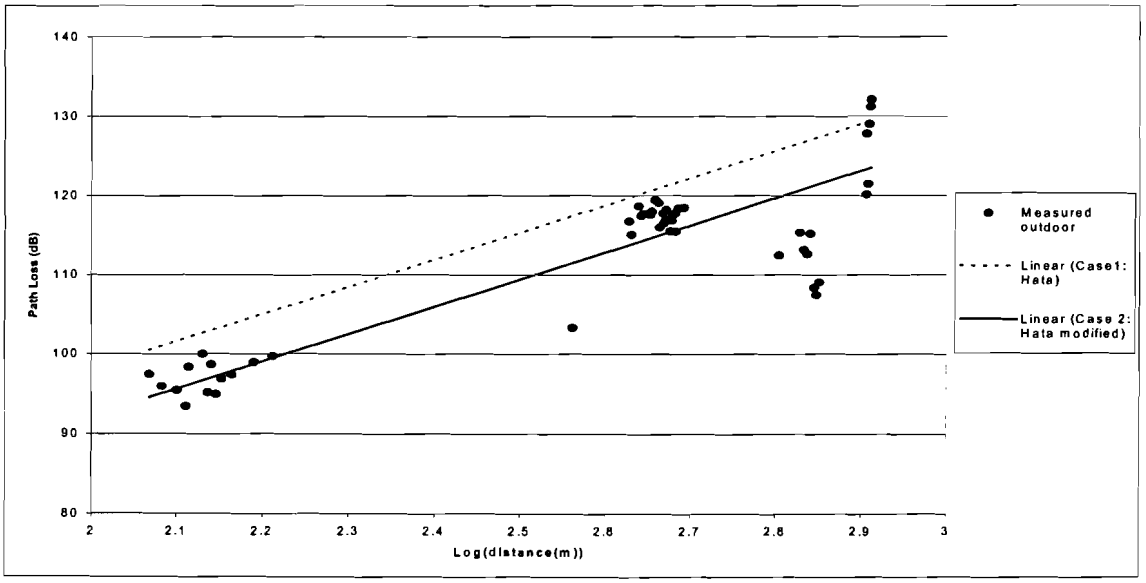

Figure 5.1 Outdoor path loss with Hata model

Case 3: In this case, the outdoor path loss was calculated with variation of both n and w_1 to get the minimum RMSE. The calculated minimum RMSE was 4.9 dB and was achieved with n=3.60 and w_1= -5 dB.

The difference in error between case two and three is not significant, therefore we can conclude that a good fit of the model to the outdoor data is achieved by applying the unmodified rate of decay n= 3.44 and subtracting 6 dB from the Hata equation.
The next step is to calculate the indoor path loss. As mentioned earlier two approaches were followed. The first one (case 4) was to use the antenna height factor $a(h_r)$ provided by the Hata model to account for the different antenna heights in SK, AB and PB (first floor), and to include a factor w_1 in the model to account for the penetration loss (see figure 5.2).

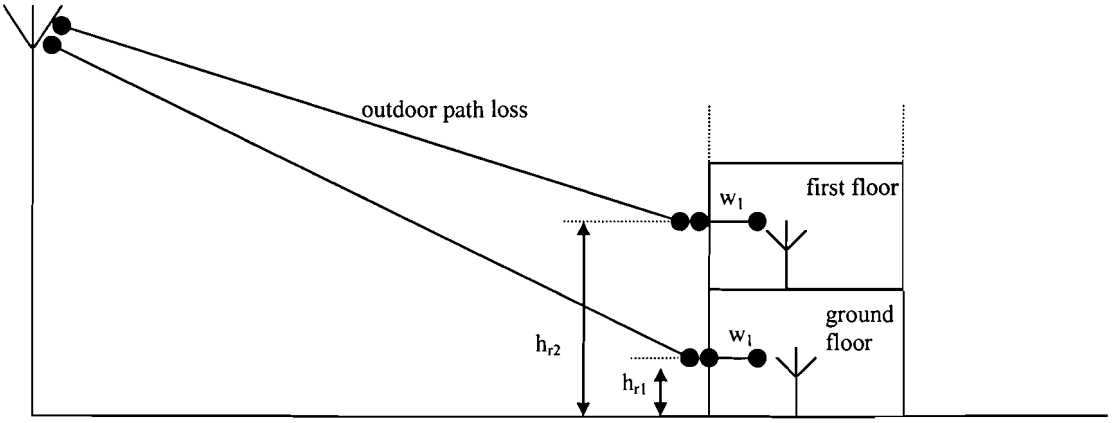

Figure 5.2 Approach to path loss calculation in case 4

$$L_{hata\_\text{int}obuilding} = 69.55 + 85.16 - 22.14 - (2.88h_r - 4.28) + (44.9 - 10.49)\log(d/1000) + w_1$$

$$= 33.71 - 2.88h_r + 34.4\log(d) + w_1 \qquad \text{[dB]} \qquad \textit{Equation 5.4}$$

Case 4: Into building path loss calculation, here the factor h_r was set to 5m for the buildings SK, AB and PB and at 1.5m for the building WA. The factor was chosen based on the receiver height on the human body and the estimated height of the first floor in meters. The exponent was n=3.44 and w_1 was varied to get the minimum RMSE. The calculated minimum RMSE was 6.5 dB with w_1= +11 dB.

In the second approach (cases 5, 6, and 7) the factor w_1 found in case 2 was used. A factor w_2 was added to account for the penetration loss and finally a factor w_3 was added as a correction for the reception at an other floor instead of the ground floor at SK, AB and PB. The receiver height was again 1.5m for all cases (see figure 5.3).

$$L_{hata\_\text{int}obuilding} = 29.39 + 34.4\log(d) + w_1 + w_2 + w_3 \qquad \textit{Equation 5.5}$$

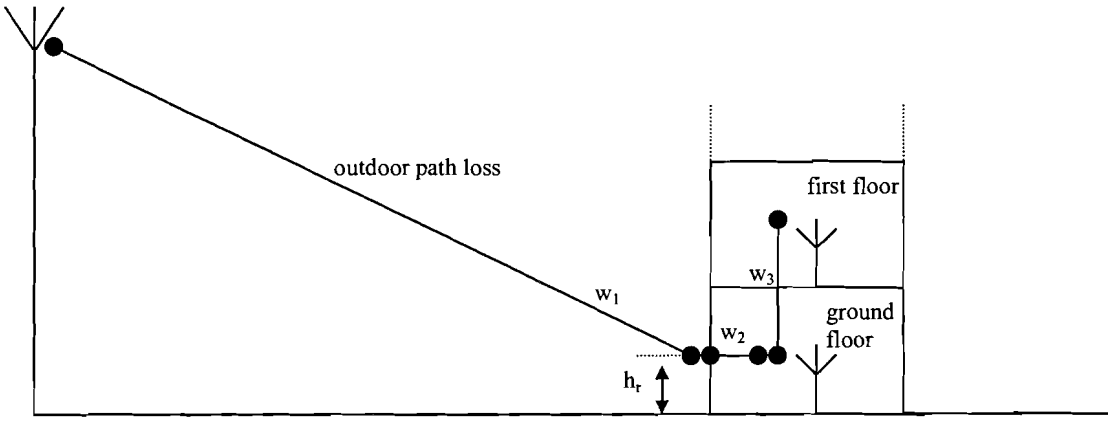

Figure 5.3 Approach to path loss calculation in cases 5 and 6

Case 5: Into building path loss calculation with n=3.44, w_1=-6dB and w_3 is 2dB. The minimum RMSE was found with a penetration loss w_2= 11 dB, here the error was 4.8 dB.

Case 6: Finally the into building path loss was calculated with the model for the outdoor path loss found in case 2, together with a 12.5 dB penetration loss (see section 4.5) and a correction of 2 dB for rooms at the first floor (see section 4.5) . With n=3.44, w_1=-6dB, w_2= 12.5 dB and w_3=2 dB the calculated RMSE was 5.0 dB. This case is plotted in figure 5.4.

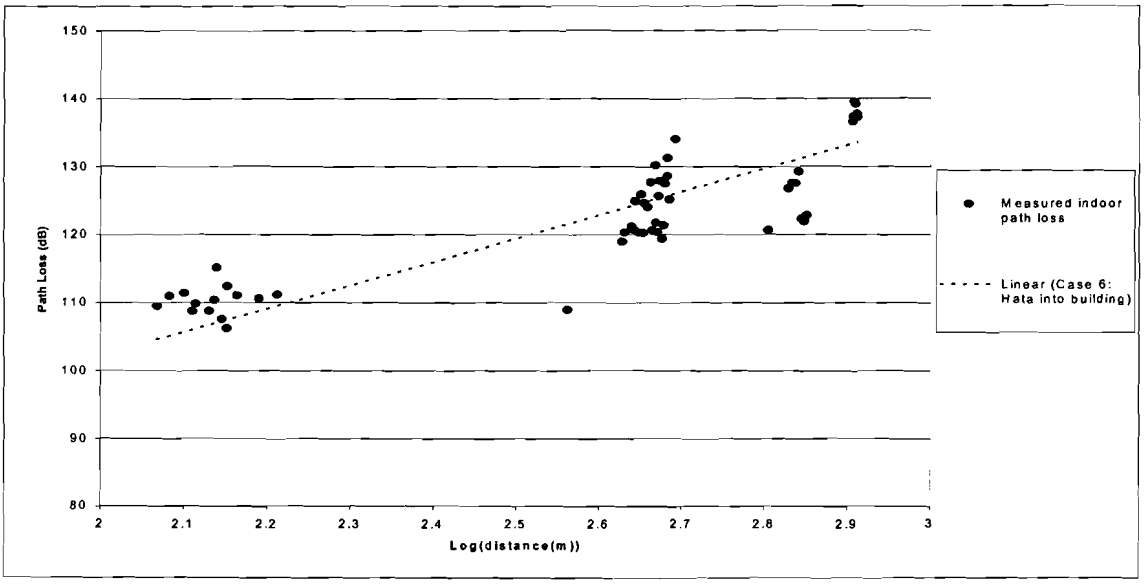

Figure 5.4 Into building path loss with modified Hata model

Case 7: In this case, the model was used to calculate the path loss in all rooms at all measured floors. The floor height was compensated with a factor w_3 = x*floor, with x in dB/floor. The lowest error calculated with n=3.44, w_1=-6 dB and the penetration loss w_2= 12.5 dB was RMSE=7.7 dB. This was calculated with x=1.7 dB/floor. When applying x=2dB/floor the RMSE becomes 7.8 dB.

The model presented here (equation 5.5) has calculated the into building path loss with a root mean square error around 5 dB for the ground floor level and around 8 dB for all floor levels. This

is not very accurate, but could be enough for the prediction of average path losses in a small cell. The amount of data used for this analysis is not enough to develop a valid model, however this analysis shows that it is possible to model the path loss with the combination of the modified well-known Hata model and extra loss factors accounting for the penetration into building.

5.3 The COST model

COST proposed two models for the case of building penetration, one for LOS and one for NLOS (equations 2.11 and 2.12). In this sections we will mainly pay attention to the LOS model. All floors having at least one side that has LOS were considered for the LOS case. Only the first floor of building AB and the building WA were omitted, this is because floor 1 of building AB has complete NLOS and building WA has only one room with partial LOS.

In the NLOS model, the outside reference $L_{outside}$ is determined in the streets adjacent to the considered rooms. Now, if we assume that 1. the reception occurs only in rooms that have an external wall (i.e. no internal walls are penetrated before reception, therefore p=0) and 2. the receiver is at a distance of 2 meters from the external wall (d=2), then the NLOS model becomes equivalent to the model already presented in section 5.2 (equation 5.5). For this reason and the small amount of rooms valid for this model, we will further consider only the LOS model.

The COST LOS model calculates the path loss as depicted in figure 2.5, we will consider 3 cases of path loss calculation.

Case1: First, the best fit of the model to the data is calculated keeping the wall losses within the boundaries recommended by COST. The parameters are:

W_e : 4-10 dB (7 dB for concrete with normal window size)
W_i : 4-10 dB (7 dB for concrete)
WG_e : 20 dB
α : 0.6 dB/m

With the frequency f=1.8 GHz, the LOS COST model is

$$L_{b\_COST\_LOS} = 32.4 + 20\log(f) + 20\log(S+d) + W_e + WG_e \cdot (1-\frac{D}{S})^2 + \max(\Gamma_1, \Gamma_2)$$

$$= 37.5 + 20\log(S+d) + W_e + 20(1-\frac{D}{S})^2 + \max(\Gamma_1, \Gamma_2) \quad [\text{dB}] \qquad \textit{Equation 5.6}$$

with

$$\Gamma_1 = W_i \cdot p$$

$$\Gamma_2 = \alpha \cdot (d-2) \cdot (1-\frac{D}{S})^2$$

The calculated minimum RMSE in this case was 8.3 dB, this value was reached with W_e=10 dB; W_i=6 dB; WG_e=20 dB and α=3 dB/m. Notice that W_e reached the upper boundary and α is considerably higher than recommended.

Case 2: Next, we varied the wall loss parameters beyond the recommended boundaries.
The calculated minimum RMSE was 5.7 dB with W_e=20 dB; W_i=2 dB; WG_e=10 dB and α=1.1 dB/m.

The error calculated here for higher floors is smaller than the RMSE calculated in case 7 of section 5.2 and a bit larger than the RMSE calculated for the ground floor in cases 5 and 6 of section 5.2. The large value of W_e can be translated into a +10 dB to +16 dB modification of the constant in the model so that W_e is within the recommended values of 4 to 10 dB. The result is plotted in figure 5.5.

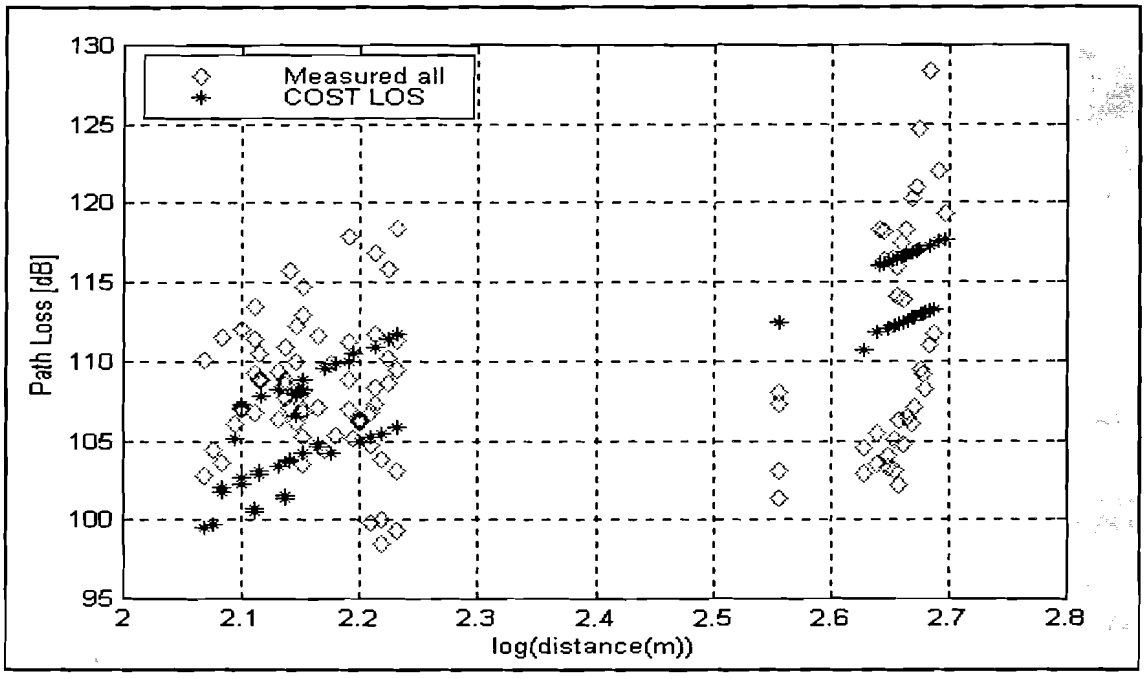

Figure 5.5 Measured and COST calculated path losses for LOS rooms

Case3: In this case, we calculated the parameters for the buildings SK and AB separately
The results are:
Building SK: RMSE= 5.2 dB with W_e=21 dB; W_i=0 dB; WG_e=20 dB and α=0 dB/m
Building AB: RMSE= 2.7 dB with W_e=12 dB; W_i=6 dB; WG_e=23 dB and α=0 dB/m

Notice the difference between the two buildings. The best fit model to the data of building SK disregards all internal information (W_i=0 dB and α=0), the calculation is based only on the angle of illumination information and an adjustment of the loss factor for best fit. The minimum error is slightly better than the error when considering all rooms. On the other hand, the parameters given for the best fit for Building AB lie within the recommended values or close to them (with the exception of α) and the internal information is included in the form of the internal wall loss factor W_i. The minimum error is smaller for building AB, indicating a better fit. In figures 5.6, 5.7 and 5.8 the measured and calculated path losses are plotted for the building SK and floors 4 and 7 of building AB. In figure 5.6 we can see the calculated and measured path losses for building SK scattered in the plot. The Hata model would give only 4 slopes for the four measured floors of SK, however the COST model scatters the calculated values to get smaller differences between the calculated and measured path losses.

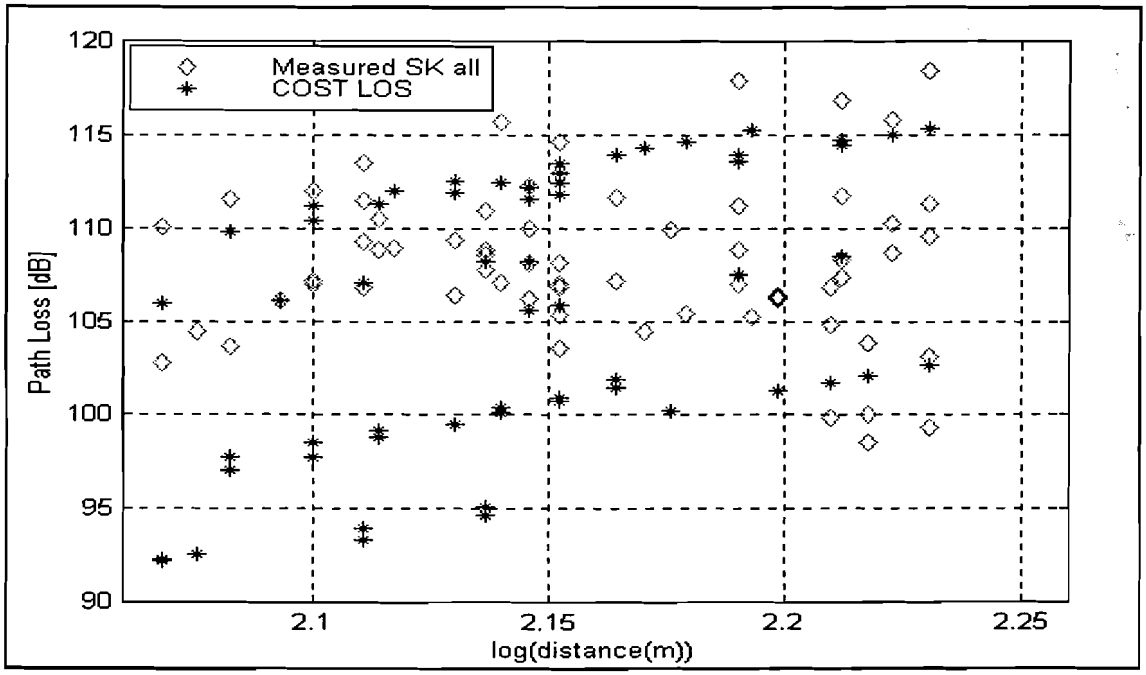

Figure 5.6 Measured and calculated path losses for LOS rooms in building SK

In figures 5.7 and 5.8, we can see the distinction made by the COST model between LOS and NLOS areas on a single floor. This division cannot be realized with the Hata model, therefore the COST model achieves a better accuracy using extra information on the internal layout of building AB.

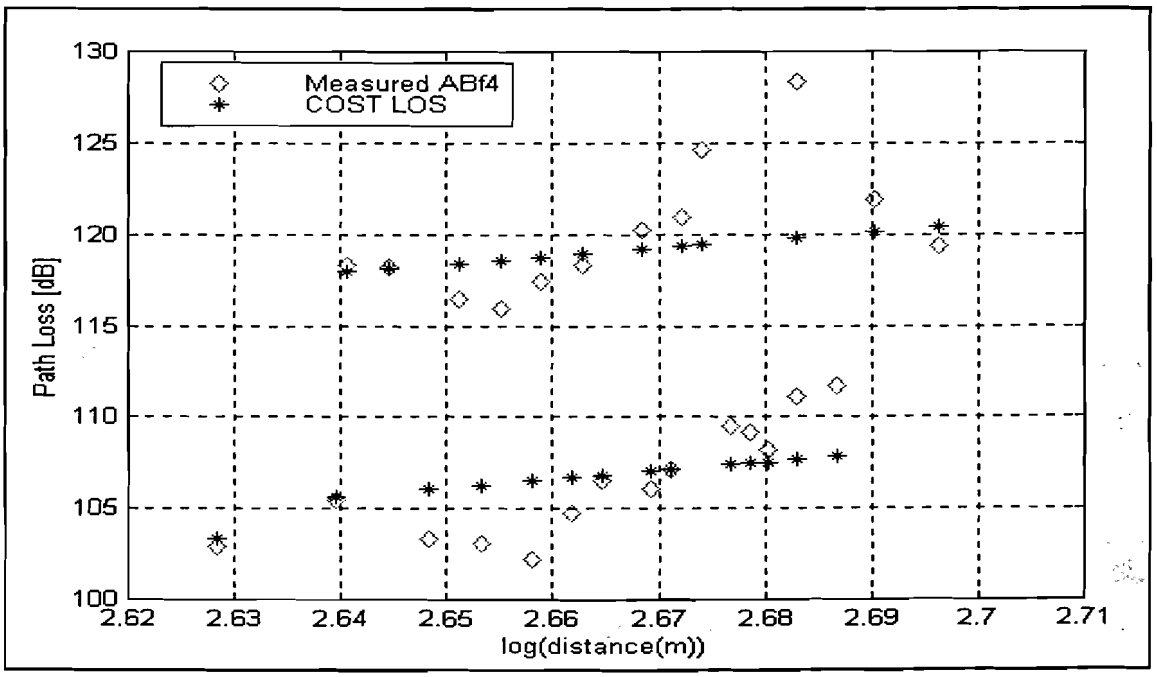

Figure 5.7 Measured and calculated path losses for LOS rooms on floor 4 of building AB

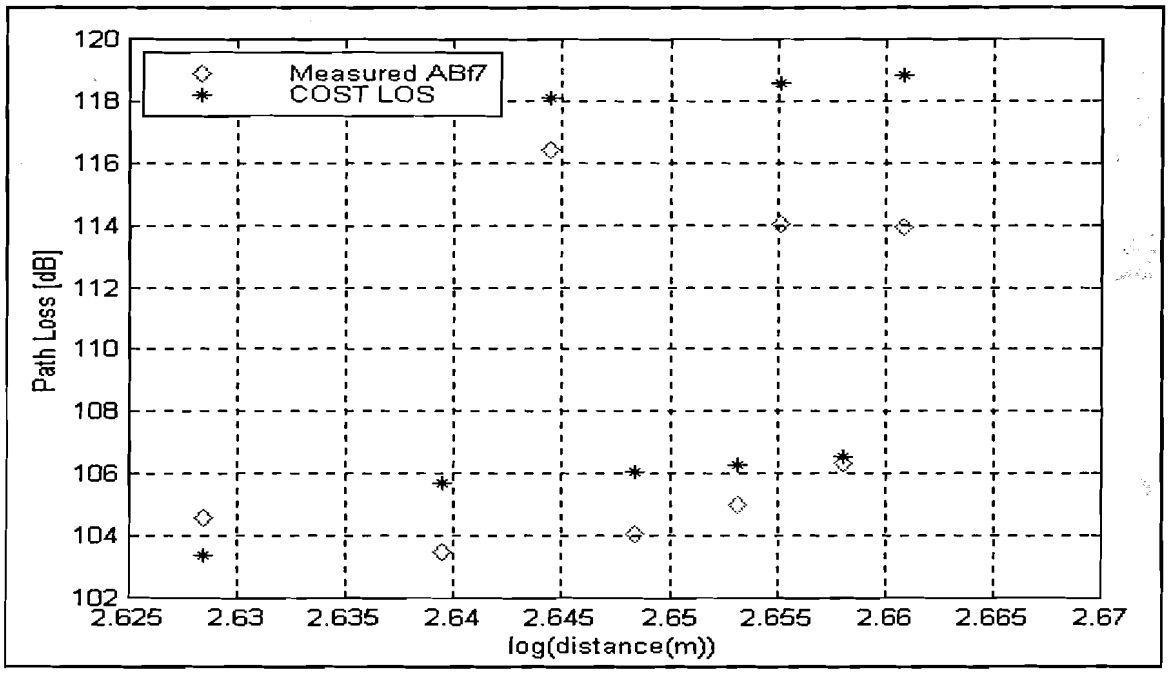

Figure 5.8 Measured and calculated path losses for LOS rooms on floor 7 of building AB

In Building SK however, the differences between areas with different conditions on a single floor are not distinguished as well as in building AB. This can in part be caused by the particular shape of the building, while building AB is of an ordinary regular shape, the SK building has an unusual U-shape with wings of different height. Furthermore, in building AB the floor layout is more regular with most rooms having the same dimensions, while the interior layout of building SK is more diverse, varying from small closed offices to more open (partitioned) working areas. Therefore, it is more difficult to assign correct values to the parameters necessary for the interior path loss, resulting in greater inaccuracy.

The LOS model presented by COST has a decay rate equal to the free space path loss exponent, n=2. The exponent was also varied between 2 and 4 together with the other parameters, but the best results were achieved with n=2. This means that the LOS COST model calculates the into building path loss by combining the outdoor freespace loss with wall losses (W_e,W_i), angle of illumination (WG_e and D/S) and other building loss factors such as α. This disregarding of other outdoor effects such as reflection, diffraction and scattering can also be the cause of a larger error for building SK. Due to its more unusual shape it is probable that significant contribution of these propagation mechanisms are present, these contributions are not included in the COST model.

In this chapter a number of attempts have been made to model the path loss in the case of indoor reception. We have applied two types of models, first the Hata model which basically uses the log-distance dependency governed by a certain decay rate and additional factors accounting for the penetration loss and floor height gain. The Hata model is a simple and easily adjustable model that may be appropriate when the average path loss of a given area (e.g. 50x50m) is required with no sharp constraints on the error margin. In cases, where more in detail analyses of the path loss is required (e.g. for a floor area), the model is not usable. The second type, the COST LOS model, used the free space loss decay rate and additional losses due to the angle of illumination, external and internal wall losses and a specific building transmission loss. The COST LOS model appears to be more suitable when path loss calculations for a specific type of building are required. Given a building of normal structure, materials and internal layout, the model could effectively include the information on building material and internal layout to calculate the path loss for that specific building.

Chapter 6 The channel sounder experiment

6.1 Introduction

The channel sounder experiment was carried out as an effort to get a better understanding of the radio wave propagation into buildings. In the first experiment, signal strength measurements were carried out in 4 KPN buildings in The Hague. From the collected data, it was possible to deduce an average building penetration loss with a certain standard deviation. It is now interesting to try to visualize the propagation into a building. How do the transmitted radio waves reach a receiver in an office room?

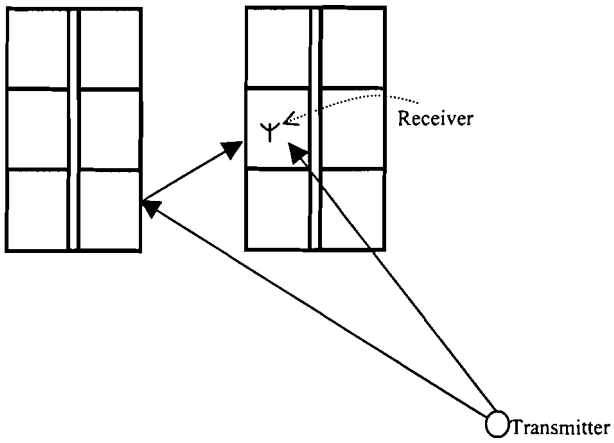

Figure 6.1 Wave propagation, reflection at and transmission through buildings

Figure 6.1 gives an illustration of two radio waves arriving at the receiver due to reflection and transmission. The signal received at the mobile station is actually a combination of a (large) number of radio waves arriving from different directions, with different magnitudes and propagation times. With the channel sounder used in this experiment it is possible to separate the different multipath components arriving at the MS. This measurement system can measure the complex impulse response (CIR) of the channel, the multipath components can then be separated in time. By using a Uniform Circular Array (UCA) antenna, it is also possible to determine the angles of arrival (AoA) of the components. The AoA are resolved with the use of the angular superresolution algorithm, MUSIC. In principle the AoA can be determined with UCA-MUSIC for every point of time of the complex impulse response.

The channel sounder, property of EUT, is normally set up for outdoor measurements were in most cases the buildings and other scatterers are at large distances compared to the UCA radius. However, in this experiment the system will be used indoors, this means that the interacting environment is much closer to the system. Therefore, we will have to consider some adaptations to the system to make it suitable for indoor measurements.

One important difference between this experiment and the first one is the height of the transmit antenna. In the first experiment the antenna was positioned above rooftop level, this setup at 1800MHz is referred to as a 'small cell' setup. The area is illuminated from above allowing 'over the rooftop' propagation. In the second experiment the transmit antenna is positioned below rooftop level, this setup resembles more the microcell concept in which the main propagation routes are not over the top of buildings but via city streets and also through buildings.

The experiment will be simulated with the ray-tracing model uFipre developed at EUT [29,30]. This model is based on geometrical optics (GO) and uniform theory of diffraction (UTD).

6.2 Impulse response model

The multipath radio channel is often described with an impulse response model. The concepts path loss and fast fading are commonly used to describe the large scale and small scale fluctuations of the signal level in a radio channel, while the impulse response is used to characterize the time dispersion in a channel. This is of importance when considering intersymbol interference caused by the channel.

The impulse response of a time-invariant channel is given by

$$h(\tau) = \sum_{n=0}^{N-1} a_n \delta(\tau - \tau_n) e^{j\theta_n} \qquad \textit{Equation 6.1}$$

where N is the number of radio waves arriving at the receiver at the time τ_n with amplitude a_n and phase θ_n. The signal received is given by the convolution of the input signal x(t) and the impulse response, and the addition of noise

$$y(t) = \int_{-\infty}^{\infty} x(\tau) h(t - \tau) d\tau + n(t) \qquad \textit{Equation 6.2}$$

One parameter often used to characterize the impulse response is the *rms delay spread* defined as [1]

$$\sigma_t = \sqrt{\overline{\tau}^2 - (\overline{\tau})^2} \qquad \textit{Equation 6.3}$$

with

$$\overline{\tau} = \frac{\sum_n a_n^2 \tau_n}{\sum_n a_n^2} = \frac{\sum_n P(\tau_n)\tau_n}{\sum_n P(\tau_n)} \qquad \textit{Equation 6.4}$$

and

$$\overline{\tau^2} = \frac{\sum_n a_n^2 \tau_n^2}{\sum_n a_n^2} = \frac{\sum_n P(\tau_n)\tau_n^2}{\sum_n P(\tau_n)} \qquad \textit{Equation 6.5}$$

where $P(\tau_n)$ is the power of the multipath components arriving at τ_n. The first arriving component sets the time τ_0=0 and all other delays are calculated relative to τ_0. In order to prevent the addition of noise in the calculations, all power levels below a certain *noise threshold* are omitted. This noise threshold was set at approximately 5 dB above the average noise level.

The relation between the time delay spread of the channel and the coherence bandwidth B_c of communication system is given by

$$B_c \sim \frac{1}{\sigma_\tau} \qquad \textit{Equation 6.6}$$

This is the bandwidth over which the signals are passed through the channel with approximately equal gain and linear phase of all spectral components [1].

$$B_c = \frac{1}{5\sigma_\tau} \qquad \textit{Equation 6.7}$$

Here the coherence bandwidth is given as the bandwidth over which the frequency correlation function is above 0.5. If this correlation is required to be above 0.9, then the rms delay spread would have to be a factor 10 smaller for the same bandwidth.

6.3 The channel sounder

6.3.1 Principle

If we consider the radio channel as a linear system with white noise, n(t) applied as the input to the system, and take the cross correlation of its output w(t) and a delayed replica n(t-τ)of the input, then the resulting cross correlation coefficient is proportional to the impulse response of the system, h(τ), evaluated at the delay time τ [4]. In formula:

$$R_n(\tau) = E[n(t)n^*(t-\tau)] = N_0\delta(\tau) \qquad \textit{Equation 6.8}$$

The factor $R_n(\tau)$ is the autocorrelation function of the noise and N_0 is the single-sided noise power spectral density. The output signal is a convolution of the impulse response and the input signal,

$$w(t) = \int h(\xi)n(t-\xi)d\xi \qquad \textit{Equation 6.9}$$

The cross correlation of the output signal and the delayed input is given by,

$$E[w(t)n^*(t-\tau)] = E[\int h(\xi)n(t-\xi)n^*(t-\tau)d\xi] \qquad \textit{Equation 6.10}$$

$$= \int h(\xi)R_n(\tau-\xi)d\xi \qquad \textit{Equation 6.11}$$

$$= N_0 h(\tau) \qquad \textit{Equation 6.12}$$

From this it follows that the impulse response of the radio channel can be evaluated by using white noise as the input and applying the crosscorrelation of output and delayed input noise.

The channel sounder used in this experiment is based on this principle. It is however unrealistic to generate a white noise signal at the transmitter and its replica at the receiver. Therefore, a

deterministic waveform with noise-like properties, the so called *pseudonoise binary sequence*, is applied in the channel sounding system. The sequence is known by both the transmitter and receiver, it consists of +1 and –1 transitions and has a period of 511 bits. The autocorrelation function is of triangular form with a base width of $2\tau_0$ and period T (the periodic reoccurrence of the sequence).

6.3.2 Specifications

The chip length τ_0, which indicates the time resolution is 20ns (chiprate=50 Mbit/s). In order to separate two radio waves of equal magnitude in time, it is necessary that they have at least a delay difference of 20 ns. This is a difference of 6 meters in total path length.

After being modulated and up converted, the pseudonoise sequence is amplified to 27 dBm and then transmitted at a carrier frequency of 1900 MHz. The bandwidth of the sounder is 100 MHz. At the receiver the signal is first down-converted and filtered. Then it is combined in the demodulator with a replica of the sequence that has a slightly lower chip rate. The small difference in chip rate causes a time shifting between the two signals, integration of the product of these two signals gives the desired cross correlation.

6.3.3 Setup

The experimental set-up is given in figure 6.2. The transmitter is located outside, while the receiver is located in the middle of an office room on the ground.

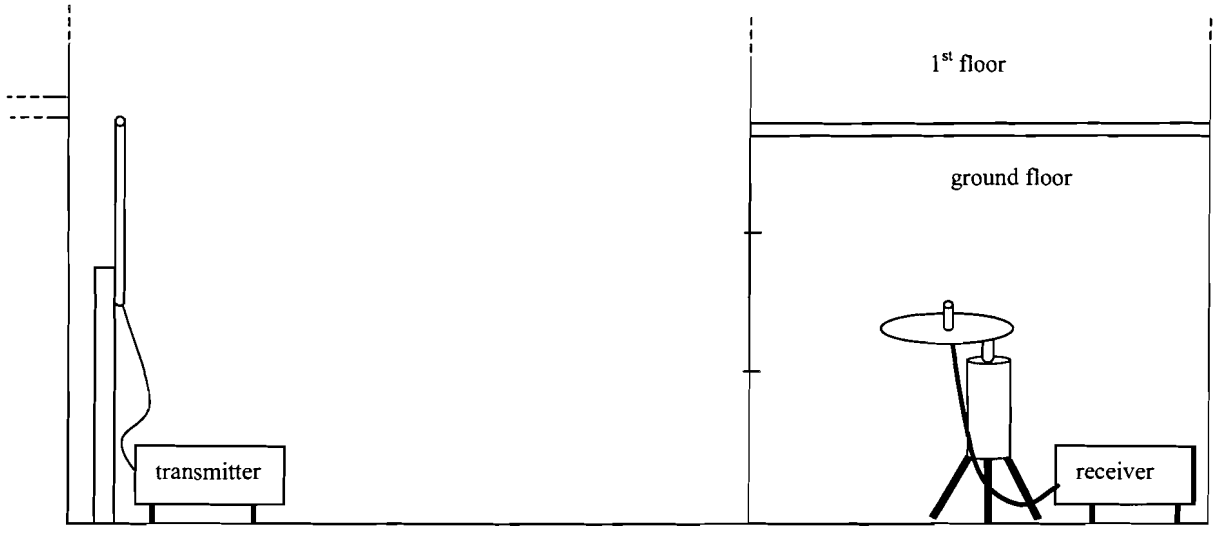

Figure 6.2 Measurement setup channel sounder experiment

6.4 Antennas

At the transmitter end, an omnidirectional collinear antenna was used. The vertical 3 dB beamwidth was only 6^0, giving a 12 dBi gain in the azimuth plane. The antenna was positioned at a height of 5.5m

At the receiver end, a rotating antenna was used. By rotating in a circle during the measurement, this single antenna emulates a UCA consisting of 157 elements. The antenna used was a 2 dBi

sleeve antenna with an omnidirectional radiation pattern in the azimuth plane. The vertical beamwidth is 60^0 and the directivity is maximum for an elevation angle of 20^0.

In theory, a radio wave arriving at the receiver from a transmitter at higher altitude (upper hemisphere) will be accompanied by a duplicate arriving from the lower hemisphere due to ground reflection at gazing angles. UCA-MUSIC cannot make a distinction between radio waves arriving at the same elevation angle from the upper hemisphere (angle has a positive sign) and lower hemisphere (angle has a negative sign). For the estimation of the angles of arrival, we are only interested in the waves arriving from the upper hemisphere. Therefore the used antenna has a lower sensitivity towards the lower hemisphere, also a 5λ groundplane was used to obstruct the components arriving from negative elevation angles. The receive antenna was positioned at a height of 1.5m.

6.5 UCA-MUSIC

The measurement method actually consists of two stages, first the reception of radio waves using a uniform circular array and second, the estimation of the angles of arrival using the UCA-MUSIC angular superresolution algorithm.

The most common antenna array geometries used for angle of arrival measurements are the uniform linear array (ULA), the rectangular lattice array and the uniform circular array (UCA). The disadvantage of the ULA is that it is not suited for estimation of both the azimuth and elevation angles of arriving radio waves. The rectangular lattice on the other hand is capable of resolving two-dimensional (azimuth and elevation) angles of arrival [31]. However the UCA is the preferred configuration, this is because 1. for this array the angular resolution is independent of the azimuth angles of the incident waves and 2. the array can be simply synthesized with one single antenna. This also eliminates the problem of mutual coupling between elements.

Consider the UCA illustrated in figure 6.3 with the origin of the coordinate system at its center.

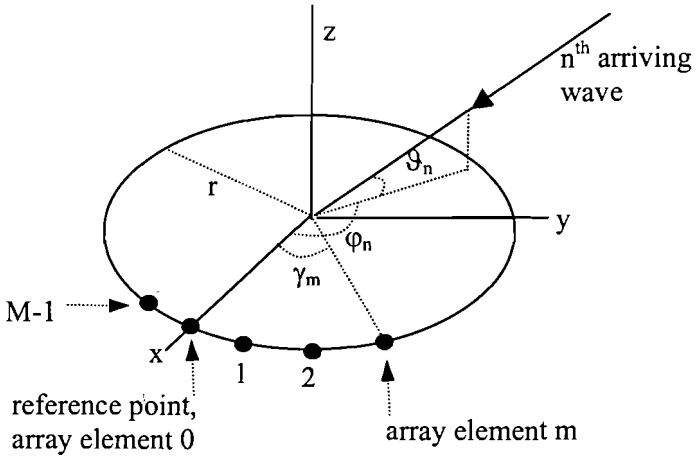

Figure 6.3 Circular antenna array

The azimuth angle of the array element m is given by

$$\gamma_m = \frac{2\pi m}{M} \qquad \textit{Equation 6.13}$$

and ϑ_n and φ_n are the elevation and azimuth angles of the n^{th} wave.

The position of the array element is given by the vector $\overline{p_m} = (r\cos\gamma_m, r\sin\gamma_m, 0)$ and the direction of the incoming wave is given by the vector $\overline{r_n} = (\cos\vartheta_n \cos\varphi_n, \cos\vartheta_n \sin\varphi_n, \sin\vartheta_n)$. The phase difference between the complex envelope of the signal received at the center of the array and the element m is

$$\psi = e^{j\frac{2\pi}{\lambda}\overline{r_n}\bullet\overline{p_m}} \qquad \textit{Equation 6.14}$$

$$= e^{j\frac{2\pi}{\lambda}r\cos\vartheta_n\cos(\varphi_n-\gamma_m)}$$

The azimuth and elevation angles of arrival of the radio waves are contained in the phase differences of the signals received at the array elements. These angles of arrival can be determined in different ways, one method is by scanning the environment with a UCA. The advantage of this method is that it is simple and gives direct results. However, the disadvantage is the limited angular resolution, the best achievable resolution is equal to λ/d. Another way of resolving the angles of arrival is with the use of a high resolution algorithm like MUSIC. The algorithm uses the complex impulse response determined at each of the antenna elements to obtain the covariance matrix used for AoA estimation.

The received correlation signal at array element m can be written as

$$y_m(\tau) = \sum_{n=1}^{N} c_n g(\varsigma_n) e^{j\varsigma_n\cos(\varphi_n-\gamma_m)} x(\tau - T_n) + \eta_m(\tau) \qquad \textit{Equation 6.15}$$

with the elevation angle given by

$$\varsigma_n = \frac{2\pi r\cos(\vartheta_n)}{\lambda} \qquad \textit{Equation 6.16}$$

The signal $x(\tau)$ is the autocorrelation function of the pseudonoise sequence, $g(\zeta)$ is the elevation voltage pattern of the array elements, c_n is the complex amplitude of the n^{th} incident wave and T_n is the delay time of that wave relative to arrival time of the first wave. The factor η represents the noise.

Equation 6.15 rewritten in vector notation is

$$\underline{y} = U(\theta)\underline{s} + \underline{n} \qquad \textit{Equation 6.17}$$

with $\theta = \zeta e^{j\varphi}$

From this equation the covariance matrix is determined. For a detailed description of UCA-MUSIC see [8, 21, 25, 31].

To approximate the true covariance matrix needed for accurate AoA estimations a large number of measurement rotations called *snapshots* are performed [25]. The matrix is then obtained by

averaging over these snapshots. In this experiment a total of 40 snapshots were taken for each measurement.

6.6 panorama camera

To visualize the environment where the measurements are taken, a panorama camera is used. This camera (Seitz Roundshot 35/35) takes a 360-degrees photo by rotating on the same axis as the rotating antenna. UCA-MUSIC uses the starting position of the rotating antenna as a reference point to calculate the azimuth and elevation angles of the incoming waves. The rotating antenna is started at a certain visual reference point, which is then captured on the photograph to be able to relate the taken photo to the angle of arrival plots.

6.7 Adaptations for indoor measurements

An important parameter of the UCA-MUSIC is the array radius. The angular accuracy decreases proportionally with decreasing array radius, therefore a large array radius is desired. However there are some important factors that limit the size of the array, these are:

1. *The plane wave assumption.* The electromagnetic field around the array is assumed by UCA-MUSIC to be comprised of a summation of plane waves. Therefore the array size must be small enough when compared to the distance of the array to the nearest scatterer.
2. *The Narrowband array assumption.* Each array element should receive a multipath wave identically, except for a phase change. Therefore, the array size should be small compared to the distance covered in one bit time (6m).
3. *Physical restrictions* (practical size and weight)

The radius of the UCA is normally 30 cm, this size is large enough to achieve good angular resolution (1^{o}-2^{o}) and complies with the assumptions 2 and 3. However, in an indoor environment the scatterers are much closer to the UCA. This means that the array radius has to be taken even smaller, resulting in less angular accuracy. Therefore, a tradeoff has to be chosen.

In practice, a radio wave is not a perfect plane wave, there is always a phase difference, either small or large, along the wave front. The 'worst case' scenario is the arrival of a spherical wave. Since the algorithm assumes the arrival of plane waves, we could expect a decomposition of a spherical wave into plane wave components. However the real effect of the 'phase error' due to the spherical nature of the radio waves on the performance of the algorithm is unknown. For this reason, the calculation of the array radius necessary for indoor measurements was done intuitively.

First we calculate the phase error, this is the phase difference φ due to the path length difference d given in figure 6.4.

$$\varphi = \frac{360^{0} * d}{\lambda} \qquad \textit{Equation 6.18}$$

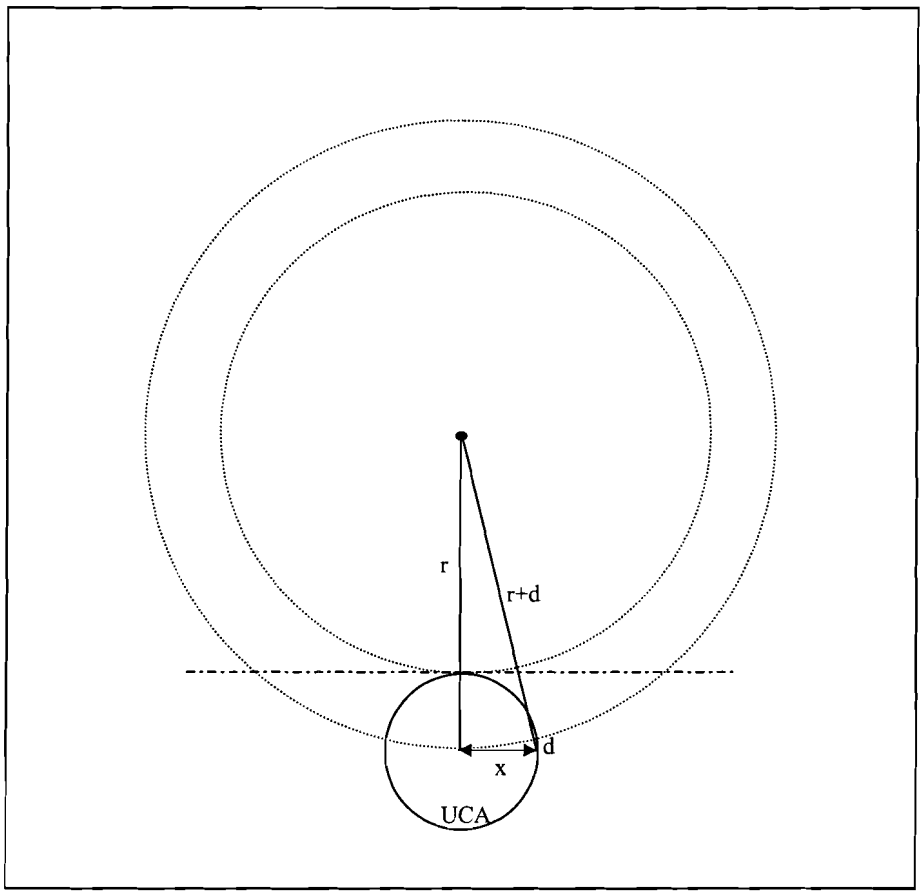

Figure 6.4 Spherical wave arriving at UCA

With the Pythagoras equation ($x^2+r^2=(r+d)^2$) , the UCA radius x is given as a function of the distance to scattering object and the path length difference. Now we can calculate the UCA radius given a certain phase error and distance to the closest scatterer. Since the maximum allowable phase error for UCA-MUSIC calculations is unknown, we considered the performance of the system for outdoor measurements with a 30cm radius as a reference [25,8]. The outdoor measurements show that the algorithm can correctly resolve radio waves coming from objects at 15 to 20m distance from the receiver. If we assume that these objects radiate a spherical wave, then the phase error will be approximately 5° to 7°.

As a reference for the indoor case we take an empty room with the dimensions 4x4m, the minimum distance r to the wall is then 2m. An allowable phase error between 5° and 7° gives a radius of 9.4cm to 11.1cm. For this experiment we chose x=10cm, this is also physically the smallest possible radius in the present configuration. The difference d in path length is then less than $\lambda/62$.

The angular resolution will be approximately 3 times (30/9.4) worse than with the original UCA. This means a new angular resolution of 3^0 to 9^0 , this is still good enough to visualize global angles of arrival of the largest wave components.

6.8 The Experiment

The experiment consisted of two indoor measurements at KPN Research in Leidschendam. One measurement was carried out in room c10 with the outer wall facing the transmitter, the other measurement was done in room c15 with the outer wall not facing the transmitter (see figure 6.5). The measurement in room c10 represents a LOS case with vegetation between the transmitter and the room. The measurement in room c15 represents an NLOS case. To approximate a static environment as much as possible the measurements were carried out after working hours.

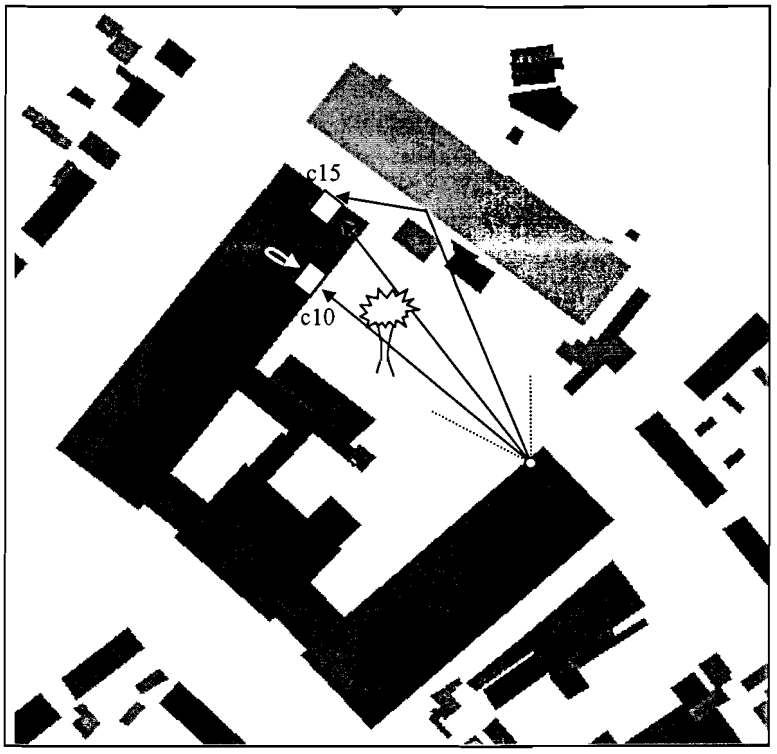

Figure 6.5 Topview of the site for the channel sounder experiment

The transmitter was positioned just in front of the E-wing of the building and the receiver was positioned in the middle of the empty rooms.

6.8.1 Link Budget

The received signal is expressed by:

$$P_r = P_t + G_t + G_r - L_t - L_r - L_b \qquad \text{[dBm]} \qquad \textit{Equation 6.19}$$

where

P_r = received power in dBm
P_t = transmitted power in dBm
G_t = gain of the transmit antenna in dBi
G_r = gain of the receive antenna in dBi
L_t = transmitter cable losses in dB
L_r = receiver cable losses in dB
L_b = path losses in dB

The path loss L_p is comprised of the free space loss L_{fs}, the building penetration loss and other additional losses. In figure 6.6 the link budget is given.

Transmit power P_t (+)	27	dBm
Gain of the transmit antenna G_t (+)	12	dBi
Gain of the receive antenna G_r (+)	2	dBi
Transmitter cable losses L_t (-)	1.3	dB
Receiver cable losses L_r (-)	5.13	dB
Maximum free space loss L_{fs} (-)	78	dB

Figure 6.6 Link budget

6.9 Experimental results

The total received power P_{tot} was calculated by integrating the measured power delay profile (pdp) from the start of the impulse response to the level where the pdp reached the noise threshold. The total received power was also calculated from the pdp simulated with uFipre. In c10 P_{tot} was –52 dBm, while the predicted total power $P_{tot\_predicted}$ was –59 dBm. The free space loss in this case was 76.6 dB, with the values given in figure 6.6 we can calculate a total additional loss of 10 dB. The P_{tot} in room c15 was –59 dBm, here $P_{tot\_predicted}$ was –66 dBm. The free space loss for c15 is approximately 78 dB, indicating a total additional loss of 15.6 dB. The additional losses include the room losses, unfortunately an outside reference is not available to calculate these room losses.

6.9.1 Analysis of small scale characteristics

The chi-square goodness of fit was used to test the distribution of the received signal amplitude. This was done for 157 positions on a circle for a total of 50 time bins per room (i.e. 50 cases). The results indicate for c15 a Rayleigh distribution for the amplitude in 23 cases, a Rician distribution in 5 cases and a lognormal distribution in 5 cases. In c10 the number of acceptances are 11 for Rayleigh and 1 for Rician. These results indicate that the amplitude of the received signal is Rayleigh distributed. In figure 6.7 the normalized theoretical Rayleigh distribution and distribution of the measured samples in the NLOS case are plotted. The standard deviation for the logarithm of the measured variable is 5.12 dB.

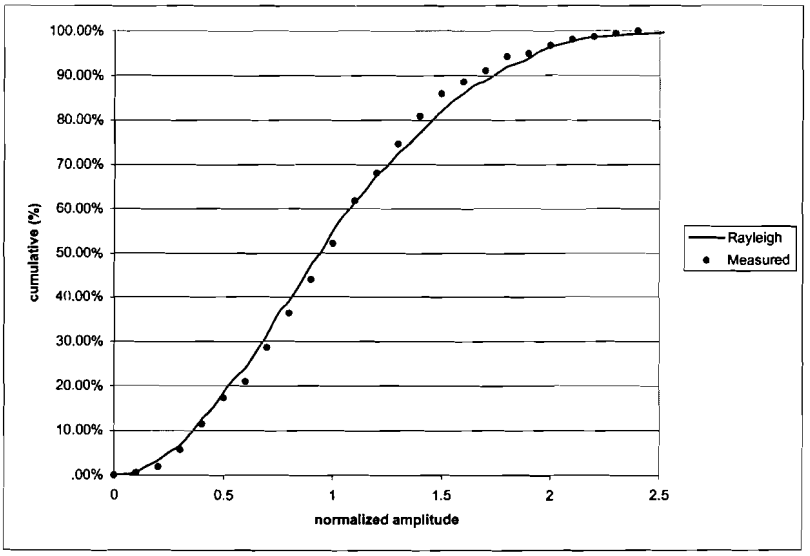

Figure 6.7 CDF of 157 normalized samples and Rayleigh process

In a LOS situation, a Rician distribution is normally expected; however, in our case the direct path from transmitter to the outer wall of the room was obstructed by vegetation, causing a spreading of the radio waves.

In [22], an analysis of the indoor radio channel was done with a similar measurement setup. The results showed that for most of the time bins the fading best fits a Rayleigh distribution. In addition, Hashemi reported in [5] that most empirical results indicate a Rayleigh distributed amplitude.

6.9.2 Impulse response and angles of arrival

The impulse response and angle of arrival results for the two rooms are presented in the form of two figures containing the following sections:

1. Ray tracing results with uFipre
2. Measured and predicted impulse responses
3. Elevation angle of arrival plot
4. Panoramic photograph of the rooms
5. Measured impulse response
6. Azimuth angle of arrival plot
7. Angular power distribution plot

In the ray tracing section, the 20 strongest rays are plotted. In the angle of arrival plots the radio waves are represented by dots, the size of the dots indicate the signal strengths relative to the total received power. The elevation plot contains the elevation and azimuth angles of the radio waves, while the azimuth angle of arrival plot gives the delay time and azimuth angle of the radio waves. The results of room c10 are plotted in figure 6.9 and the results of room c15 are plotted in figure 6.10. Additionally, the sections 3 to 7 are plotted in figure 6.11 for room c15 measured with an array with a radius of 30 cm.

Impulse response
For room c10 the simulated impulse response has a reasonable coincidence with the measured impulse response. The first and second single peak of the response measured in room c15 are reproduced by uFipre with a shift in time for the second peak. This single peak is probably caused by the component travelling according to the path marked with the dot in section (1) in figure 6.8. The channel shows a wider response over time than the response produced with uFipre (space after first peak). The first peaks of the simulated response are also higher than the measured peaks.

Notice also the similarity between the impulse responses for room c15 measured with the 10 cm and 30 cm radius (e.g. the single peak at 0.7 usec). These two measurements were taken on different days, nevertheless the impulse responses show a similarity indicating that the channel is reasonably stationary.

The measured and simulated rms delay spread are given in figure 6.8.

Room	$\sigma_{t\ measured}$ (ns)	$\sigma_{t\ simulated}$ (ns)
c10	54.2	79.9
c15	65.3	55.2
c15 (r=30m)	65.7	55.2

Figure 6.8 Measured and simulated rms delay spread

The channel bandwidth for DCS1800 is 200 KHz while the coherence bandwidths calculated with equation 6.7 are well above 200 KHz. In this case the measured delay spread satisfies even the more strict condition ($Bc=1/50\sigma_t$).

Angles of arrival

In room c10 (figure 6.9), the radio waves arrive mainly from the window. The first contributions arrive from the right side of the window, slightly to the right of the transmitter position indicated with the dashed vertical line. These contributions are mainly waves coming straight from the transmitter that were scattered by the vegetation and radio waves reflected at the *main entrance* section of the building. The second group of radio waves arrives through the left part of the window, these waves are reflected at the *neighbor* building. These two observations correspond with the uFipre prediction, the waves reflected from the neighbor building travel a longer path than the direct waves and waves reflected at the *main entrance*. One observation not captured by uFipre is the reflection at the inner walls of the building. The contributions due to internal reflections can be seen at the edges of the plot.

In room c15 (figure 6.10), the first contributions arrive through the wall between transmitter and receiver. Here the waves do not arrive exactly from the transmitter position. This is possibly due to a worse angular resolution and errors made in the positioning of the system and the reference points. Nevertheless, the plot indicates that the first and strongest contributions arrive through the wall in question. From the window in the external wall we can notice delayed contributions scattered over the window width. Again, the contributions due to internal reflection are visible.

The results for the 30 cm radius array in room c15 (figure 6.11) indicate good resolution of the azimuth angles of arrival through the wall, but less strong components arriving from the room window when compared with the results for the 10 cm radius. Furthermore, the majority of the components are resolved as coming from elevation angles larger than 30 degrees. This indicates that the plane wave assumption is probably not valid for the 30 cm radius array in the indoor environment.

In this experiment we have demonstrated that the system can be used indoors for impulse response and angle of arrival measurements. From the results we can deduce that propagation through building walls can be the main propagation mechanism, even through multiple building walls as is the case in room c15. We can say that the choice of an array with smaller radius was a good one in the sense that the modified configuration still indicates the approximate angles of arrival despite a decrease in resolution. Secondly, the adaptation provided the information for comparison with the unmodified 30cm radius array in an indoor situation. The 30 cm radius measurement showed problems with the elevation angles and differences with the components arriving from the window area when compared with the 10 cm measurement.

The exact behavior of the UCA-MUSIC algorithm in the case of indoor reception is still not known. This could be studied by taking measurements with different UCA configurations in an aneochoic chamber with known close-by reflectors.

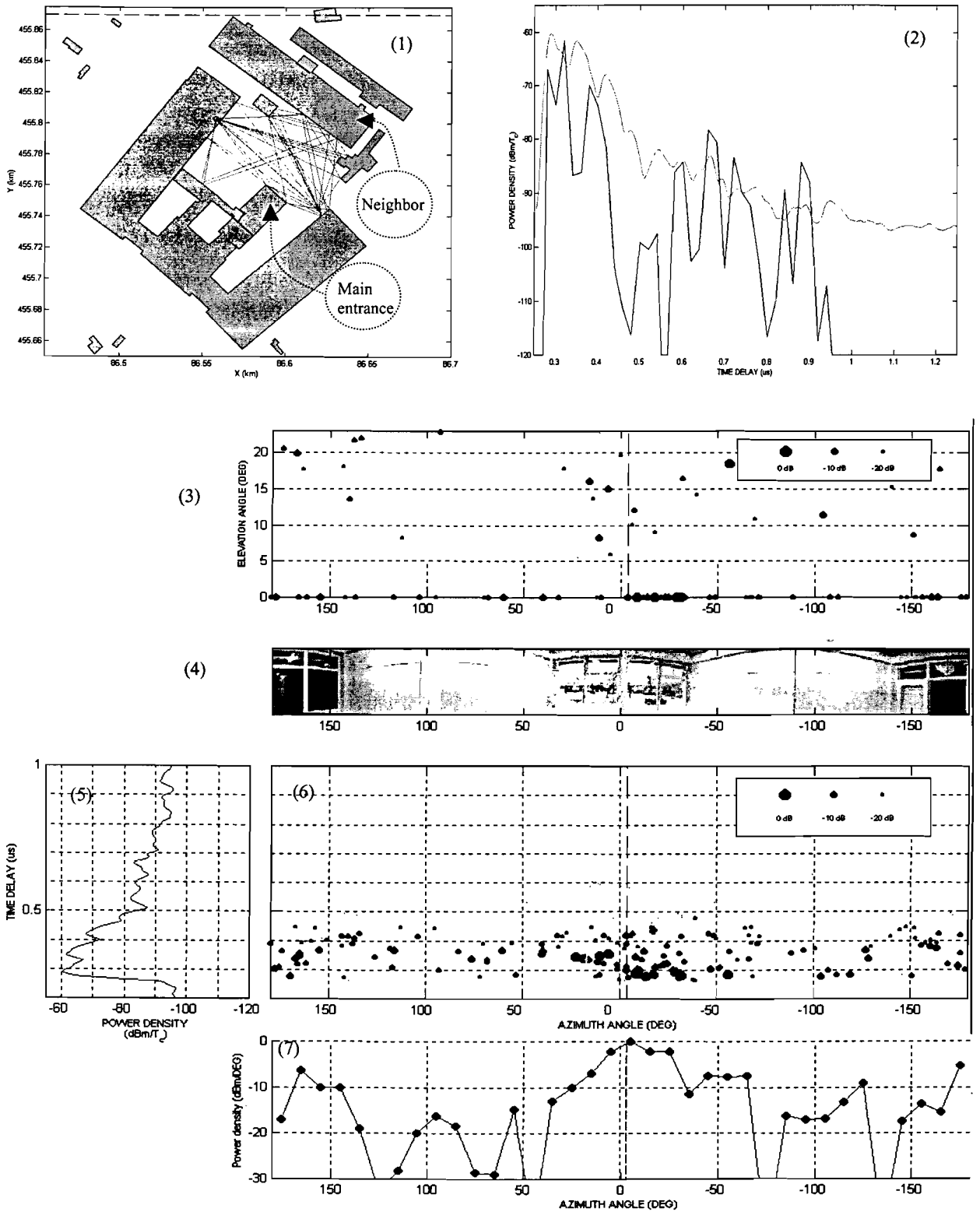

Figure 6.9 Impulse response and angle of arrival plots of room c10

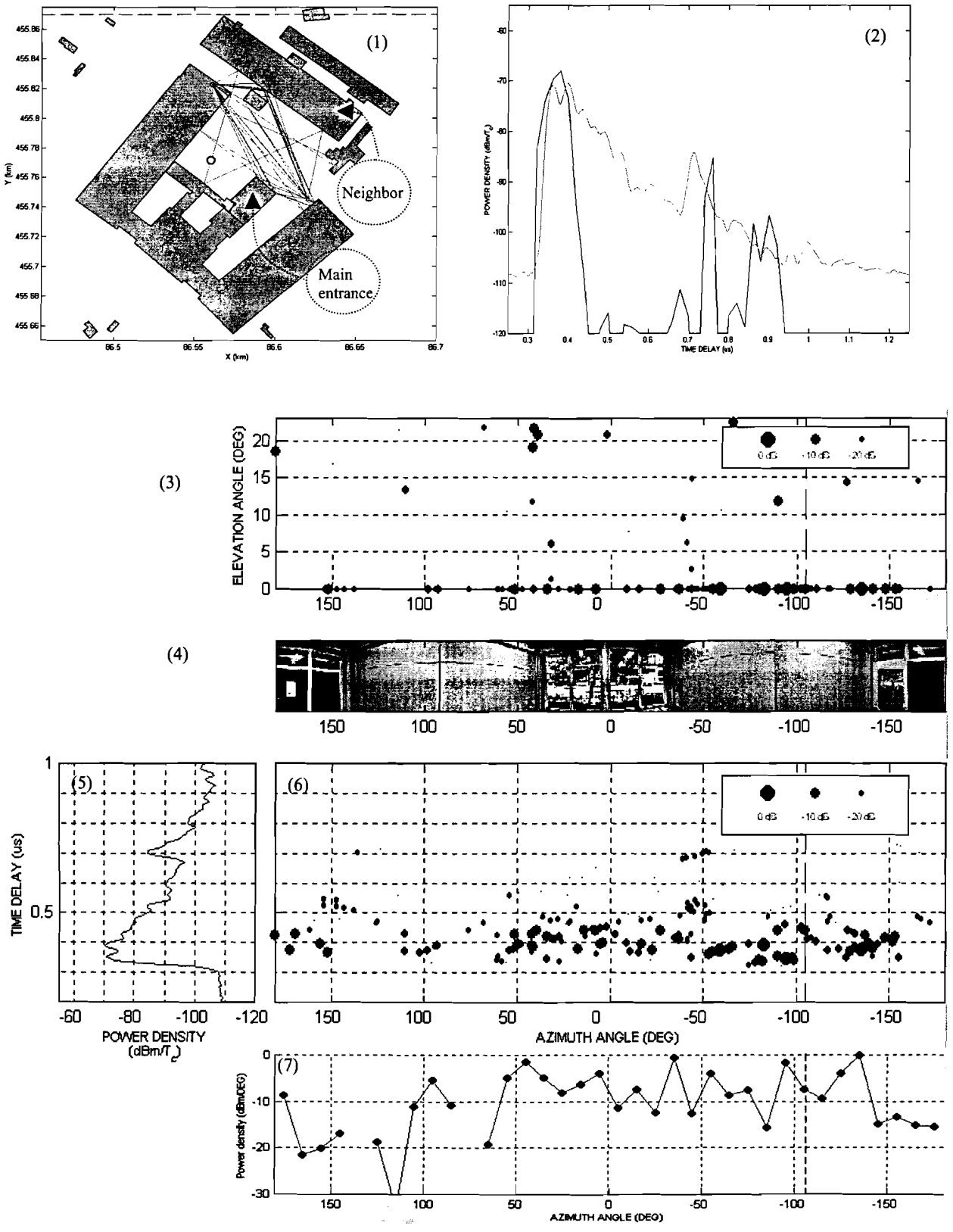

Figure 6.10 Impulse response and angle of arrival plots of room c15

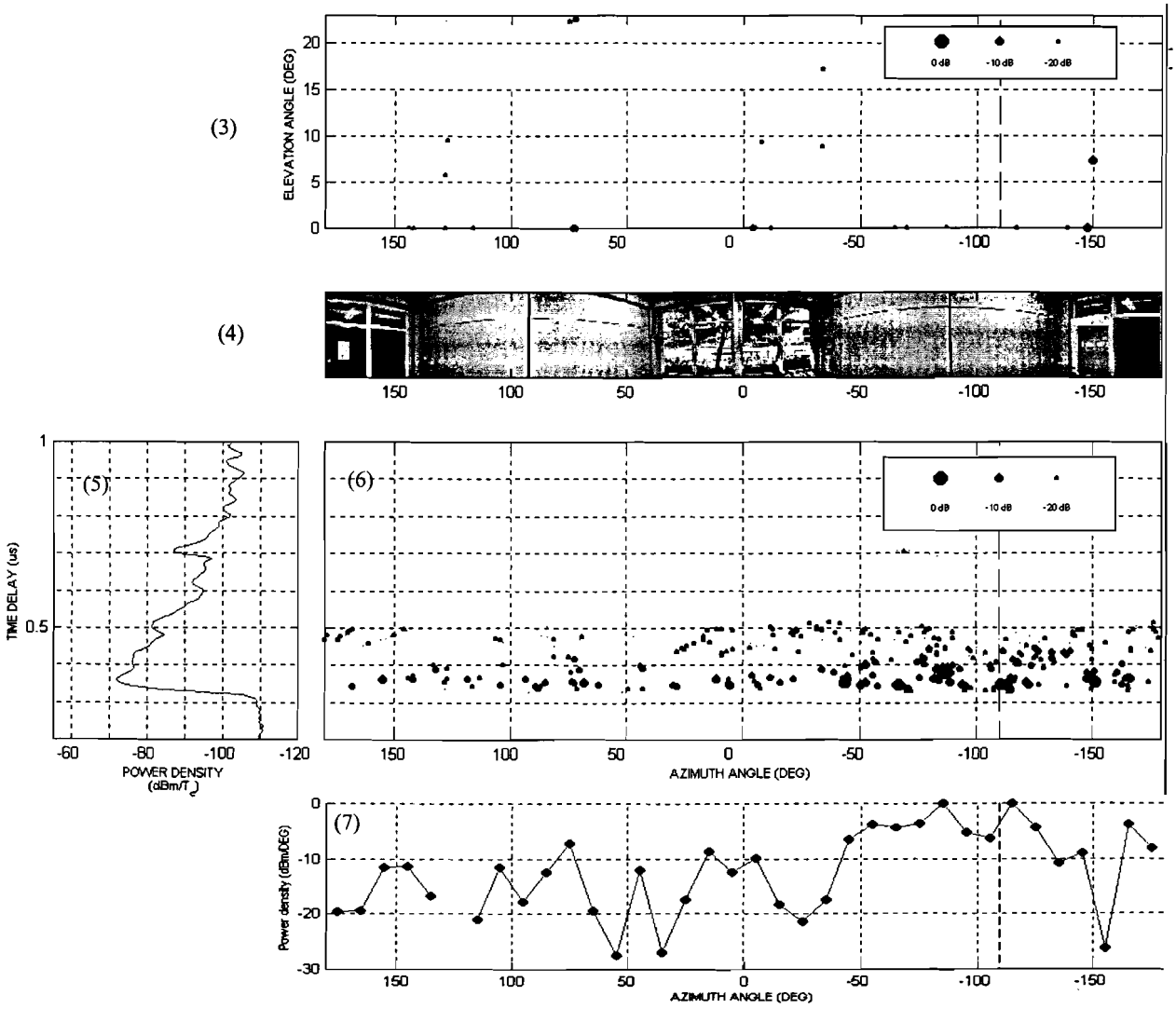

Figure 6.11 Impulse response and angle of arrival plots of room c15 with array radius=30cm

Chapter 7 Conclusions & Recommendations

7.1 Conclusions

In this project, two experiments have been carried out to characterize the propagation of radio waves into buildings. In the first experiment, results from measurements taken in office buildings situated in an urban small cell in The Hague indicated an average penetration loss of approximately 12 to 13 dB with a standard deviation of 5 to 6 dB. The correlation between the outdoor and indoor measured signal strengths used for the penetration loss calculations showed a correlation of 0.7. This indicates a certain relation between the signal strength measured in a room and the signal strength measured just outside the room.

In general, there is an increase in the average signal strength when the receiver is moved upward in a building (up to floor seven), the worst case situation is at ground floor. This is in accordance with several other studies done on this subject. The observed increase has been found to be dependent on factors such as the antenna radiation pattern in buildings close to the transmitter (with (partial) line of sight), and the local urban clutter. The relationship between the floor height and extra gain with respect to the ground floor level is not linear; even on the same floor significant differences can be noticed between rooms with line of sight (LOS) and rooms with no line of sight (NLOS). On higher floors, the difference between rooms with LOS and NLOS is larger than at the lower floors. However, the floor height gain is often represented as a linear relationship governed by a single factor. This factor has been found to be approximately 2dB/floor.

Statistically, the small-scale variations can be modeled as having a Rayleigh probability density function. This has been demonstrated in several other studies and has been confirmed here. In other studies, the large-scale fluctuations have been often modeled as having a lognormal distribution, in this project this was shown to be the case when considering the lower floors. Significant differences have been observed at higher floors between areas directly facing the transmitter (LOS) and areas not facing the transmitter (NLOS).

We have seen that in general there is more variability in the indoor average received signal strength compared to the outdoor average received signal strength. This causes larger errors when predicting the path losses. For cells with radii of 1km or more the predictions are done for grids not smaller than 50X50m. In these cases simple and a coarser modeling is enough to predict the coverage. In general, a model containing three ingredients can be used to describe urban propagation, the components are 1. an n*log(d) dependence with d being the range from transmitter to the area where the receiver is located, 2. lognormal fluctuations (slow fading) of the local mean within the reception area and 3. superimposed fast fading which follows a Rayleigh distribution. This approach can also be used in the case of building penetration. We used the model of Hata as a starting point and showed that it is possible to calculate path losses with RMS errors of 5 dB for the ground or first floor and up to approximately 8 dB for higher floors .

In the second model presented, the COST model, more information was used to calculate the path losses. When including extra information on the losses due to indoor radio wave propagation such as transmission through internal walls, the model can make distinctions between areas on the same floor. This was not possible with the Hata model. Consequently it was possible to further decrease the error; in our analysis the COST model calculated the path loss in LOS rooms with a root mean square error of 5.7 dB.

In the second experiment, measurements were taken in a microcell type of scenario. Here an existing uniform circular array antenna for outdoor measurements was adapted in order to measure the impulse response of the channel and angles of arrival of the radio wave components. The choice of an

array with smaller radius resulted in still a reasonable indication of the true angles of arrival despite a decrease in resolution. We have seen that propagation through building walls can be the main propagation mechanism, even through multiple building walls. Furthermore, the adaptation provided the information for comparison with the unmodified antenna array in an indoor situation. This indicated the problem areas of the unmodified configuration.

The modeling in microcells can be done in a different way. In this case, the ray tracing model uFipre was used for the simulations. This model used a detailed database of building structure information to calculate the propagation parameters (path loss, power delay profile and rms delay spread) by means of ray tracing including all the propagation mechanisms. It showed capable of correctly calculating received signal strengths and the time dispersion of the channel.

With the further increase in mobile communication, the need for more capacity will have to be satisfied with implementation of smaller cell configurations. When moving from large cells to smaller cells, the modeling of radio wave propagation moves from calculations with simple, empirical-statistical models to more complex deterministic models. The addition of extra building information (and propagation mechanisms in deterministic models) gives on one hand the possibility for more accurate calculations, but on the other hand it makes the calculations more complex and time consuming. Therefore a compromise has to be found. Recently, researchers have been developing models that use a combination of empirical-statistical and deterministic methods. In any case the main problem in the prediction of into building coverage in small cells will be the acquisition of enough measurement data for empirical-statistical modeling. In microcells on the other hand both indoor measurements and further improvement of deterministic models and advanced tools like angle of arrival measurement systems will be of great importance.

7.2 Recommendations

In this experiment only four office buildings in an urban area were considered. In order to adequately include radio wave propagation into buildings in empirical-statistical path loss models, more measurements should be done in different environments. The range of types of buildings and types of environments should be divided in subcategories. Since the ground floor is the worst case situation, efforts could be first concentrated on getting more data on the ground floor or first floor of buildings. Then in addition it could be interesting to further study building penetration at higher floors, for example the phenomena of smaller variations of the mean at lower floor levels against the larger variations at higher floor levels. Buildings with glass covered by special reflective coating should be considered as a special case since the coating could cause large differences (larger losses) with other buildings with normal glass.

Another possible experiment could be outdoor measurements at higher floor levels to determine the direct outdoor-indoor dependency. This experiment is not easily executed, but could provide important information on the relation between the signal strength outdoor and indoor.

The second experiment was comprised of a small number of measurements. This type of experiment could also be performed more extensively to obtain more information on the subject. However, the exact behavior of the algorithm that calculates the angles of arrival is still not known for the case of indoor reception. This could be studied by taking measurements with different configurations of the uniform circular array antenna in an aneochoic chamber with known close-by reflectors.

References

[1] Rappaport T.S., "Wireless Communications", Prentice Hall, New Jersey, 1996.

[2] Dooren G.A.J. van, "A deterministic approach to the modeling of electromagnetic wave propagation in urban environments", Ph.D. thesis, Eindhoven University of Technology Eindhoven, The Netherlands, 1994.

[3] Herben M.H.A.J., "Collegedictaat Antennes & Propagatie", Eindhoven University of Technology, Eindhoven, The Netherlands.

[4] Parsons D., "The Mobile Radio Propagation Channel", Pentech Press, pp. 189-200, 224-225.

[5] Hashemi H., "The Indoor Radio Propagation Channel", Proceedings of the IEEE, vol. 81, Iss 7, 1993, pp. 943-968.

[6] ITU Recommendations on Radiowave propagation, "The concepts of transmission loss for radio links", ITU-R p.341-4.

[7] Lee C.Y., "Mobile communications engineering", second edition, 1998, pp. 128-130.

[8] Koelen M.H.J.L., "Measurements and modeling of transmission of radio waves through buildings", M.Sc. final report, Eindhoven University of Technology, Eindhoven, The Netherlands, 2000, pp. 19-56, 39-42.

[9] COST 231 Final Report, Digital mobile radio: COST 231 view on the evolution towards 3rd generation systems,: European commission – COST Telecommunications, Brussel, Belgium, 1998, pp. 167-174.

[10] Hata M., "Empirical formula for propagation loss in land mobile radio services", IEEE Transactions on Vehicular Technology, vol. VT-29, No. 3, 1980, pp. 317-325 .

[11] Okumura Y, et. al., "Field strength and its variability in VHF and UHF land mobile service", Rev. Elec. Comm. Lab., vol. 16, 1968, pp. 825-873.

[12] Rice L.P. "Radio transmission into buildings at 35 and 150 MHz", The Bell System Technical Journal, vol. 38, no.1, 1959, pp. 197-210.

[13] Kreyszig E., "Advanced engineering mathematics", Wiley, New York, 7th edition, 1993, pp. 1255-1257.

[14] Lennartz C.H.F., "Modelling, simulation and design of Land Mobile Satellite systems", Stan Ackermans Institute, Eindhoven, The Netherlands, 1995, pp. 17-23.

[15] A. Picquenard, "Radio wave propagation", Wiley, New York, 1974, p.296.

[16] Toledo A.F. de and A.M.D. Turkmani and J.D. Parsons, "Estimating coverage of radio transmission into and within buildings at 900, 1800 and 2300 MHz", IEEE personal communications, April 1998 pp. 40-47.

[17] Turkmani A.M.D. and A.F. de Toledo , "Radio transmission at 1800 MHz into and within multistory buildings", IEE Proceedings-I, vol. 138, No. 6, 1991.

[18] Tanis W. J. and G. J. Pilato, "Building penetration characteristics of 880 MHz and 1922 MHz radio waves", Vehicular Technology Conference, 1993., 43rd IEEE , 1993, pp. 206 – 209.

[19] Horikoshi J. and K. Tanaka and T. Moringa, "1.2 GHz band wave propagation measurements in concrete building for indoor radio communications", IEEE Transactions on Vehicular Technology, vol. VT-35 No. 4, 1986.

[20] Barry P.J. and A.G. Williamson, "Modeling of UHF radio wave signals within externally illuminated multi-story buildings", J. IERE, 1987, 57, (6), (supplement), pp. S231-S240.

[21] Schmidt R.O., "Multiple emitter location and signal parameter estimation", IEEE Trans. Antennas Propagation, vol. 34, March 1986, pp. 276.

[22] Scully N., "An impulse response model for cordless systems: A combined statistical and deterministic approach", Final report of postgraduate program: Information and Communication Technology, Stan Ackermans Institute, Eindhoven, The Netherlands, 1999, pp. 63-64.

[23] Mawira A., "Variability of monthly time fraction of excess of atmospheric propagation parameters", Ph.D. Thesis Eindhoven University of Technology, Eindhoven, The Netherlands, 1999, pp.52.

[24] Gumbel E.J., "Statistics of extremes", Columbia University Press, 1967.

[25] Jong Y.L.C. de, "High-resolution time delay/angle-of-arrival measurements in microcellular environments", Final report internship at Swisscom Corporate Technology, 1998.

[26] Walker E.H. ,"Penetration of radio signals into buildings in the cellular radio environment", Bell System Technical Journal, vol.62, no.9, 1983, pp.2719-2734.

[27] Borjeson H., "Radio wave propagation in confined environments, measurements and models", Ph.D. Thesis, Lund Institute of Technology, Lund, Sweden .

[28] Molkdar D., "Review on Radio Propagation into and Within Buildings"
IEE Proceedings-H Microwaves Antenna and Propagation, vol.138, Iss. 1, 1991, pp. 61-73.

[29] Dooren G.A.J. van and M.H.A.J. Herben, "A deterministic approach for the modelling of wave propagation around buildings", Journal of Electromagn. Waves and Appl., vol.8,1994, pp. 175-194.

[30] Jong Y.L.C. de and M.H.A.J. Herben, "Experimental verification of ray-tracing based propagation prediction models for urban microcell environments", IEEE Trans. Veh. Technol., vol. 3, 1999, pp.1434-1438.

[31] Mathews C.P. and M.D. Zoltowski, "Eigenstructure techniques for 2-D angle estimation with uniform circular arrays", IEEE Trans. on Signal Processing, vol. 42, no. 9, 1994, pp. 2395-2407.

Appendices

Building Maps with measured rooms per floor

The building maps of all floors of the four buildings SK, PB, AB and WA measured in the TEMS experiment are plotted. The arrow indicates the direction of the transmitter, the measured rooms are indicated with *k<number>* and the floor areas are indicated with *front*, *left* and *right*.

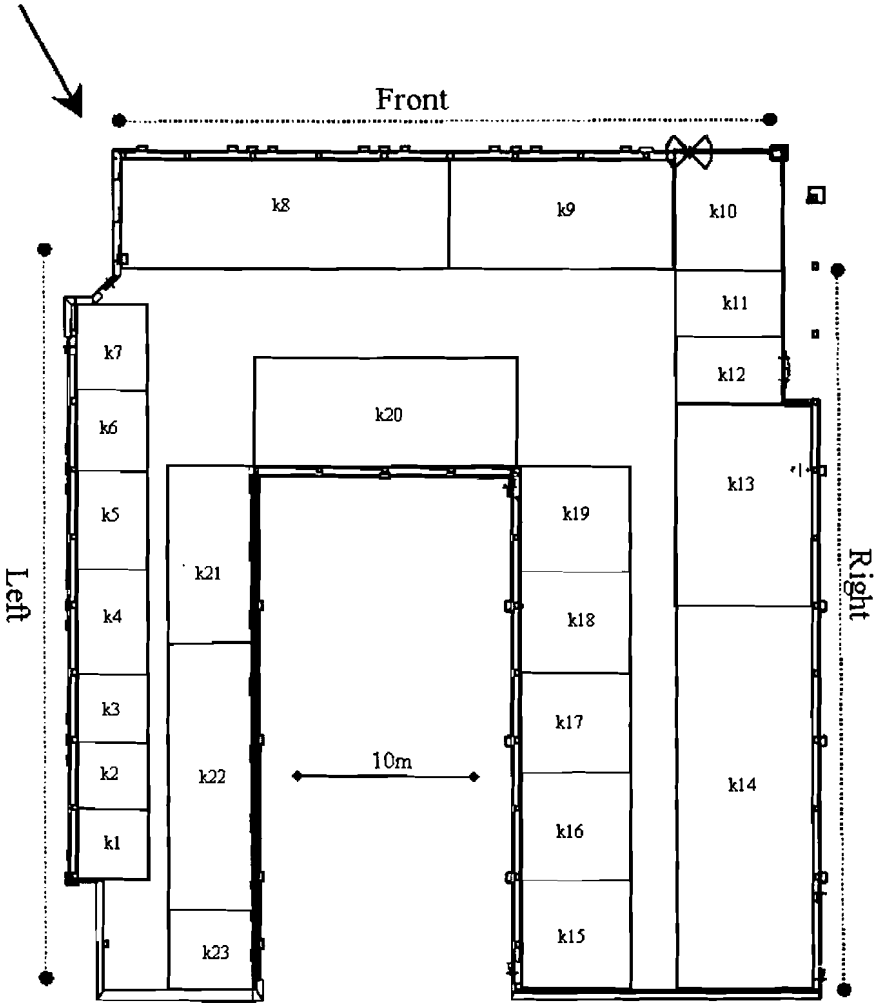

Fig. A.2 Building SK Floor 3

Fig. A.1 Building SK Floor 1

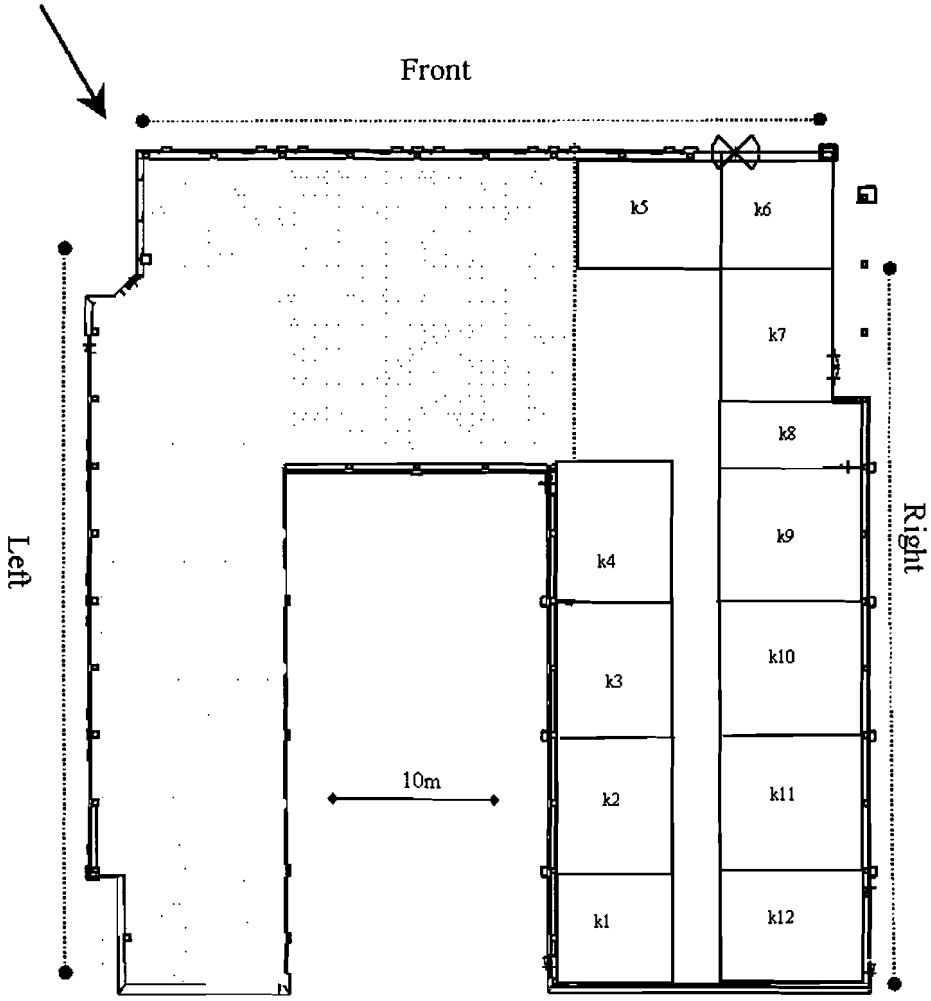

Fig. A.3 Building SK Floor 5&7

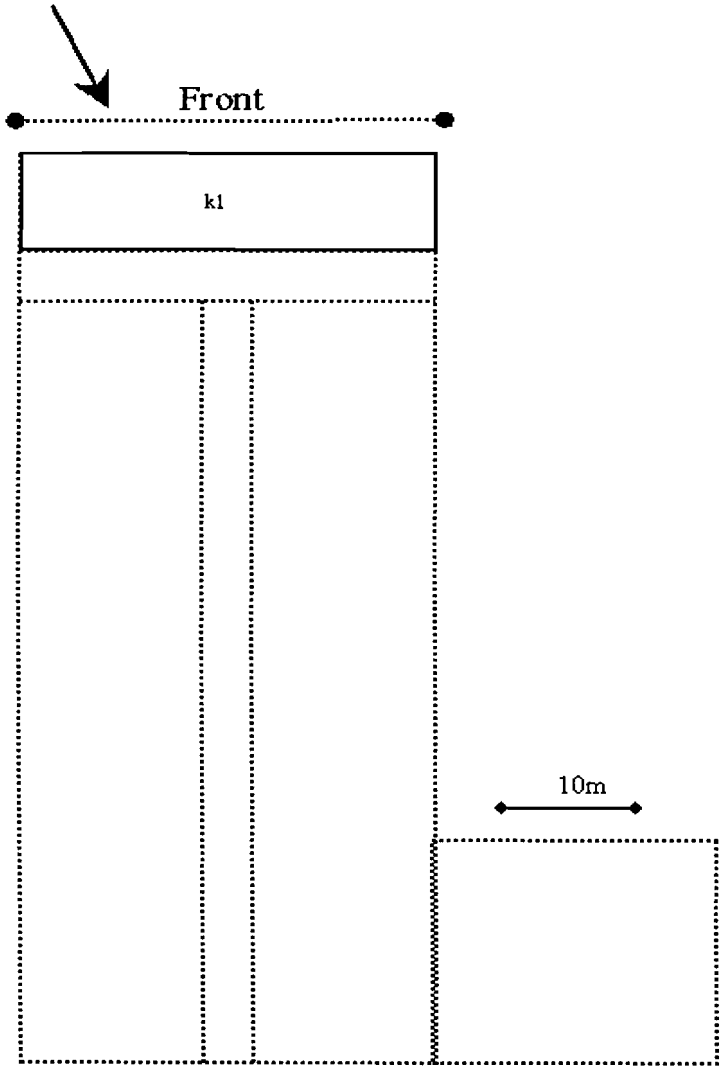

Fig. A.4 Building PB All floors

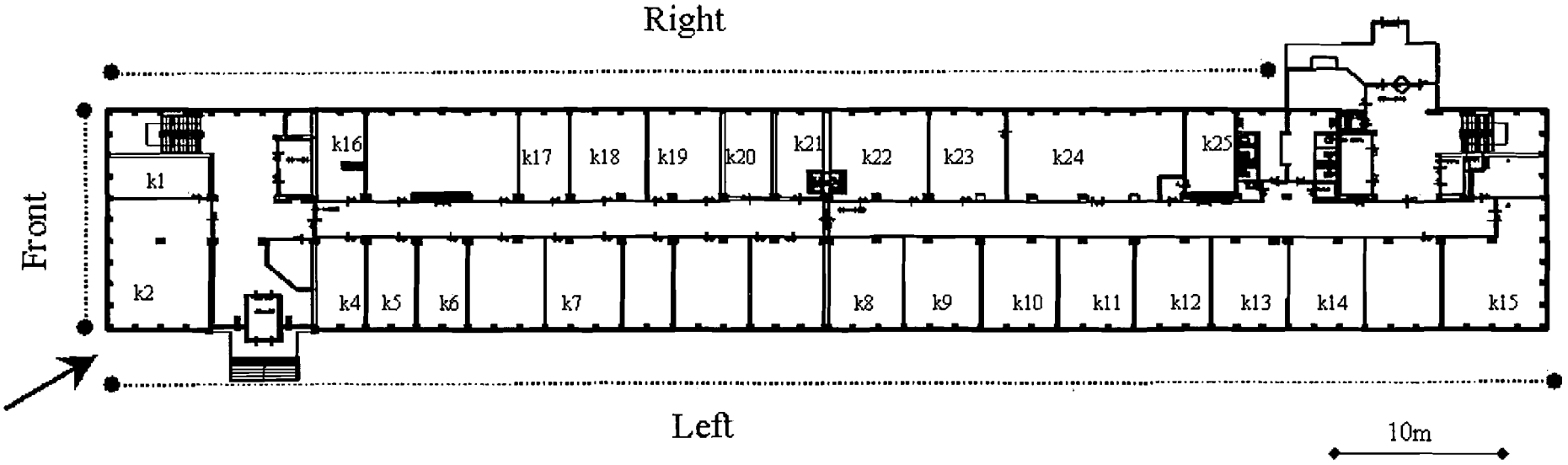

Fig. A.5 Building AB Floor 1

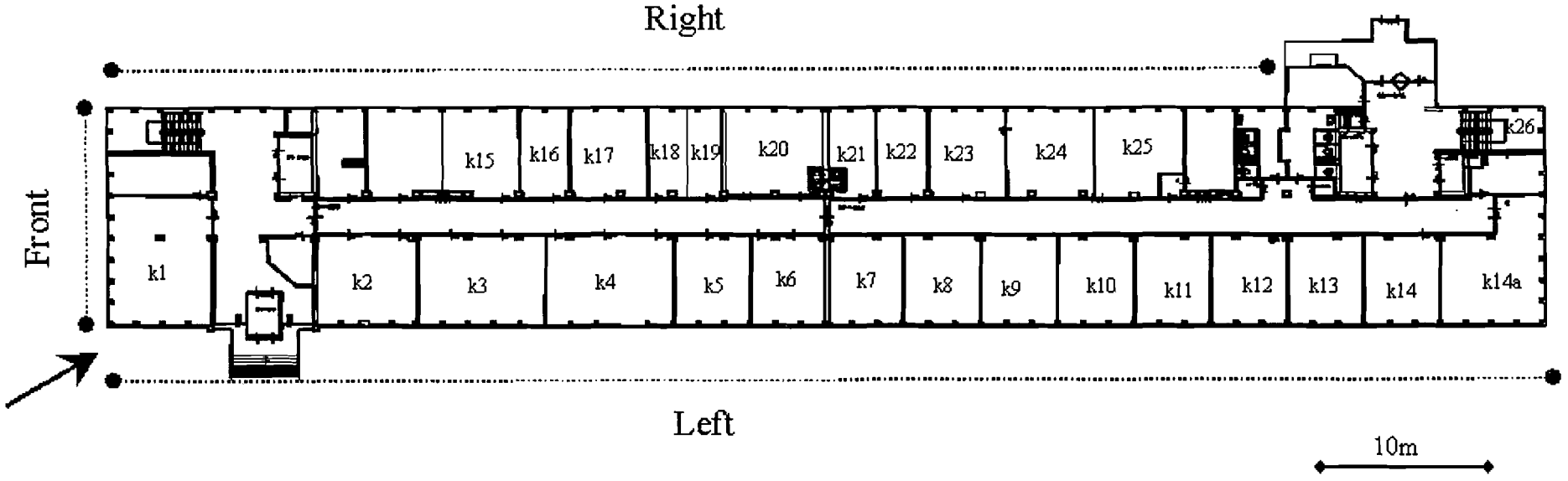

Fig. A.6 Building AB Floor 4

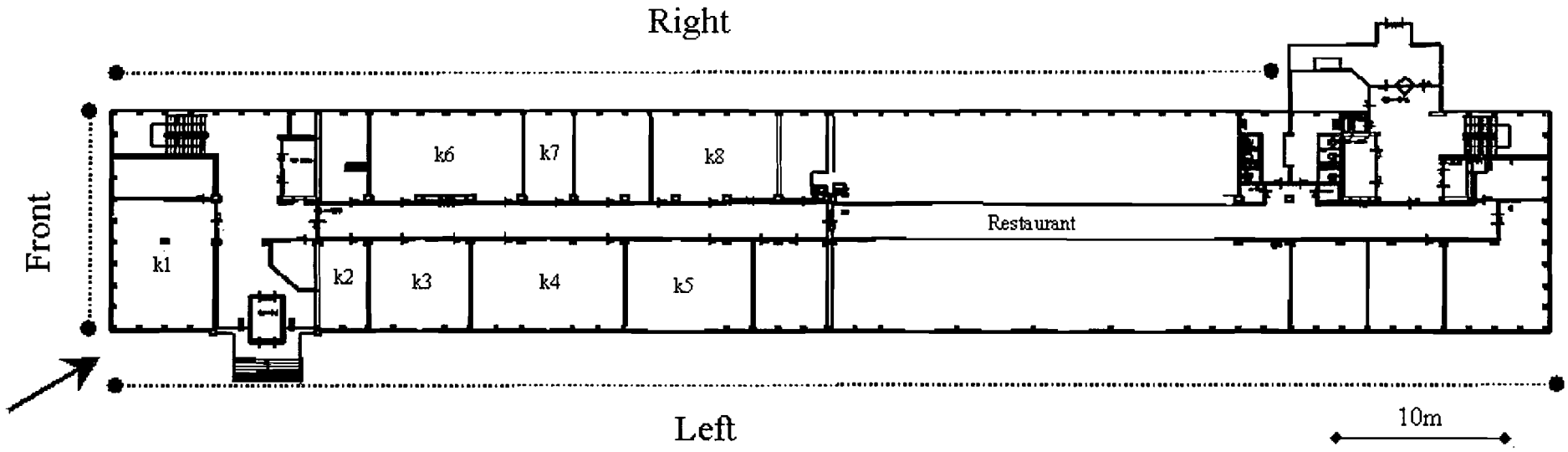

Fig A.7 Building AB Floor 7

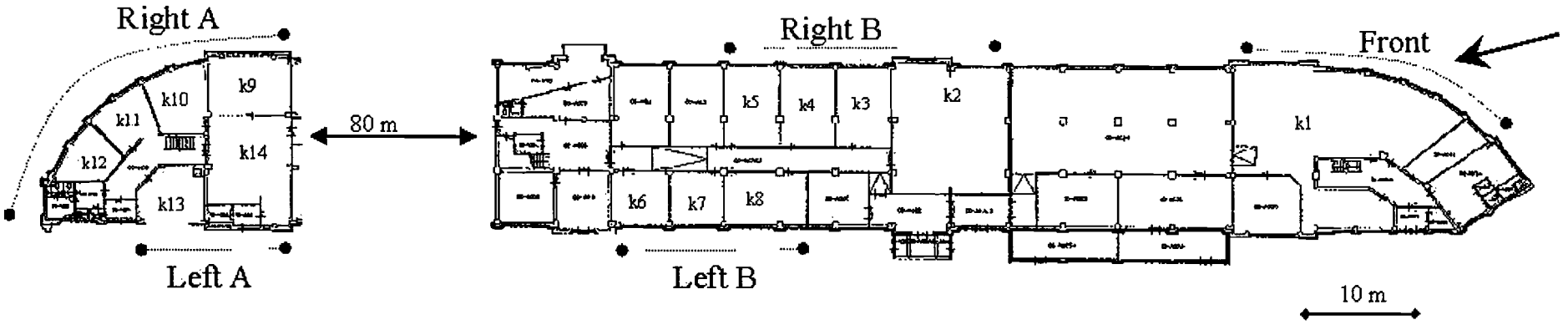

Fig. A.8 Building WA Ground floor

Measurement results per room of all floors in the four buildings

The average of the measured RxLev is given for outdoor and all measured rooms of the four measured buildings SK, PB, AB and WA. Also the room losses, transmitter-receiver distance for rooms on the first floor (Tx-Rx distance) and floor height factors are given. Finally the building loss and standard deviation are given in the gray sections.

Mean RxLev per room for building SK									
room	outdoor	floor 1	floor3	floor5	floor7		Room loss (dB)	Tx-Rx distan-ce (m)	floor height factor (dB/floor)
k1	52,6	39,0	40,8	54,7	56,9		13,7	146	1,9
k2	53,0	37,6	41,0	55,5	56,2		15,4	142	3,0
k3	51,3	34,9	40,9	54,1	53,2		16,4	138	0,6
K4	50,0	41,2	39,2	47,8	53,7		8,8	135	
k5	51,6	40,1	40,9	47,2	48,6		11,5	130	
K6	54,6	38,6	44,4	45,2	52,3		16,0	126	
k7	54,1	39,1	43,5	44,0	47,8		15,0	121	
K8	52,5	40,5	45,2	45,9	45,3		12,0	117	
K9	56,6	41,3	34,5	45,2	42,1		15,3	129	
K10	54,8	39,6	39,5	45,7	43,2		15,2	137	
K11	55,1	42,5	41,8	43,8	44,2		12,6	140	
K12	53,2	43,8	42,7	42,7	41,6		9,4	142	
K13	51,0	39,4	41,0				11,6	155	
K14	50,3	38,9	40,6				11,4	163	
k15		36,8	39,3						
k16		36,7	38,5			Building loss (dB):		13,2	
k17		34,3	48,0			sd(dB):		2,5	
k18		35,1	43,2						
k19		30,0	41,6						
k20		34,2	38,1						
k21		35,6	41,9						
k22		36,3	41,0						
k23		32,6	39,1						
k24			41,6						
k25			44,4						
k26			43,6						
k27			42,6						
k28			42,8						
Average	52,9	37,7	41,5	47,6	48,8				
SD	1,9	2,1	2,6	4,5	5,5				

Mean per room for building AB							
room	outdoor	floor 1	floor4	floor7	Room loss (dB)	Tx-Rx distance (m)	Floor height factor (dB/floor)
k1	44,9	41,7	58,1	56,4	3,2	428	3,5
k2	43,2	43,1	55,5	57,5	0,1	425	1,0
k3	xxx	xxx	57,7	56,9	xxx	xxx	
K4	41,3	40,8	57,9	56,0	0,5	436	
k5	42,5	41,3	58,8	54,7	1,2	439	
K6	42,3	41,7	56,3	47,0	0,6	445	
k7	42,4	41,8	54,5	44,6	0,6	450	
K8	43,9	41,4	54,9	47,1	2,6	462	
K9	43,4	40,3	53,9		3,2	467	
K10	43,1	41,7	51,5	Rest. R:43,2	1,5	469	
K11	44,5	42,6	51,8	Rest. L:50,0	1,8	475	
K12	43,1	40,7	52,8		2,4	477	
K13	42,3	34,5	49,9		7,8	479	
K14	42,2	33,4	49,3		8,7	482	
k15	41,6	36,9	41,6		4,8	485	
k16	41,5	27,9	42,7		13,6	493	
k17	42,3	37,1	42,8		5,2	441	
k18	42,3	36,2	44,5		6,1	448	
k19	42,0	37,4	45,0		4,5	452	
k20	40,6	38,0	43,6		2,6	456	
k21	40,9	34,3	42,7		6,6	460	
k22	42,2	31,8	40,7		10,4	466	
k23	41,8	36,4	40,0		5,3	470	
k24	43,0	34,1	36,4		8,9	472	
k25	44,5	30,7	32,7		13,8	482	
k26		k14a: 48,9	39,1				
Average:	42,6	37,7	48,3	51,3	Building loss (dB):	4,8	
	1,1	4,2	7,5	5,6	sd (dB):	4,0	

Mean RxLev per room for building WA					
room	outdoor	floor 0		Room loss	Tx-Rx distance (m)
k1	47,5	39,4		8,2	638
k2	44,6	33,3		11,3	675
k3	46,8	32,5		14,3	682
K4	47,3	32,5		14,8	688
k5	44,8	30,8		14,0	694
K6	51,6	37,7		13,9	701
k7	52,6	38,1		14,5	705
K8	50,9	37,2		13,7	710
K9	32,2	22,7		9,5	808
K10	31,0	20,8		10,1	813
K11	28,8	22,3		6,5	816
K12	27,9	22,8		5,1	817
K13	39,8	23,4		16,4	807
K14	38,5	20,5		18,1	810
Average:	41,7	29,6	Building loss:		12,2
	8,7	7,2	sd:		3,8

Mean RxLev per floor for building PB		
floor	indoor	Floor height factor (dB/floor)
1	53,0	0,7
2	53,7	1,4
3	xxx	1,7
4	xxx	-0,6
5	57,9	-0,8
6	59,6	-0,1
7	59,0	-0,6
8	58,2	-2,3
9	58,1	
10	57,5	
11	xxx	
12	52,9	
Outdoor RxLev:	56,6	
Room loss:	3,6	
Tx-Rx distance (m)	365	